TECHNICAL REPORT STANDARD PAGE

1. Report No. **FHWA/LA.03/379**	2. Government Accession No.	3. Recipient's Catalog No.
4. Title and Subtitle Evaluation of Interaction Properties of Geosynthetics in Cohesive Soils: LTRC Reinforced-Soil Test Wall	5. Report Date January 2004	
	6. Performing Organization Code	
7. Author(s) Khalid Farrag, Ph.D., P.E. & Mark Morvant, P.E.	8. Performing Organization Report No. 379	
9. Performing Organization Name and Address Louisiana Transportation Research Center 4101 Gourrier Ave. Baton Rouge, LA 70808	10. Work Unit No.	
	11. Contract or Grant No. State Project No. 736-99-0658	
12. Sponsoring Agency Name and Address Louisiana Department of Transportation and Development Louisiana Transportation Research Center 4101 Gourrier Ave. Baton Rouge, LA 70808	13. Type of Report and Period Covered Final Report July 1997 – December 2003	
	14. Sponsoring Agency Code 92-4GT	

15. Supplementary Notes
Conducted in Cooperation with the U.S. Department of Transportation, Federal Highway Administration

16. Abstract

This report presents the construction and performance evaluation of the LTRC reinforced-soil test wall. The 20 ft. high, 160 ft. long wall was constructed using low quality backfill. Its vertical front facing was constructed with modular blocks. It consisted of three sections reinforced with various geogrid reinforcement types and spacing. The backside of the wall was a one-to-one slope reinforced with woven and non-woven geotextiles.

The test wall was constructed to evaluate the design procedure and performance of geosynthetic-reinforced structures constructed with marginal silty-clay backfill over soft clay foundation. The instrumentation program consisted of monitoring wall deformation, foundation settlement, strains in the reinforcement, vertical and horizontal stresses in the soil, and pore water pressure under the wall. Results of the monitoring program from construction through four months after completion of the wall are detailed in this report.

The results of the instrumentation program showed relatively high deformations due to both the design of the wall with low factors of safety and to the high settlement of the foundation soil. These deformations, however, occurred mostly during construction. The results of strain measurements in the reinforcement were used to evaluate the effect of reinforcement stiffness and spacing on the shape of the failure surface and on the distribution and magnitude of stresses in reinforcement layers.

The results show promising performance of silty-clay soils as a backfill material in reinforced-soil walls providing proper design and control of soil compaction and moisture. However, long-term performance of the wall needs to be monitored for a complete evaluation of these types of walls.

17. Key Words Geosynthetics, Geogrids, full-scale test, mechanically stabilized earth wall, reinforced steep slope, reinforcements, marginal soils	18. Distribution Statement **Unrestricted. This document is available through the National Technical Information Service, Springfield, VA 21161.**	
19. Security Classif. (of this report) None	20. Security Classif. (of this page)	21. No. of Pages 136	22. Price

Project Review Committee

Each research project has an advisory committee appointed by the LTRC Director. The Project Review Committee is responsible for assisting the LTRC Administrator or Manager in the development of acceptable research problem statements, requests for proposals, review of research proposals, oversight of approved research projects, and implementation of findings.

LTRC appreciates the dedication of the following Project Review Committee members in guiding this research study to fruition.

LTRC Administrator/ Manager
Mark J. Morvant
Pavement & Geotechnical Research Administrator

Members
Doug Hood, DOTD
Kim Martindale, DOTD
Mike J. Boudreaux, DOTD
Mike B. Boudreaux, LTRC
Zhongjie "Doc" Zhang, Ph.D., LTRC
Murad Abu-Farsakh, Ph.D., LTRC/LSU

Directorate Implementation Sponsor
William T. Temple, DOTD Chief Engineer

Evaluation of Interaction Properties of Geosynthetics in Cohesive Soils: LTRC Reinforced-Soil Test Wall

By

Khalid Farrag, Ph.D., P.E.

and

Mark Morvant, P.E.

The contents of this report reflect the views of the author/principal investigator who is responsible for the facts and the accuracy of the data presented herein. The contents do not necessarily reflect the views or policies of the Louisiana Department of Transportation and Development the Federal Highway Administration the Louisiana Transportation Research Center. This report does not constitute a standard, specification, or regulation.

January 2004

ii

ABSTRACT

This report presents the construction and performance evaluation of the LTRC reinforced-soil test wall. The 20 ft. high, 160 ft. long wall was constructed using low quality backfill. Its vertical front facing was constructed with modular blocks. It consisted of three sections reinforced with various geogrid reinforcement types and spacing. The backside of the wall was a one-to-one slope reinforced with woven and non-woven geotextiles.

The test wall was constructed to evaluate the design procedure and performance of geosynthetic-reinforced structures constructed with marginal silty-clay backfill over soft clay foundation. The instrumentation program consisted of monitoring wall deformation, foundation settlement, strains in the reinforcement, vertical and horizontal stresses in the soil, and pore water pressure under the wall. Results of the monitoring program from construction through four months after completion of the wall are detailed in this report.

The results of the instrumentation program showed relatively high deformations due to both the design of the wall with low factors of safety and to the high settlement of the foundation soil. These deformations, however, occurred mostly during construction. The results of strain measurements in the reinforcement were used to evaluate the effect of reinforcement stiffness and spacing on the shape of the failure surface and on the distribution and magnitude of stresses in reinforcement layers.

The results show promising performance of silty-clay soils as a backfill material in reinforced-soil walls providing proper design and control of soil compaction and moisture. However, long-term performance of the wall needs to be monitored for a complete evaluation of these types of walls.

ACKNOWLEDGMENTS

IMPLEMENTATION STATEMENT

Current design specifications of reinforced-soil walls require the use of high quality granular soil as a backfill material. This project investigated the utilization of available silty-clay soil as a backfill material. The use of the marginal silty-clay soil (up to Plasticity Index 15) presented an economical and practical solution for the construction of reinforced walls.

The performance of the reinforced-soil wall demonstrated the applicability of using marginal silty-clay soil as a backfill material. The high deformations of the wall sections were mainly due to low safety factors in the design procedure and the settlement of the base soil. However, the use of these materials requires the proper control of soil moisture content during construction and a proper drainage system behind the wall facing. Long-term performance of the wall was not evaluated in the testing program.

The performance of the reinforced slopes suggested the applicability of using woven and non-woven geotextiles in reinforcing steep slopes with marginal soils. There were no results that concluded the advantage of using one type of geotextile over the other.

TABLE OF CONTENTS

x

LIST OF TABLES

LIST OF FIGURES

INTRODUCTION

Using available low quality silty-clay soil as a backfill material presents an economical and practical solution for the construction of reinforced-soil walls. Design specifications of reinforced-soil walls to date have focused on the use of high quality granular soil as a backfill material [1], [2]. This is primarily due to their higher frictional resistance and their stable mechanical properties with time and with changes in soil moisture. However, sandy-silt and silty-clay soils of medium plasticity [PI < 15] have been used in reinforced slopes, and they could be suitable as backfill in reinforced walls, provided that their interaction mechanism and their long-term performance have been thoroughly investigated.

For this purpose, the Louisiana Transportation Research Center (LTRC) has constructed a full-scale reinforced test wall with low quality backfill. The two major objectives of the test wall's construction were to investigate the interaction mechanism between various geosynthetic materials and the silty-clay and to monitor the state of stresses and deformations of the wall. The test wall was 20 ft. high and consisted of a vertical side and a one-to-one slope side at the back. The vertical side of the wall was constructed with modular block facing and consisted of three test sections reinforced with various geogrid types. The strength, geometry, and vertical spacing of the geogrids varied in each section to evaluate the effect of these design parameters on the wall performance.

The first section of the wall (section 1) was constructed using low strength geogrid placed at a minimum vertical spacing of 16 in. Section 2 was constructed using higher strength geogrid placed at a maximum vertical spacing of 40 in. The vertical spacing of section 3 was variable so as to obtain relatively uniform stresses in the reinforcement layers along most of the wall height. Field pullout tests were performed on various types of geosynthetic-reinforcements installed for this purpose in section 3 of the wall. The results of the field pullout tests are presented in a separate report [3].

Another section of the vertical side of the wall was constructed using Geoweb cells to investigate the construction procedure and performance of such systems around culverts. The

backside of the wall is a one-to-one slope reinforced with two types of woven and non-woven geotextiles.

The design criteria of the wall was based on using low factors of safety to obtain measurable deformations in the test sections. Accordingly, the instrumentation program monitored the during-construction and short-term deformations of the silty-clay backfill, the mobilized strains in the reinforcement, vertical and horizontal earth pressures in soil and near the facing, and the settlement of the wall over the soft soil foundations.

The construction of the test wall started in February 1998 and was completed in July 1998. This report presents the results of the monitoring program during construction through the first four months after completion of construction. Some measurements of wall deformations and strains were also taken until the beginning of 2002, those results are presented as well.

The "Methodology" section of the report describes the construction and the instrumentation of the test wall. The results of the monitoring program and an evaluation of the performance of the test wall are presented in the "Discussion" section of the report.

OBJECTIVES

The test wall was constructed to evaluate the behavior of reinforced soil walls constructed with silty-clay soils through comparison between the predicted and field measurements, and to provide guidelines for the selection of the design parameters. The primary objectives of the construction of the LTRC reinforced test wall were to:

- Monitor the performance of the reinforced-soil wall constructed with low quality backfill (silty-clay soil with of Plasticity Index of 15).
- Evaluate the effect of reinforcement type, strength, geometry, and vertical spacing on the distribution of the stresses along the height of the wall.
- Correlate the results of lab pullout tests to field tests for various types of geosynthetic reinforcement.

Other secondary objectives were addressed in the design, construction, and instrumentation of the test wall. These objectives were to:

- Investigate the effect of settlement of the base-soil on wall deformation.
- Monitor the performance of steep slopes reinforced with woven and non-woven geotextiles.
- Evaluate the performance of 'Geoweb Cells' in the wall as a flexible wall system around culverts.
- Evaluate the performance of several erosion control products in steep slopes.

This report addresses the first two primary objectives and the secondary objectives of the wall construction. The evaluation of field and laboratory pullout tests is presented in a separate report.

SCOPE

The design, construction, and instrumentation of the LTRC test wall were based on the following considerations:

- Using geogrid for the reinforcement of the vertical test wall. The strengths of the geogrids varied widely between sections 1 and 2 in order to cover the two design configurations of flexible walls with minimum and maximum vertical spacing between the reinforcements.

- Designing the walls with an overall low factor of safety to obtain measurable deformations and higher reinforcement loads. Sections 1 and 2 were designed with a low safety factor for creep and safety factors of one for construction damage and degradation. Section 3 was designed using standard geogrid type and procedure in order to safely perform pullout tests in the field.

- Monitoring the wall deformations, stresses, and strains in the reinforcement to evaluate the applicability of the current design procedures for use in reinforced walls with silty-clay soils.

- Evaluating the use of woven and non-woven geotextiles in the reinforcement of steep slopes.

The research program focused on monitoring and evaluating the performance of the test wall during-construction and in the short-term period of four months after construction. The report presents some measurements at longer periods.

The scope of future investigations of the test wall may include the following:

- Long-term monitoring of wall deformations and stresses.

- Field pullout tests on facing blocks in order to evaluate the connection strength of the modular block facing.

- Evaluating the effect of construction damage on the various types of reinforcements in the wall.

- Determining the ultimate loads and deformations at the critical state by adding surcharge over the wall.

METHODOLGY

Description of the LTRC Test Wall

The test wall was constructed in 1998 by LTRC at its Pavement Research Facility (PRF) site. It consisted of a 20 ft. vertical wall of modular block facing and was constructed using silty-clay backfill of medium plasticity (PI = 15). The wall was reinforced with various types of geogrids. The height of the wall was uniform for a length of 100 ft. and then sloped down at one end for a length of about 60 ft. This three-to-one slope facilitated the construction of the wall. Figure 1 shows a view of the vertical wall.

The other end of the vertical wall consisted of a 15 ft. long gravity type Geoweb section. Figure 2 shows a view of the Geoweb section of the vertical wall.

Figure 1
View of the LTRC test wall

Figure 2
View of the Geoweb section of the vertical wall

The back side of the wall had a slope of one-to-one and was reinforced with two types of woven and nonwoven geotextiles. Figure 3 shows the slope side of the wall.

The wall was constructed over a soft clay foundation. A 2-ft.-thick stone base layer was constructed under the wall to provide a working platform and a global stability to the wall against foundation failure. The base was reinforced with two layers of geogrids Tensar UX-1600.

The vertical wall consisted of three sections reinforced with various types and configurations of reinforcement. Section 1 was reinforced with a relatively low strength geogrid placed at minimum vertical spacing of two modular blocks while section 2 of the wall was constructed with relatively stronger geogrid placed at a maximum spacing of 5 modular blocks.

8

Figure 3
The slope side of the wall during construction

Section 3 of the vertical wall was reinforced with strong geogrid, and the section was used in performing field pullout tests on various geosynthetic specimens placed between the main reinforcement.

The backside slope consisted of two sections reinforced with woven and non-woven geotextiles. The width at the top of the wall was 25 ft. Figure 4 shows a plan and elevation of the wall.

Figures 5 through 7 show cross sectional details of the three vertical wall sections and the two slope sections. Section 1 of the vertical wall was reinforced with geogrid Tensar UX-750, which is a relatively low-strength geogrid not commonly used in wall reinforcement. The 11-ft.-long geogrid was placed at minimum vertical spacing of two block heights (16 in.). The section was designated as the "Weak Geogrid – Minimum Spacing" section. The facing of the section was compact type "Keystone" modular blocks of 8 in. high, 18 inches wide , and 12 in. deep.
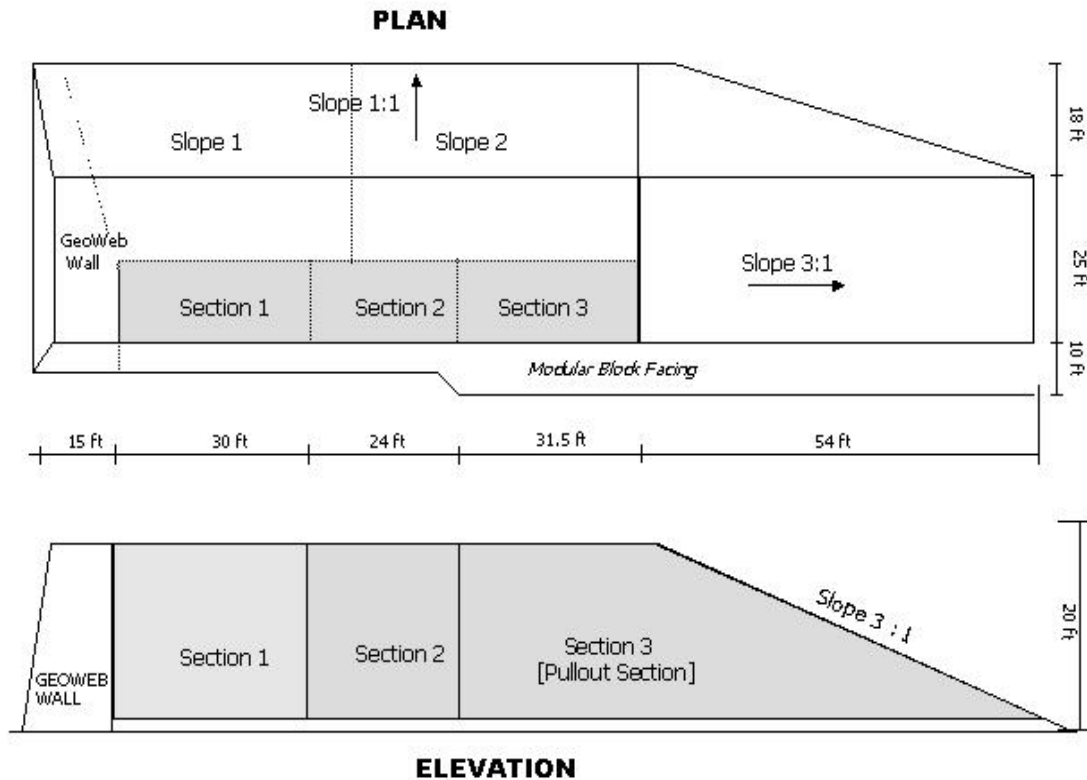
PLAN

Figure 4
Plan and Elevation of the test wall

Section 2 of the wall was reinforced with geogrid Tensar UX-1400, which is a relatively stronger geogrid. The geogrid was placed at the maximum vertical spacing of five block heights (40 in.) and had the same length of 11 ft. This section was designated the "Strong Geogrid – Maximum Spacing" section.

Section 3 was reinforced with geogrid Tensar UX-1500. The 11-ft.-long geogrid was placed at various vertical positions. Geosynthetics specimens were one ft. wide and three to five ft. long. They were placed between the main reinforcement of the wall in order to perform field pullout tests. Figure 7 shows the locations of the pullout specimens in the cross section. The specimens were connected to one-ft.-wide metal plates. The plates extended outside the wall facing through wooden boxes, which replaced the modular block units. Figure 8 shows the

10

pullout specimens and the wooden boxes at the facing of section 3. The modular blocks at the facing of sections 2 and 3 were standard "Keystone" blocks (8 in. high x 18 in. wide x 21 in. deep).

Section 1 of the slope side was reinforced with woven geotextiles "Geotex 4x4" of Synthetic Industries. The geotextile length varied from 11 ft. at the top of the wall to 19 ft. at the bottom layer (figure 5).

The non-woven geotextile type "Evergreen TG-700" was used in reinforcing section 2 of the slope. The geotextiles were placed at equal vertical spacing of 2 ft. (three soil lifts) and had length of 7 ft. at the top half of the wall and 14 ft. at the bottom half. Figure 7 shows a cross section of the non-woven slope section.
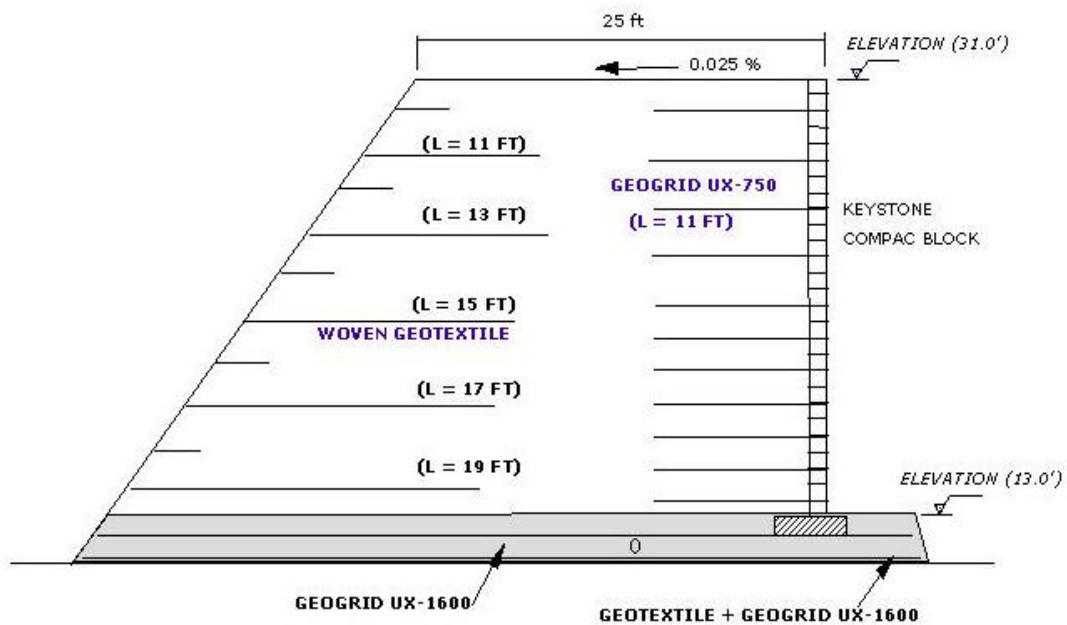
Figure 5
Cross-section of section 1 of the wall

11
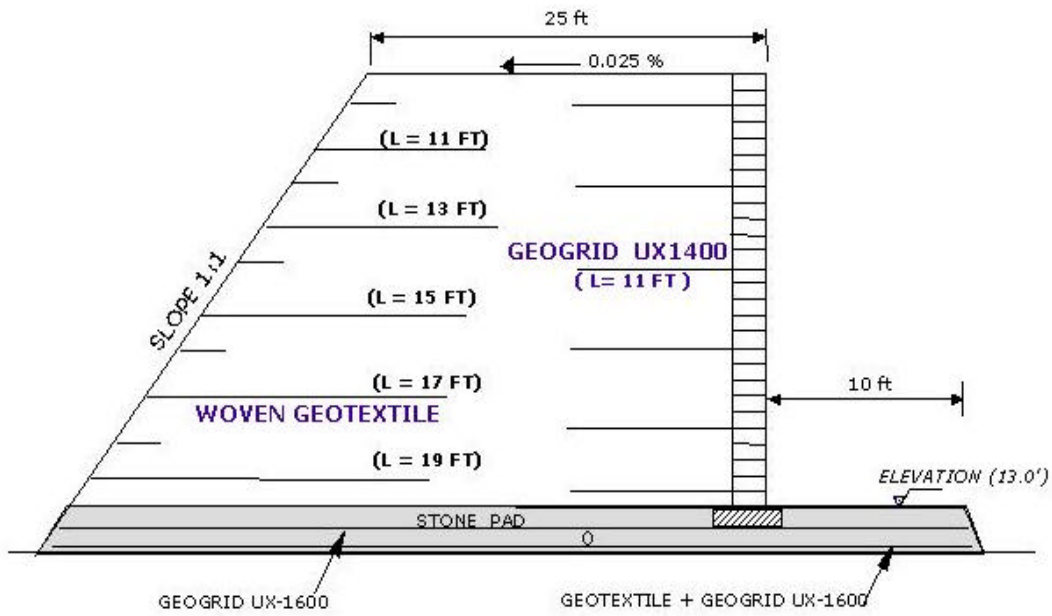
Figure 6
Cross-section of section 2 of the wall
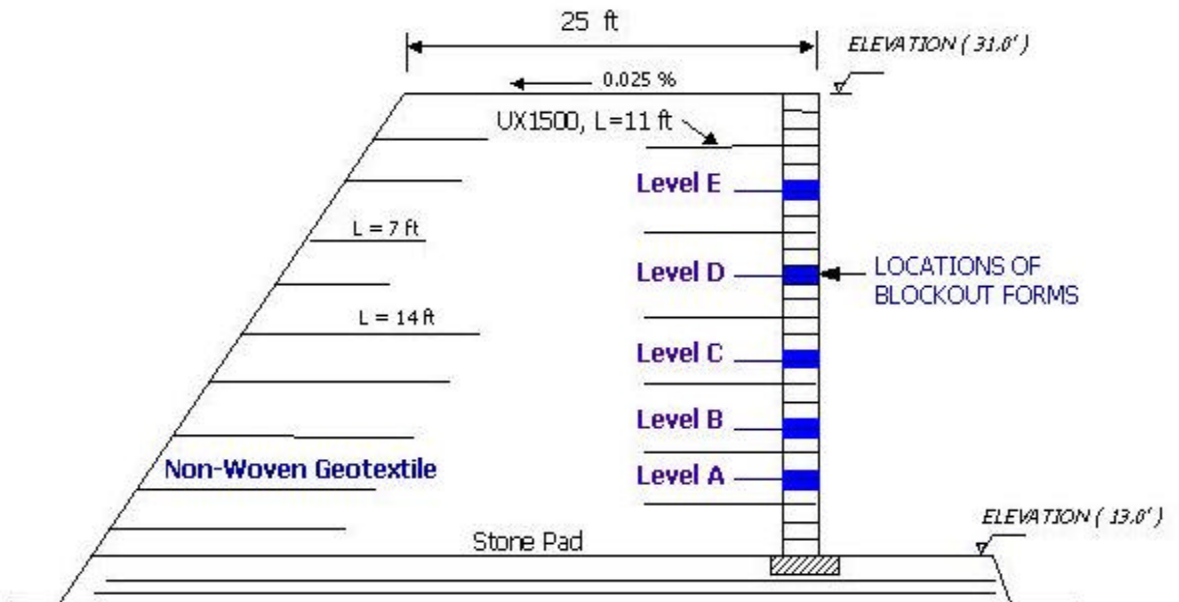
Figure 7
Cross-section of section 3 of the wall

12

Figure 8
View of the pullout specimens in section 3 of the wall

Material Properties

Base Soil Properties

The test wall was constructed over a soft soil foundation which consisted of a soft to medium 3-to-4 ft.-deep organic-clay layer, a 20-ft.-deep soft-clay layer, followed by a stiff-clay to a very stiff-clay layer. The results of unconfined compression tests on samples from various depths are shown in figure 9.

A 2-ft.-thick stone base soil layer was placed on the top of the foundation soil. The stone was reinforced with two layers of geogrid Tensar UX-1600 in order to provide a leveled base and to increase the global stability of the wall. Figure 10 shows the grain size distribution of the stone base layer.
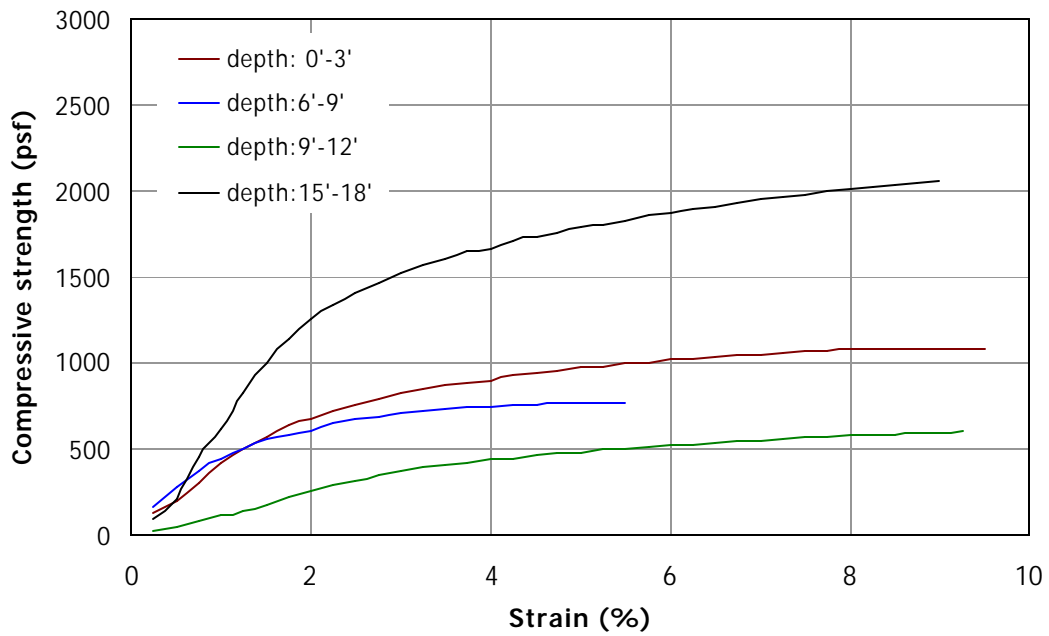
Figure 9
Unconfined compression tests on foundation soil
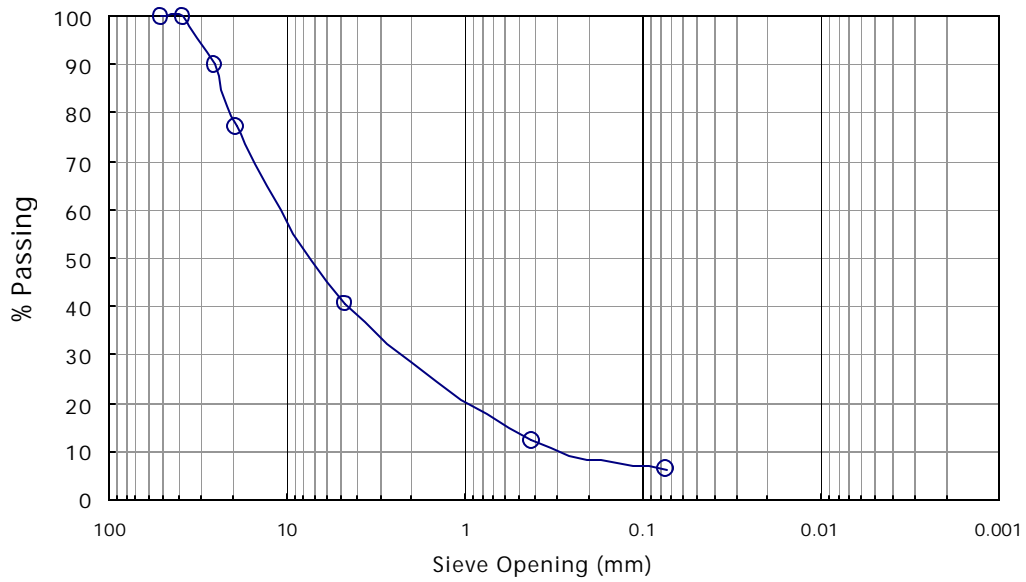
Figure 10
Grain size distribution of the stone base layer

Backfill Soil Properties

The backfill used in the wall was a silty-clay soil, AASHTO classification A-4, with the properties shown in table 1. The shear strength parameters were measured in the direct shear test according to ASTM D-6528. Maximum soil dry density and optimum moisture content were determined from the Standard Proctor test according to AASHTO test T-99. Figure 11 shows the moisture-density relationship obtained from the compaction test.

The soil was compacted in the wall in 8-inch lifts (equals the height of the modular block facing). Measurements of soil densities and moistures were performed at each compacted layer using the Nuclear Density Gauge. Figure 12 shows the average dry soil density in each soil layer. The figure shows an average dry soil density of 102 pcf which was about 95 percent of the maximum dry density.

Table 1
Properties of the soil backfill

% Silt	% Clay	PI	φ (degree)	Cohesion C (psf)	Optimum Moisture (%)	Max. γ_{dry} (pcf)
72	19	15	24	30	18.5	105
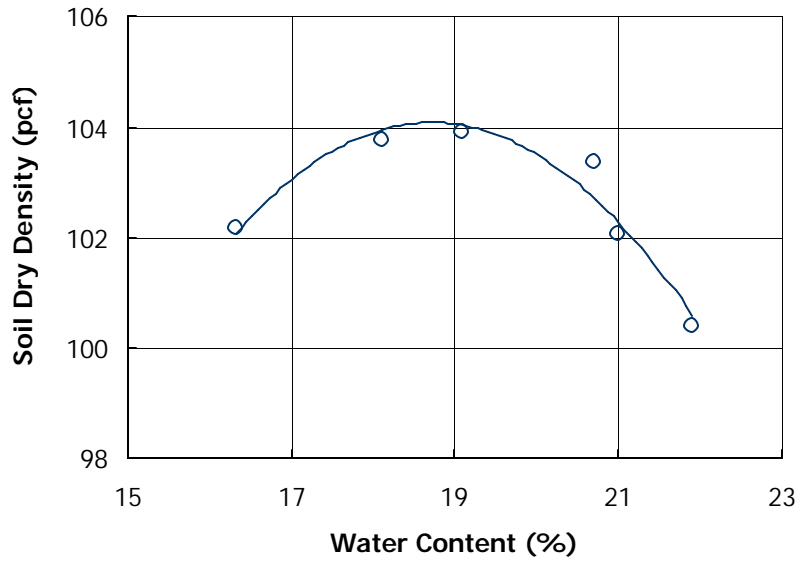
Figure 11

Moisture-density relationship of the silty-clay soil
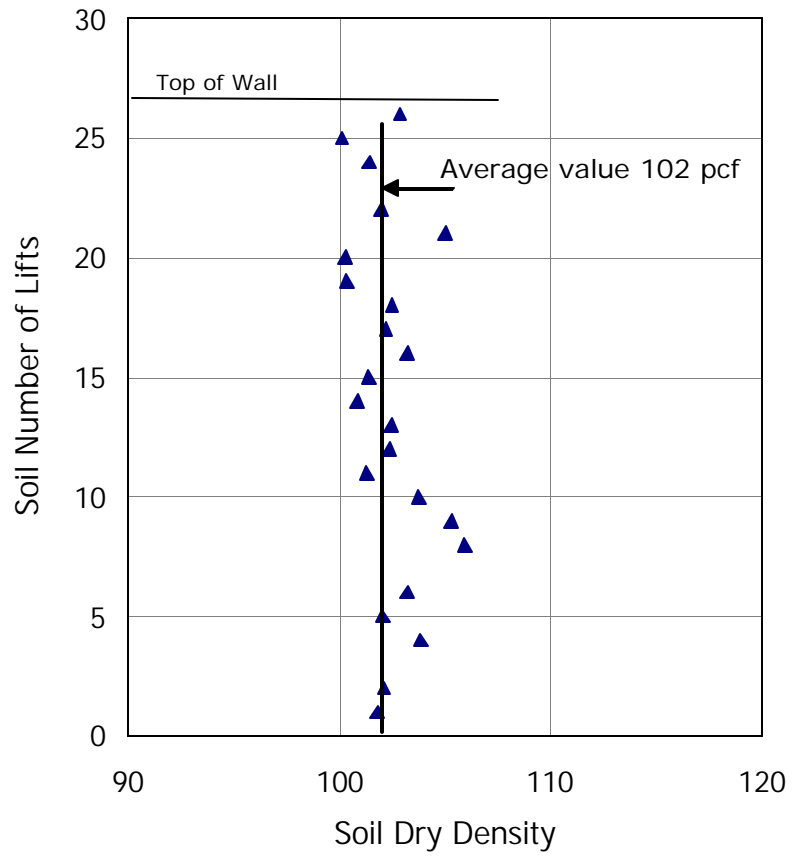
Figure 12 Profile of soil dry density at each soil lift if the wall

Geosynthetics Material Properties

The vertical side of the wall consisted of three sections reinforced with different types of geogrids. The first section was reinforced with a weak geogrid (Tensar UX-750) placed at a minimum vertical spacing of two soil lifts. The second section contained a relatively stronger geogrid (Tensar UX-1400) placed at a maximum vertical spacing of five soil lifts. The third section was designed for field pullout tests and it was reinforced with geogrid Tensar UX-1500.

The slope side of the wall consisted of two sections. One section was reinforced with woven geotextile "Geotex 4x4" and the other section was reinforced with 8-oz. non-woven geotextile type "Evergreen TG700."

The properties of geosynthetics reinforcement are presented in the following sections.

Geogrid UX-1600

The geogrid is a uniaxial High Density Polyethylene (HDPE) manufactured by the Tensar Corp. Table 2 shows the properties of the geogrid that was used in reinforcing the stone layer at the base of the wall. One layer of the geogrid was placed under the stone layer and another layer was placed at the middle of the 2-ft.-thick layer.

Geogrid UX-1500

This geogrid is also a uniaxial HDPE geogrid manufactured by the Tensar Corp. It has identical aperture size as the UX-1600 with a thinner rib, which results in a lower strength and modulus. The geogrid was used to reinforce the standard wall section (section 3), which was used in field pullout tests. Table 3 shows the properties of the geogrid and figure 13 shows the results of unconfined-extension tests on the geogrid. The extension tests were performed at an extension rate of 1 percent/min. on specimens that were 8-in. (7 strands) wide and 3 longitudinal units in length. Figure 14 shows the specimen setup in the "United" extension testing machine.

Table 2
Properties of the Geogrid UX – 1600HS

Property	Value	Unit

Aperture size:
     Machine Direction (MD)
     Cross-Machine Direction (CMD)
 Open Area
	14.5
	 0.66
	 68
		inch
		 inch
		 %

Initial Tensile Modulus	144,620	lb/ft

Long-Term Allowable Strength – MD
   in sand & silt
   in aggregate
	3,771
	 3,300
		lb/ft
		 lb/ft
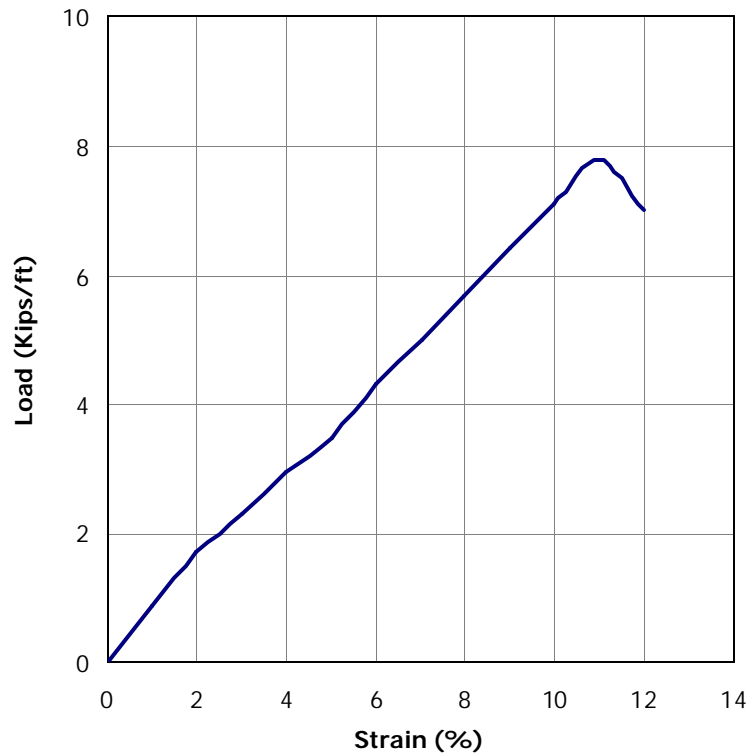
Figure 13
Results of extension test on the UX-1500 geogrid

18

Table 3
Properties of the Geogrid UX-1500HS

Property	Value	Unit
Thickness		
Ribs	0.065	inch
Junction	0.0167	inch
Ultimate Strength – MD	7,800	lb/ft
Tensile Modulus	90 –100	Kips/ft
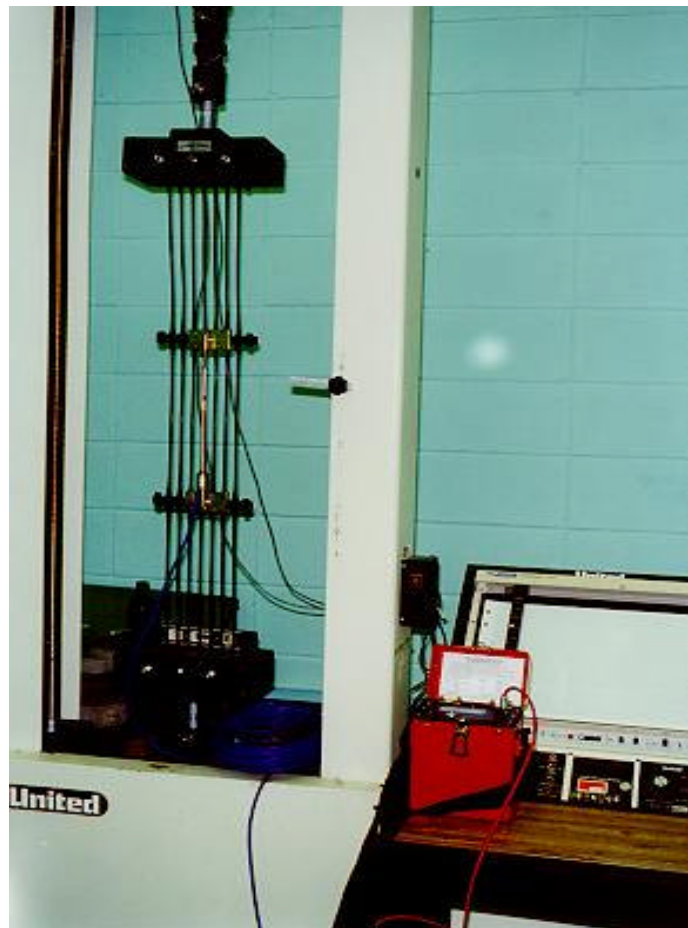
Figure 14
View of the extension test on the UX-1500

Geogrid UX-1400

This geogrid is a uniaxial HDPE geogrid manufactured by the Tensar Corp. It was used to reinforce section 2 (strong geogrid-maximum spacing) of the test wall. Table 4 shows the properties of the geogrid.

Table 4
Properties of the Geogrid UX-1400

Property	Value	Unit
Initial Tensile Modulus	75,737	lb/ft

Long-Term Allowable Strength – MD
    in sand & silt
    in aggregate
	1,876
	 1,642
		lb/ft
		 lb/ft

Geogrid UX-750

The Geogrid Tensar UX-750 is a high-density polyethylene (HDPE) uniaxial geogrid with relatively low tensile modulus and strength. The geogrid was used to reinforce section 1, "weak geogrid-minimum spacing" reinforcement. The properties of the geogrid are shown in table 5. Unconfined-extension tests were performed on the geogrid and the results are shown in figure 15. The tests were performed on 8-in.-wide specimens (9 strands) with total length of 18.75 in. (3 units in the machine direction) at an extension rate 2.5 percent/min.

Table 5
Properties of the Geogrid UX-750SB

Property	Value	Unit
Aperture size:		
Machine Direction (MD)	6.00	inch
Cross-Machine Direction (CMD)	0.66	inch
Open Area	60	%
Thickness:		
Ribs	0.018	inch
Junction	0.072	inch
Ultimate Strength – MD	2,200	lb/ft
Tensile Modulus	27	Kips/ft
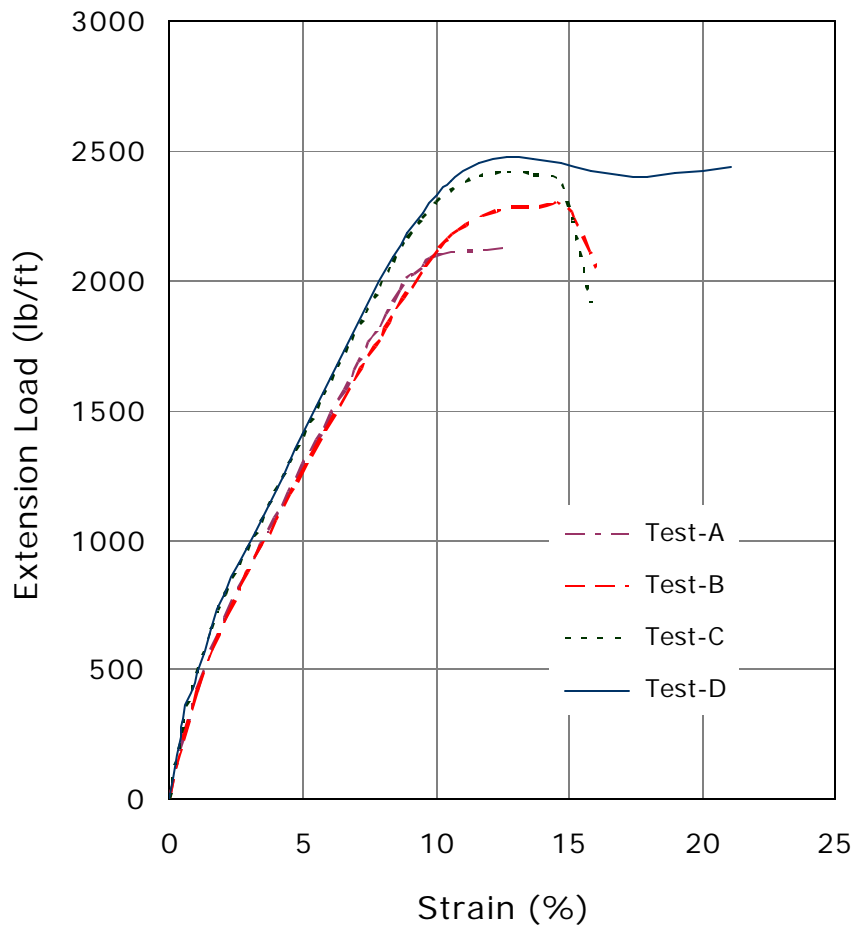
Figure 15
Wide-width strength tests on the UX-750 geogrid

Woven Geotextile

The woven geotextile used in reinforcing the slope side of the wall was Geotex 4x4. It is a polypropylene (PP) woven geotextiles manufactured by "Synthetic Industries". Table 6 shows the properties of the geotextile.

Table 6

Material properties of the woven geotextile

Property	Geotex 4x4	Units
Mass/unit area	13	oz/yd^3
Wide Width Strength- MD	4,800	lb/ft
Strength at 5% strain- MD	2,400	lb/ft

Non-Woven Geotextile

The non-woven geotextile used in the test slope was type "Evergreen TG700". It is a polypropylene (PP) fabric with mass/unit area of 8 oz./yd^3. Figure 16 shows results of extension tests on 8-in. wide and 20-in. long specimens.
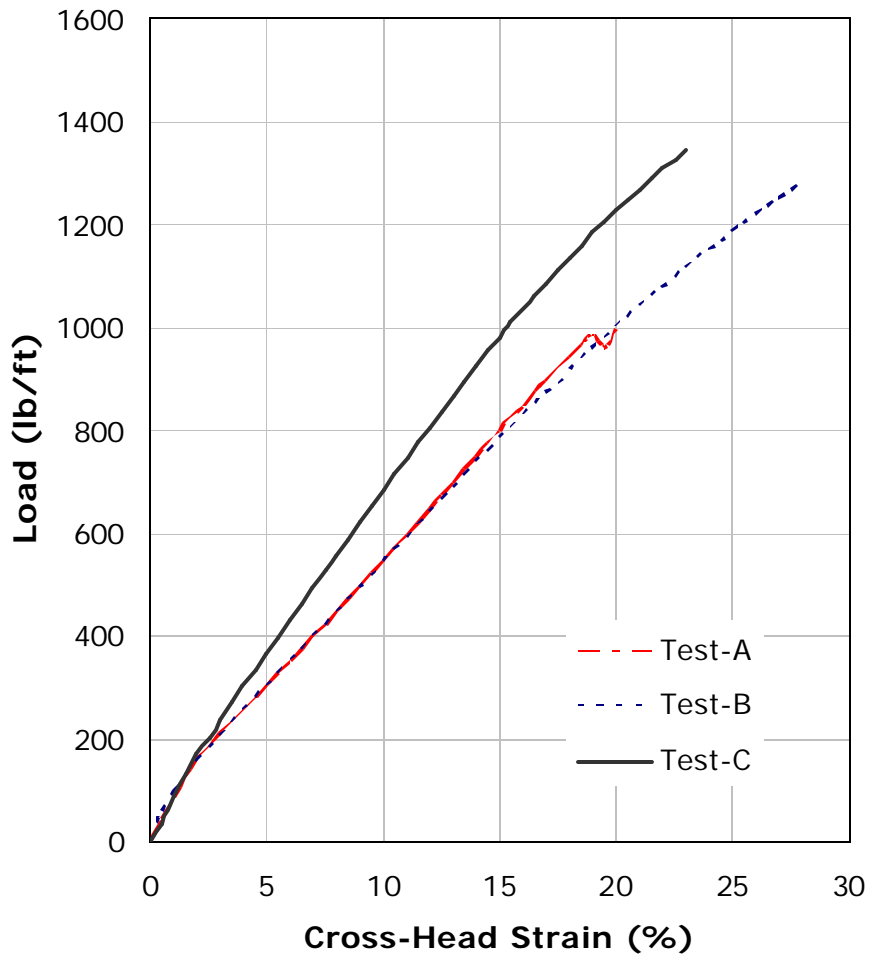
Figure 16
Extension tests on the non-woven geotextile TG-700

Construction of the Test Wall

The design of the wall was based on the following considerations:
- Drained soil condition for the cohesive soil with cohesion, c equals zero, and a drained friction angle ϕ of 25°.
- A surcharge load of 200 psf is assumed in the design for equipment loads during construction.
- The design for the external stability of the wall is based on standard safety factors against wall sliding, overturning, and bearing failures.
- The internal stability design of the wall considered factors of safety of unity for construction damage and material degradation. A safety factor of 3 was taken for creep load in the design of sections 1 and 2 in order to obtain measurable deformations.

The major steps of the construction of the test wall were:
- A of 2-ft.-thick stone base layer was compacted on the top of the foundation soil. A woven geotextile layer was placed as a separator between the stone base and the foundation soil. A drainage pipe was installed in the layer (figure 17). The stone base was reinforced with two layers of geogrid UX-1600 placed at the bottom and at mid-height of the stone base. Figure 18 shows the placement of the stone base on the top of the first geogrid layer.
- A leveling pad was constructed of plain concrete under the modular block facing (figure 19). The blocks were placed at a maximum height of two layers above soil level. Figure 20 shows the placement of the facing blocks.
- The facing blocks were filled with open graded stone for drainage. A geotextile fabric was placed as a separator between the stones and the compacted backfill.
- The soil was compacted at the optimum moisture content of 18 percent. Each soil lift was 8 in. high after compaction. Instrumentations (strain gauges, inclinometers, pressure cells, etc.) were placed according to the plans shown in the following sections.

24

Figure 17
Placement of the drainage pipe in the stone base layer

Figure 18
Placement of the stone layer on the top of the base reinforcement

Figure 19
Construction of the leveling pad of the block facing

- Pullout boxes replaced some of the facing blocks in section 3 of the wall (figure 21). Metal plates were connected to the geosynthetics specimens and extended through the boxes.

- The Geoweb cells were filled and compacted using the same type of backfill material. The cells near the facing were filled with open graded stone for drainage. Figure 22 shows the alignment of the cells during construction.

- A corrugated drainage pipe with a 5-ft. diameter was placed in the Geoweb section (figure 23) to evaluate the construction procedure and the applicability of using the Geoweb cells as wing walls around culverts.

- Woven and non-woven geotextiles were placed in the slope sections. The geotextiles were extended 2 ft. outside the slope facing to provide drainage and erosion control. Figure 24 shows the geotextile layers in the slope section during construction.

- At the completion of wall's construction, the slope section was treated with two different types of erosion control materials, standard DOTD mulch and sugar cane by-product mulch. Figure 24 shows the spraying of the sugar-cane mulch on the slope surface.

Test wall construction lasted four months. Figure 25 shows the construction time schedule of the soil layers. It took three months of construction time to complete the first half height of the wall (14 soil lifts) while the top half was built in one month. The slow construction period at the beginning was mainly due to the time needed to dry the soil, the dense instrumentation at the bottom half of the wall, and to the large volume of soil backfill at the bottom of the slopes.

Figure 20
Placement of the facing blocks with drainage stone layer

Figure 21
Installation of the pullout boxes in section 3 of the wall

Figure 22
Installation of the Geoweb cell in the section

Figure 23
The 5-ft. drainage pipe in the Geoweb section

Figure 24
Spraying of erosion control material on the slope surface
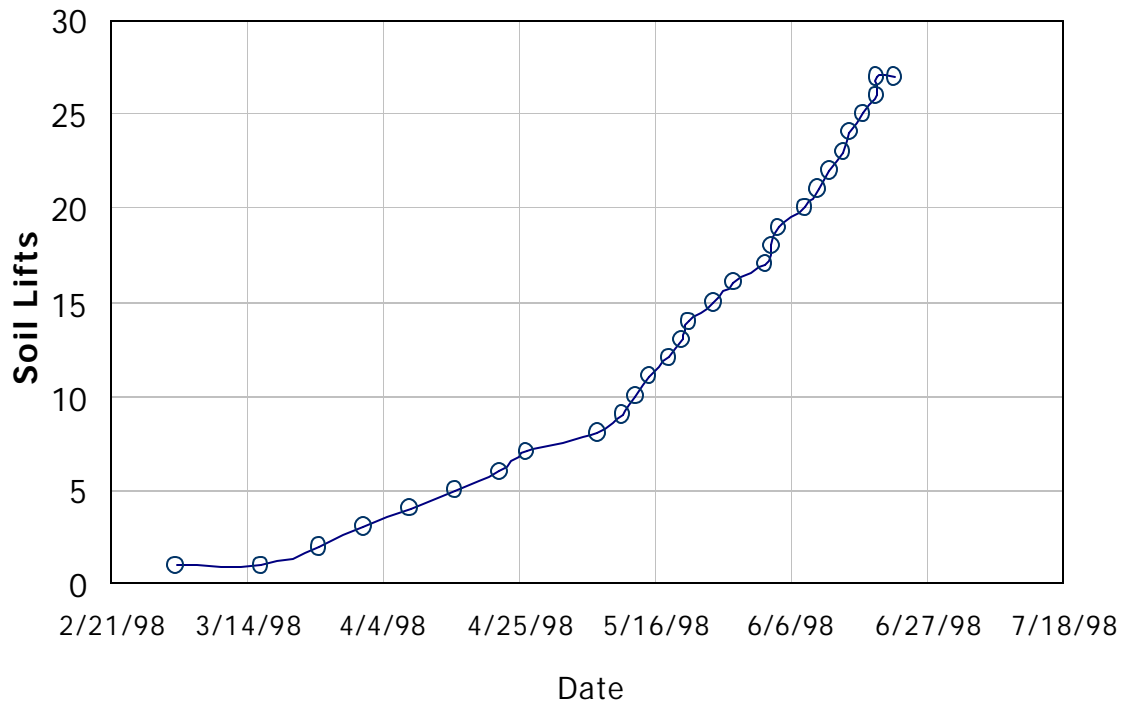
Figure 25
Construction of the test wall with time

<h1 style="text-align:center">Instrumentation of the Test Wall</h1>

A comprehensive literature review of instrumentation programs on reinforced-soil walls and slopes was performed. Appendix A presents a summary of the instrumented walls and slopes from the literature review. The review was used in planning the instrumentation program of the LTRC test wall, in evaluating the instrumentation suitability to monitor the response parameters, and providing guidelines for the selection of the appropriate instruments that meet the program objectives.

The instrumentation of the test wall consisted of the following measurements:

A. Deformation of base soil reinforcement, using strain gauges and vibrating wire (VW) extensometers.

B. Pore water pressure at foundation soil, using VW pressure transducers.

C. Wall settlement, using survey points, settlement plates, and horizontal inclinometers.

D. Horizontal wall deformation, using survey points and vertical inclinometers.

E. Earth pressure at wall facing and in the soil, using resistance type and VW earth pressure cells.

F. Strains in the reinforcement, using strain gauges and extensometers.

G. Temperature at the facing, using thermisters.

Installation of the Strain Gauges

This section presents the procedure used for installing and calibrating strain gauges on the geogrid and geotextile reinforcement of the test wall. The reinforcements of the wall varied in their polymer type (polyethylene (PE), polypropylene (PP) and polyester (PET)), surface texture, and geometry. Accordingly, strain gauge types, installation procedure, and calibration varied for each reinforcement type.

The objectives of strain gauge installation were to monitor the expected high strains (up to 5 percent) in the test sections of the wall and to monitor the long-term strains. The gauges

monitored the strains satisfactorily in both the geogrids and woven geotextiles. However, the installation procedure was not successful in the non-woven geotextile and the readings did not correlate to the measured strains in the lab for this type of geotextile.

Strain Gauge types

The strain gauges used in the test wall were Micro-Measurement (MM) type produced by "Measurements Group." The selection of the gauge types was based on several manufacturers' recommendations for large strain measurements [*4*], [*5*]. For such measurements (about 5 percent strains), an annealed constantan grid material was selected (EP type). It should be noted that this alloy might exhibit some permanent resistance after loading, which makes it unsuitable for cyclic type loading. The constantan alloy was supplied in a self-temperature compensated form (S-T-C) in order to match the thermal expansion coefficient of the material tested. A high S-T-C number of 40 were recommended in the manufacturer's literature for use with plastics [*5*]. The gauges were supplied in polyimide packing to provide the large elongation capability. The length of the gauges varied from 0.25 inches to 2 inches. The relatively longer gauges were easier to handle and to install, and they provided a better heat dissipation. The width of the rib dictated the dimension of the strain gauges in the geogrid. Gauges 0.125 inches wide were used in the geogrid while larger sizes were used in the geotextiles. Table 7 lists the types of strain gauges used in the test wall.

Table 7
List of strain gauges used in the geosynthetics instrumentation

Gauge type	Length (inch)	*Width* (inch)	Resistance (ohms)	Application
EP-08-250BG-120	0.25	0.125	120	(HDPE grid) UX-750
EP-40-250BF-350-L	0.25	0.125	350	UX-1400, UX-1500, and UX1600
EP-08-10CBE-120	1.0	0.25	120	Woven geotextiles
EP-08-20CBW-120	2.0	0.188	120	Strata-500 (PET geogrid)

Surface Preparation

Surface preparation for gauge installation was modified from the manufacturer's technical notes [*6*]. For the smooth and glossy surface of the geogrid, the surface was roughened with

32

sand paper (150-250 grit). Mild surface roughness was applied in diagonal directions to create a rough cross-hatching pattern for maximum bonding with the adhesive. The surface was cleaned with Methyl Alcohol using gauze sponges for removal of dirt contaminants and residue from abrasion. A mild phosphoric acid conditioner for cleaning was applied to remove oxides (MM Conditioner A). An ammonia-based liquid was then applied to neutralize the surface (MM Neutralizer 5A). A more aggressive technique using sulfuric acid in surface preparation was recommended for plastic materials. However, when tried on the woven fabric, this procedure did not prove to yield better adhesion.

Gauges Installation

Bondable terminals were installed 1/16 in. from the gauges. Flexible jumper wires were used as lead wires and the bondable terminals used were type MM CPF-75C. For the HDPE geogrid and the PP geotextiles, which do not absorb water, a two-component epoxy adhesive was used (M-Bond A-15). This adhesive is transparent with medium viscosity and has elongation capability of 15 percent at room temperature. The components were mixed to the recommended manufacturer's ratio (10 parts by weight of the "AE Resin" to 0.8 parts of the "Curing Agent 15"). The adhesive was thoroughly mixed for five minutes and then allowed to stand for additional five minutes before being applied to the surface. The gauges were placed on the adhesive and were clamped to the geogrid specimen during curing. Figure 26 shows the installation of the gauge on the geogrid.

The adhesive required a minimum curing time of six hours at elevated temperature of 125°F. Heat lamps were placed on top of the strain gauges in order to produce the curing temperature, which was measured by thermometers at the surface of the gauge. Figure 27 shows the curing of the instrumented geogrid in the lab.
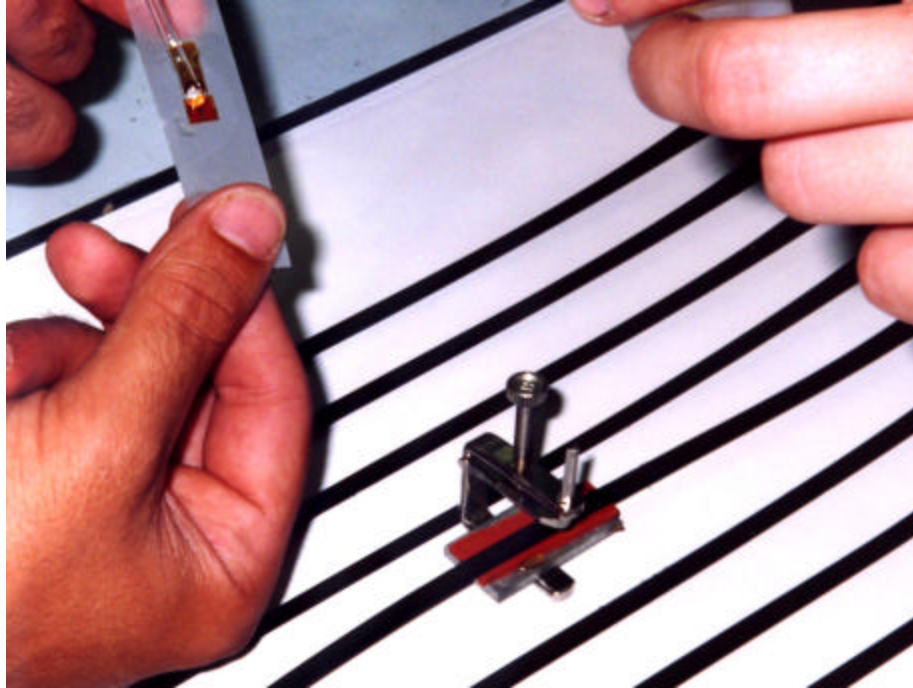
Figure 26
Installation of the strain gauge on the geogrid

For the woven geotextiles and polyester-coated geogrids, another adhesive type (M-Bond A-12) was used. This adhesive had similar elongation capabilities. However, it was more easily absorbed through the fabric, which produced better moisture insulation. The A-12 adhesive has two components, which were mixed to a ratio of two-to-three. The mix was blended with a spatula to a uniform color (figure 28). Dead weights were placed on the gauges to produce a uniform pressure and the gauges were cured for six hours at a temperature of 120°F. Figure 29 shows the installation of the gauge on the woven geotextile.

Figure 27
Curing the gauges at elevated temperature

Figure 28
Preparation of the A-12 adhesive of the woven geotextile

Figure 29
Installation of the gauges on the woven geotextile

Coating for Field Conditions

A resin solvent was applied on the gauges in order to remove soldering flux and to provide a clean surface. The procedure for coating the gauges was as follows.

- A Teflon film layer was placed on the gauges. The gauges and lead wires were coated with a layer of RTV silicon rubber. A non-corrosive type of 'Measurements Group' RTV 3145 was used. The coating was cured at elevated temperature for 24 hours.
- A layer of aluminum foil was placed around the coating.
- A layer of M-Coat FBT is placed on the gauge. M-Coat FBT is a butyl rubber compound, which forms an effective sealant to moisture without restricting the flexibility of the system. Figure 30 shows the coated strain gauge in the woven geotextile specimen.
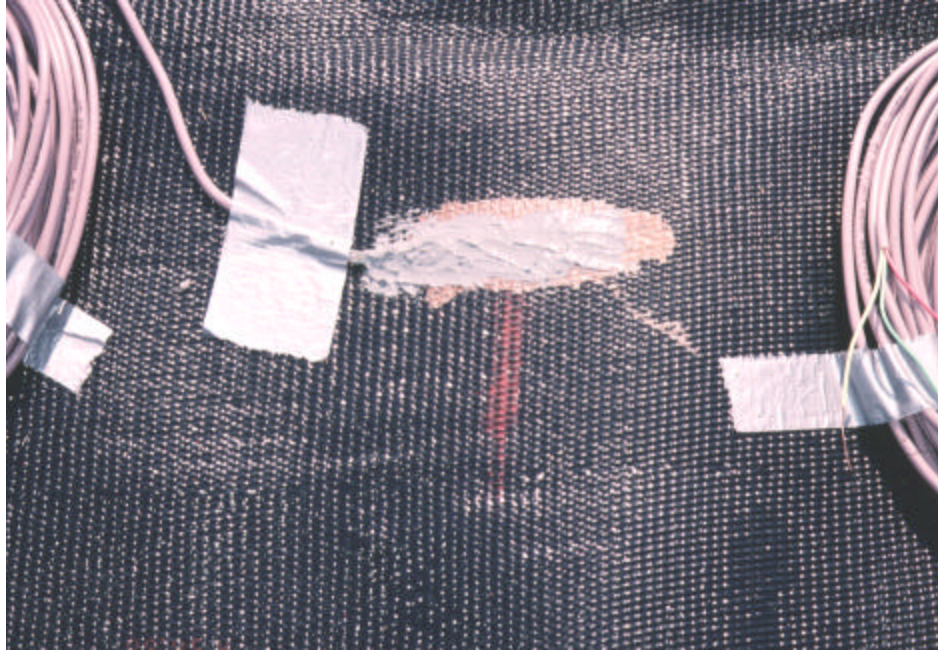
Figure 30
The coated strain gauge in the woven geotextile

Calibration of Strain Gauges

The installation of strain gauges on the geosynthetics material causes the specimen to stiffen at the location of the gauge. Proper selection of adhesive and coating materials may reduce this effect and result in a more flexible system that closely resembles the un-reinforced part of the specimen. However, strain gauges measure the local strains at the location of the gauge. This measurement may differ from the overall strain along the section where strain measurement is desired. Accordingly, calibration of the gauge measurements is necessary in order to correlate gauge readings to the actual strain along the specimen section.

Calibration was performed on instrumented specimens in unconfined extension tests. Extensometers were placed on the specimen and the gauge readings were correlated to machine travel and to the extensometers readings. Figures 31 and 32 show the instrumented geogrid and geotextile specimens during the extension test, respectively.

The results of calibration tests of the various types of reinforcement are shown in Figures 33 to 36. The tests resulted in calibration factors of 0.8 for the UX-750, 0.85 for the UX-1500 and UX-1600, 0.75 for the Strata-500, and 0.8 for the woven geotextile. The lowest calibration factor of about 0.1 was obtained on the non-woven geotextile. The results were not repeatable. Accordingly, no strain gauges were installed in the non-woven geotextile in the slope section.
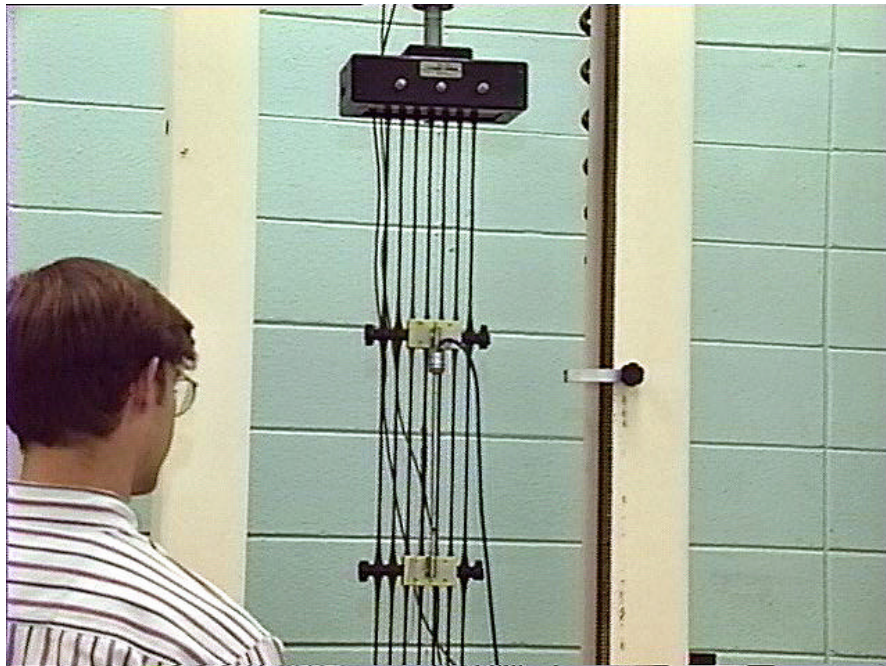
Figure 31
Strain measurement of the geogrid specimen in the lab
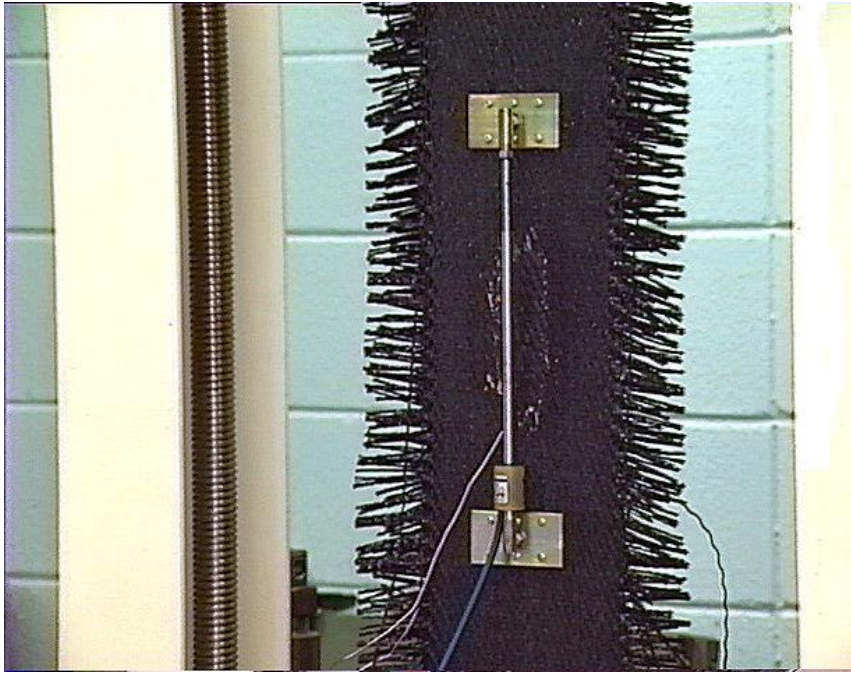
Figure 32
Measurement of strain of the woven geotextile specimen
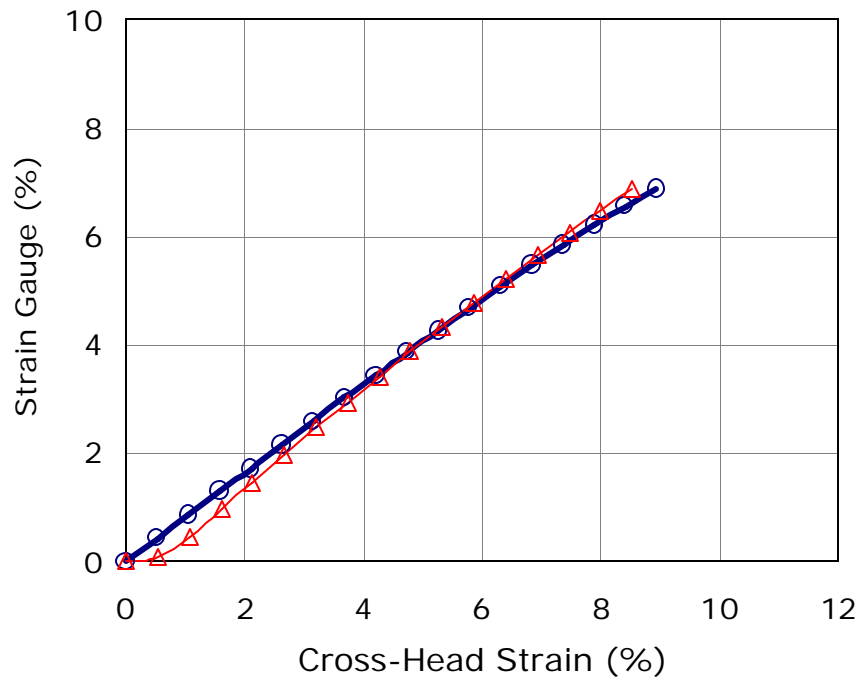
Figure 33
Results of strain calibration in geogrid UX-750
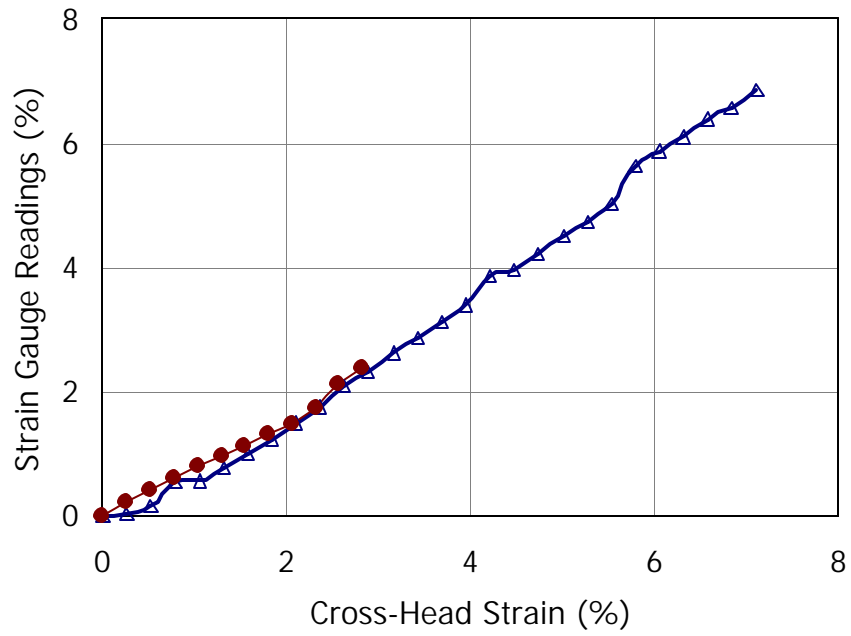
Figure 34
Results of strain calibration in geogrid UX-1500
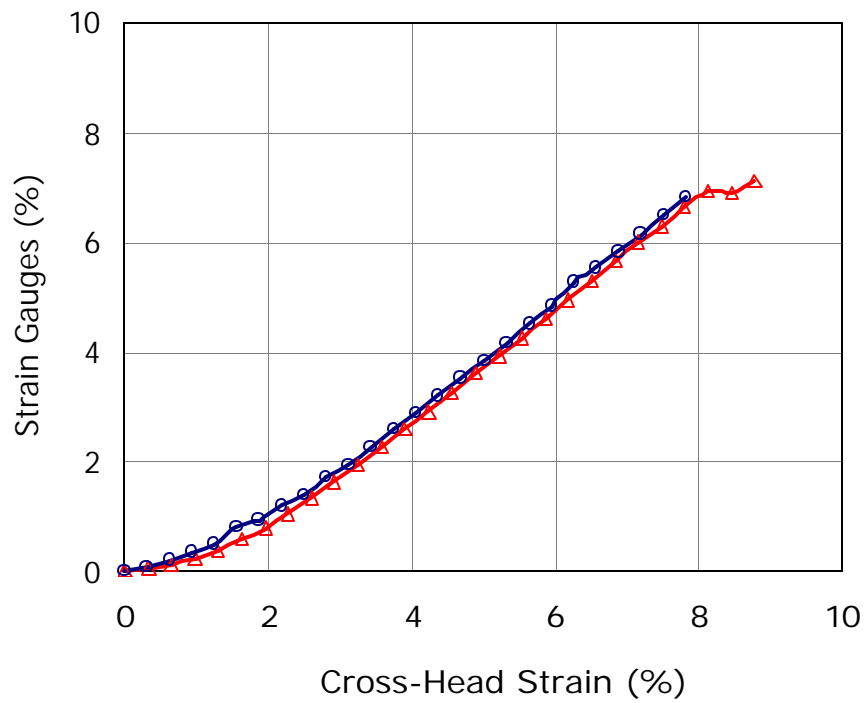
Figure 35
Results of strain calibration in woven geotextile

40
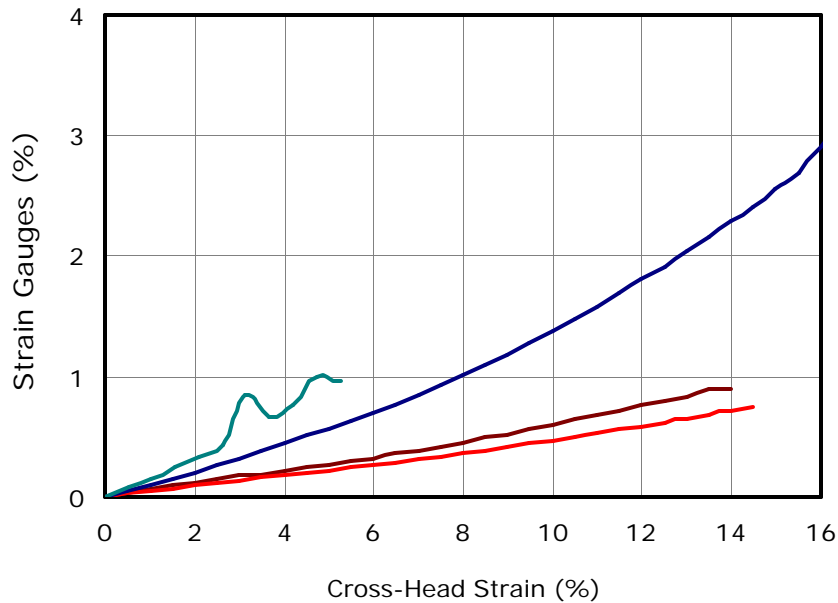
Figure 36
Results of strain calibration in non-woven geotextile

Instrumentation of Base Soil Reinforcement

Type MM EP-40-250BF-350 strain gauges were installed in the top geogrid UX-1600 layer of the stone base. Figure 37 shows a schematic of the configuration of the strain gauges in the geogrid layer.

Rod extensometers were installed at various locations on the geogrid. The rods were placed inside plastic pipes and were extended outside the wall to monitor their movement. Figure 38 shows a view of the instruments in the base reinforcement.

Vibrating wire (VW) extensometers model "Geokon 4420-X" of 2-inch extension were also mounted on the cross ribs in order to measure the elongation of the longitudinal ribs. Measurements of the rod extensometers and the VW extensometers did not show consistent readings and many of them did not respond at later stages of wall construction. Most of the extensometer failures could be due to wall settlement, which resulted in large deformations in the extensometer pipes. These deformations consequently restrained the movement of the extensometer rods.
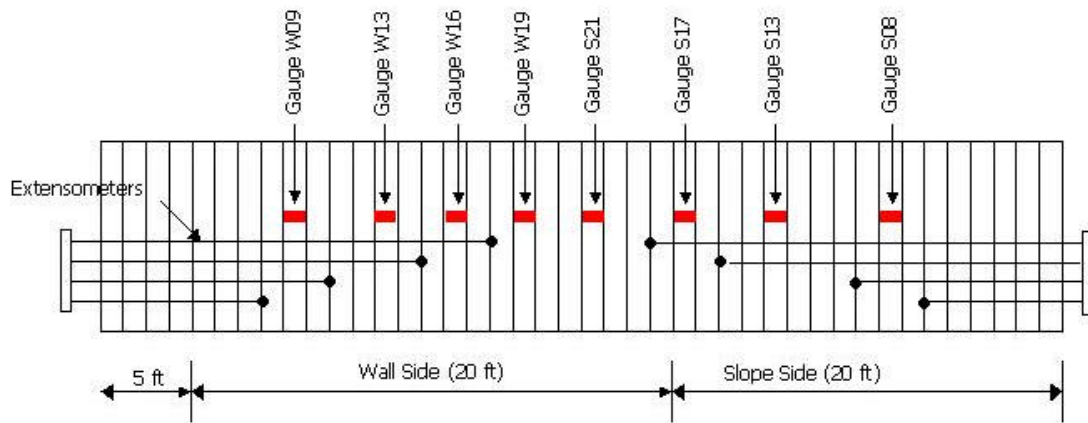
Figure 37
Locations of strain gauges and extensometers in the base reinforcement

Figure 38
View of the instrumentation at the base reinforcement

Instrumentation for Pore-Pressure Measurements

Vibrating wire piezometers were installed in two locations under the centerline of the wall. The piezometers were "Geokon" model 4500 with 50-psi pressure range. Figure 39 shows the VW piezometer in a lab test. This type of transducer allows for measurements of negative pore pressures in case the soil was initially partially saturated. However, both piezometers were installed in the saturated zone.

The piezometers were installed at 6 ft. and 12 ft. below ground level to monitor the development of pore-water pressure during and after the construction of the wall. The transducers were placed in sand bags in the holes in order to allow for water flow, and the holes were cement-grouted to ground level. Figure 40 shows the drilling process for the installation of the transducers.

The ground water level was monitored in an open well at the test site and the results did not show significant changes during the four-month period of wall construction.
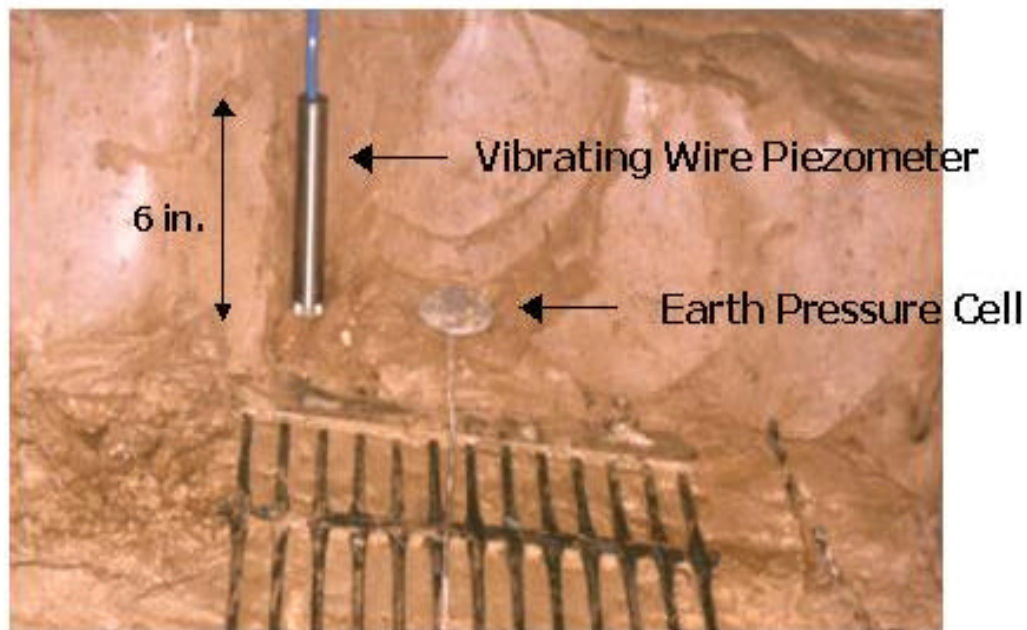
Figure 39
View of the VW piezometer in a lab test

Figure 40
The drilling equipment for installing of the pore-pressure transducers

Instrumentation for Wall Settlement

The vertical movement of the wall due to the settlement of the soft foundation soil was monitored during and after construction. The monitoring procedure included the measurements of the elevations at the base of the wall, elevations of settlement plates installed at the wall base, and measurements of horizontal inclinometers. Figure 41 shows the locations of these instruments.

Survey of the Wall Facing

The vertical movement of the wall facing was monitored by surveying the elevations of several points at the leveling pad at the base of the vertical wall.

Settlement Plates

Fours settlement plates (A to D) were installed at the top of the stone base layer. Figure 42 shows a view of the settlement plates during the construction of the base layer. The vertical rods were placed inside steel pipes that extended to the top elevation of the wall in order to allow the movement of the rods and measuring the levels of the rods at the top of the wall.
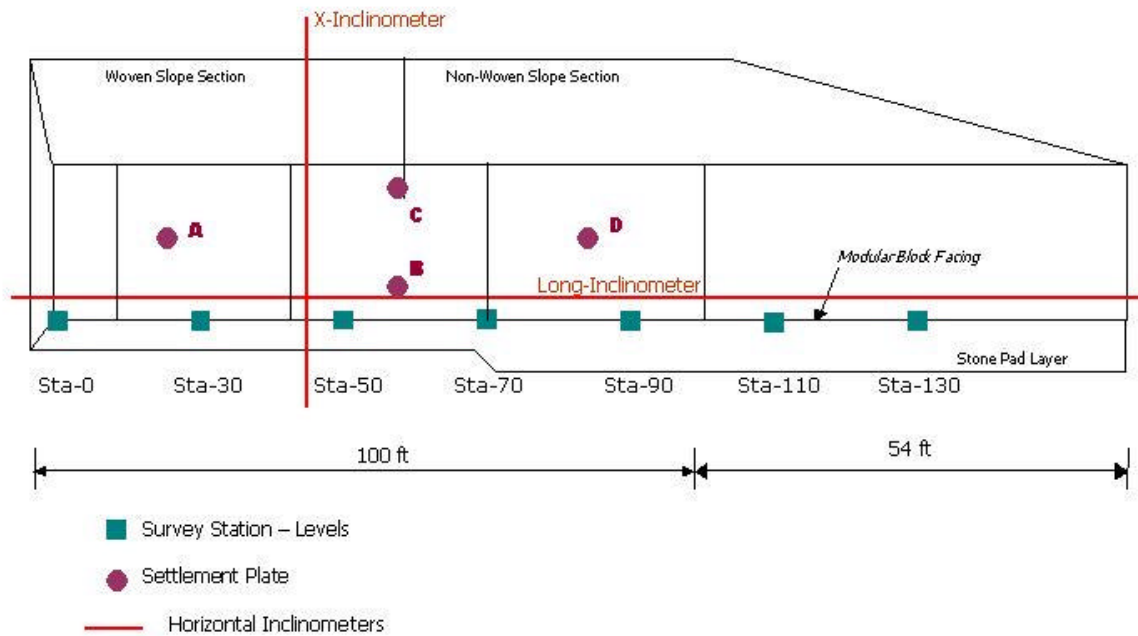
Figure 41
Schematic of the instruments used in monitoring wall settlement

Figure 42
Installation of the settlement plates on the base layer

Horizontal Inclinometers

Two horizontal inclinometers pipes were placed in the stone base layer to monitor wall settlement in the longitudinal and cross directions. The longitudinal inclinometer was placed near the front wall facing (see figure 45) to monitor the settlement near the vertical side of the wall. The locations of the inclinometers are shown in figure 43.

Figure 43
Location of the longitudinal inclinometer pipe near the front leveling pad

Horizontal Deformation of Wall

The horizontal deformations of the vertical side of the wall were monitored by survey points located at various locations in the modular block facing. The horizontal movement of the facing at each section of the wall was also measured using vertical inclinometers placed at a distance of 1 to 2 ft. behind the modular block facing. Figure 44 shows a schematic of the locations of the survey points and the vertical inclinometers.
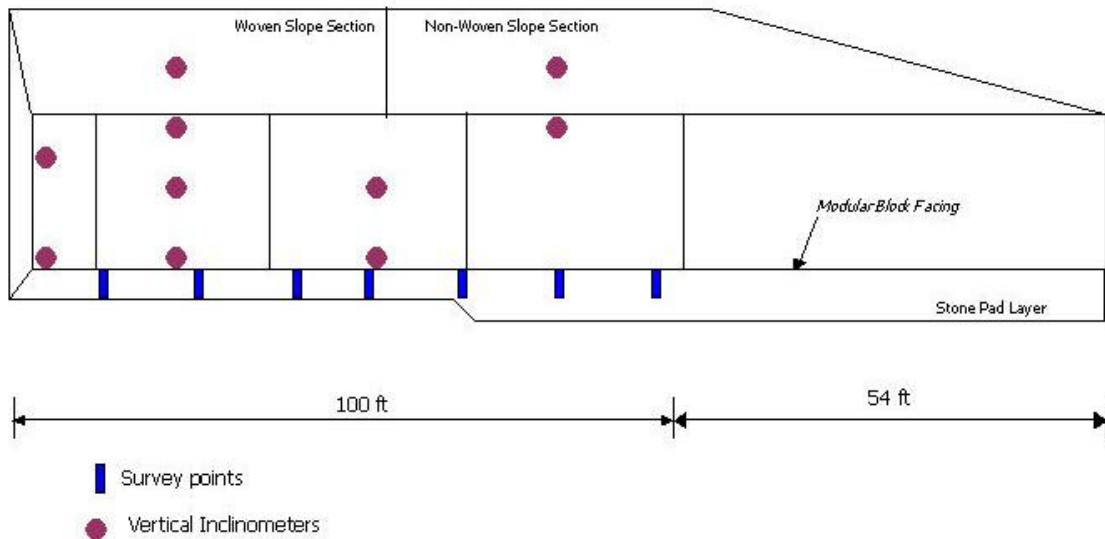
Figure 44
Schematic of the instruments for monitoring horizontal deformations

Survey Points

The survey points consisted of measuring tapes placed at various locations in three elevations of the vertical wall facing. Figure 45 shows the measuring tapes installed in the block facing. The tapes were monitored from a fixed reference point in order to determine the horizontal movement of the wall. Figure 46 shows a side view of the wall facing and the reference point. The locations of the survey points are shown in table 8, and figure 47 shows a schematic of the measuring points at each level.

Figure 45
The measuring tapes installed at the wall facing

Figure 46
View of the measurements on the wall facing

Table 8
Locations of the measuring tapes at each wall layer

Layer	Layer No.	Height (ft)
A	4	2.7
B	14	9.3
C	24	16.0
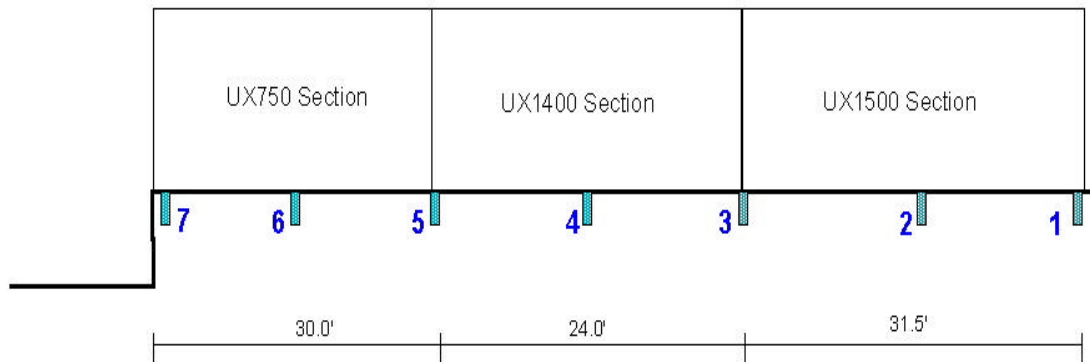
Figure 47
Schematic of locations of survey points for measuring horizontal movement

Vertical inclinometers

Vertical inclinometers were placed in sections 1 and 2 of the vertical wall, in the Geoweb section, and in the two slope sections. In each of the wall sections, a front inclinometer was placed behind the block facings and a second inclinometer was placed behind the reinforcement at a distance of 11 ft from the facing. In the slope sections, one inclinometer was placed at the top of the slope and another one was placed at mid-height of the slope. Figure 48 shows the vertical inclinometers near the wall facing during construction.

Figure 48
The vertical inclinometer pipes during construction

Measurements of Earth Pressure

Earth pressure cells were installed in various locations near the vertical wall facing to monitor the development of vertical and horizontal earth pressures during construction. Two cells were also placed horizontally under the facing blocks in order to monitor the loads induced from the blocks on the leveling pad. The locations of cells are shown in figures 49 and 50.

Vibrating wire and resistance type gauges of various diameters were used in the instrumentation program. Table 9 shows a list of the cells. The pressure cells were installed by digging the soil after compaction and placing the cells in the vertical and horizontal positions. Sand was placed around the cells and was manually compacted. Figure 51 shows the placement of the pressure cells near the facing of the wall.

Table 9
Locations of the earth pressure cells

Cell No.	Type	Wall Section	Position	Location	Layer
VW-684 VW-685	9-inch Vibrating Wire cells 0-25 psi	Compact Block– UX750 Standard Block-UX1400	Horizontal	Under blocks	0
247 248	6-inch resistance type 0-30 psi	Compact Block– UX750 Standard Block-UX1400	Vertical	Near the facing	0
212 213	6-inch resistance type 0-30 psi	Standard Block-UX1400 Standard Block-UX1400	Vertical Horizontal	Near the facing	5
214 215	6-inch resistance type 0-30 psi	Standard Block-UX1500 Standard Block-UX1500	Vertical Horizontal	Near pullout specimen	17
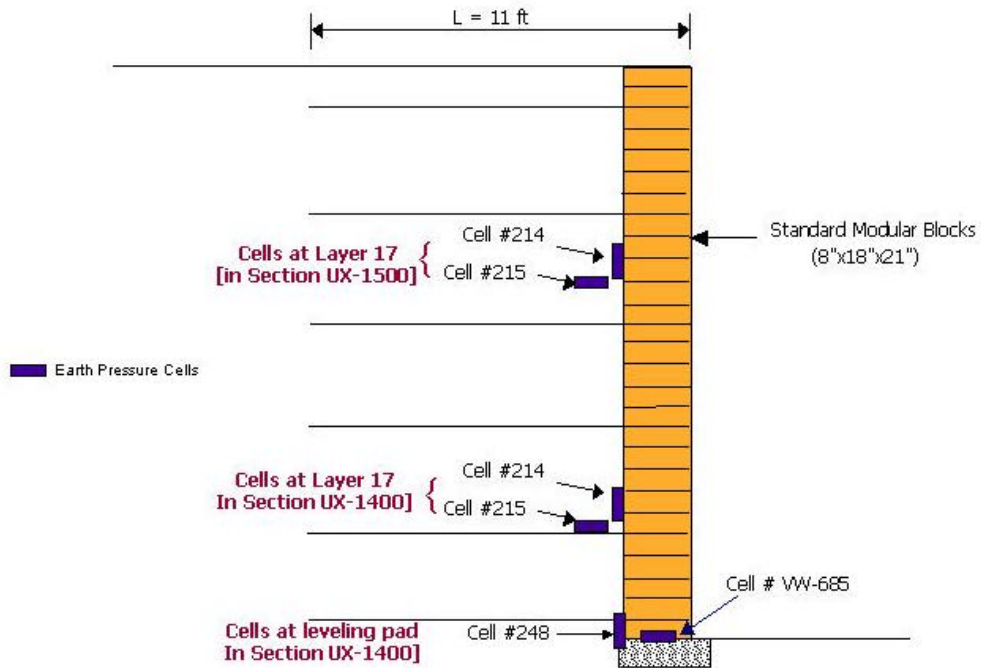
Figure 49
Locations of the pressure cells in the standard block sections
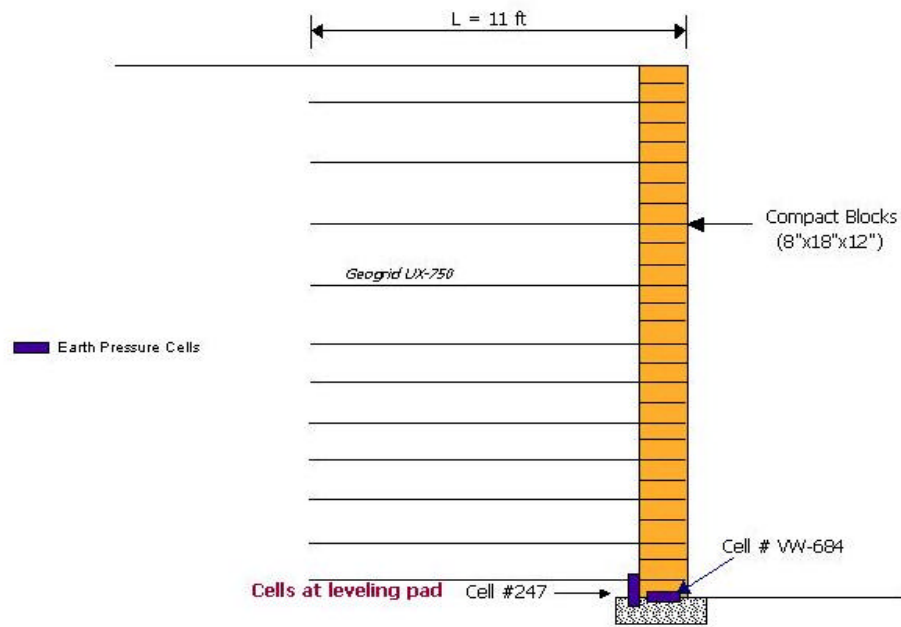
Figure 50
Locations of the pressure cells in the compact block section

Figure 51
Installation of earth pressure cells near the wall facing

Measurements of Reinforcement Strains

Wall Section 1 (Weak Geogrid- Minimum Spacing)

This wall section was reinforced with geogrid Tensar UX-750. Refer to the construction section for details of the test section and the properties of the geogrid. The strains in the reinforcement were measured using strain gauges installed along the reinforcement. Table 10 shows the locations of the strain gauges at each layer. In the table, the gauges are identified by the layer level and the longitudinal rib number where they were installed. The longitudinal ribs of this geogrid were about 6 in. in length and the reinforcement had about 21 strands with the first one practically between the front facing blocks.

Figure 52 shows a schematic of the locations of the strain gauges in each layer and figure 53 shows the instrumented section of the geogrid layer in the wall. The gauges were closely arranged near the facing blocks at the bottom part of the wall. They were more widely spaced far from the facing at the upper part in order to capture the anticipated maximum strains along the height of the wall. Similar configurations of the strain gauges were followed in the other sections of the wall.

Wall Section 2 (Strong Geogrid- Maximum Spacing)

The section was reinforced with geogrid Tensar UX-1400. The distribution of strain gauges is shown in figure 54. Table 11 shows the locations of the strain gauges in each layer of the section.

The gauges in the table are identified by the level of the layer and the rib number where they were installed. The length of the geogrid ribs is about 13.75 in. and, accordingly, the number of the gauge is an approximate figure of its distance from the facing. Two sets of strain gauges were installed in two sections in layer F to evaluate the repeatability of the measurements.

Table 10
Locations of strain gauges in wall section 1

Wall Layer	Locations of the strain Gauges
A	A-2, A4, A-6, A-9, A-12
B	B-1, B-2, B-4, B-6, B-9, B-12
D	D-1, D-2, D-4, D-6, D-9, D12
E	E-3, E-5, E-7, E-13
F	F-2, F-5, F-8
G	G-3, G-6, G-9, G-12, G-15
H	H-3, H-6, H-12, H-15
I	I-5, I-8, I-11, I-14
K	K-3, K-5, K-7, K-9, K-12, K-15
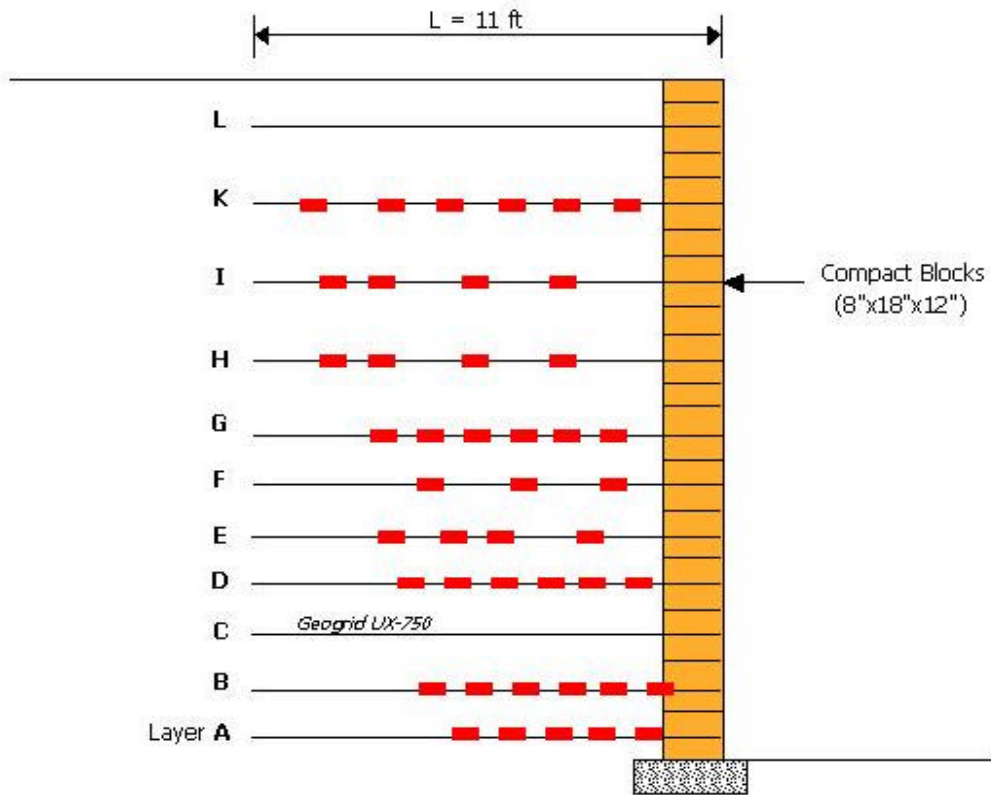
Figure 52
Schematic of the locations of strain gauges in the UX-750

Figure 53
The instrumented section of the UX-750 geogrid in the wall

Table 11
Locations of strain gauges in wall section 2

Wall Layer	Locations of the strain Gauges
A	A-2, A3, A-4, A-6
B	B-1, B-2, B-3, B-6
C	C-1, C-2, C-3, C-6, C-8
D	D-3, D-4, D-6
E	E-1, E-2, E-3, E-7
F	F-3A, F-3B, F-4, F-5A, F-5B, F-7, F-9
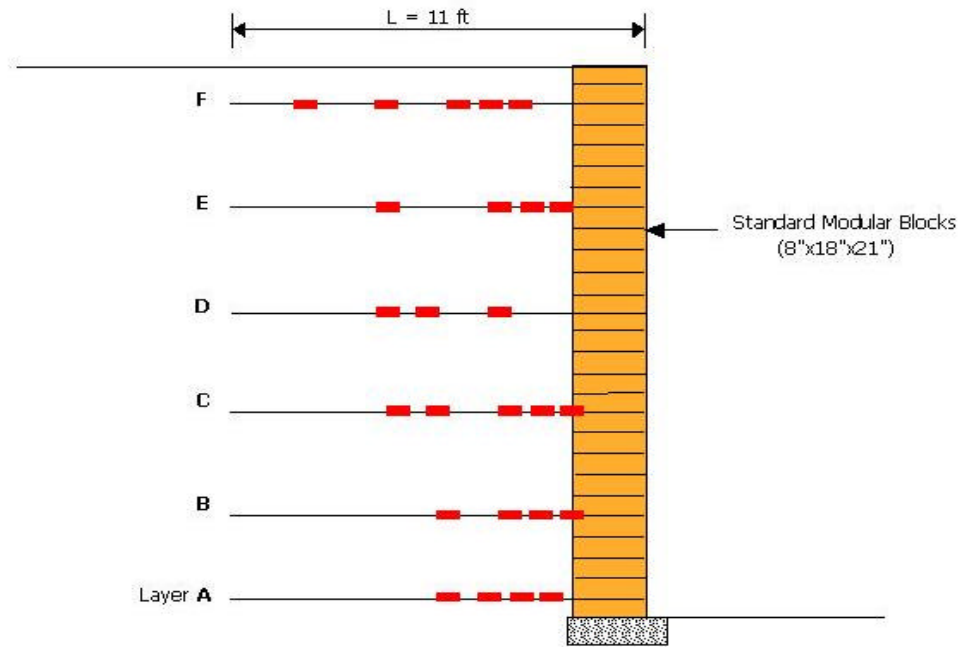
Figure 54
Schematic of the locations of strain gauges in the UX-1400

Wall Section 3 (Standard Section)

Section 3 of the test wall was constructed with geogrid Tensar UX-1500. The vertical spacing of the geogrid was set to accommodate the field pullout specimens. The locations of the strain gauges are shown in figure 55 and a list of the gauges is shown in table 12.

Table 12
Locations of strain gauges in wall section 3

Wall Layer	Locations of the strain Gauges
A	A-2, A-2, A3, A-4
B	B-1, B-2, B-3, B-7
C	C-1, C-2, C-3, C-5, C-7
E	E-1, E-2, E-3, E-7
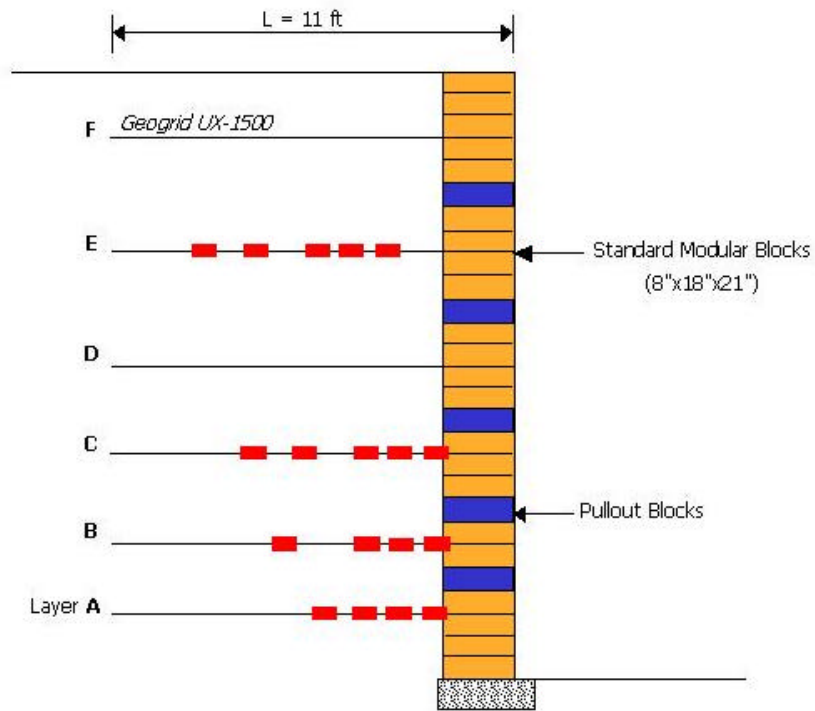
Figure 55
Schematic of the locations of strain gauges in the UX-1500

Woven Slope Section

Strain gauges were installed on the woven geotextiles in the slope section. The locations of the gauges are shown in figure 56. The numbers of the gauges indicate their distance from the slope facing in feet. Figure 57 shows the installation of the gauges in the woven geotextile.
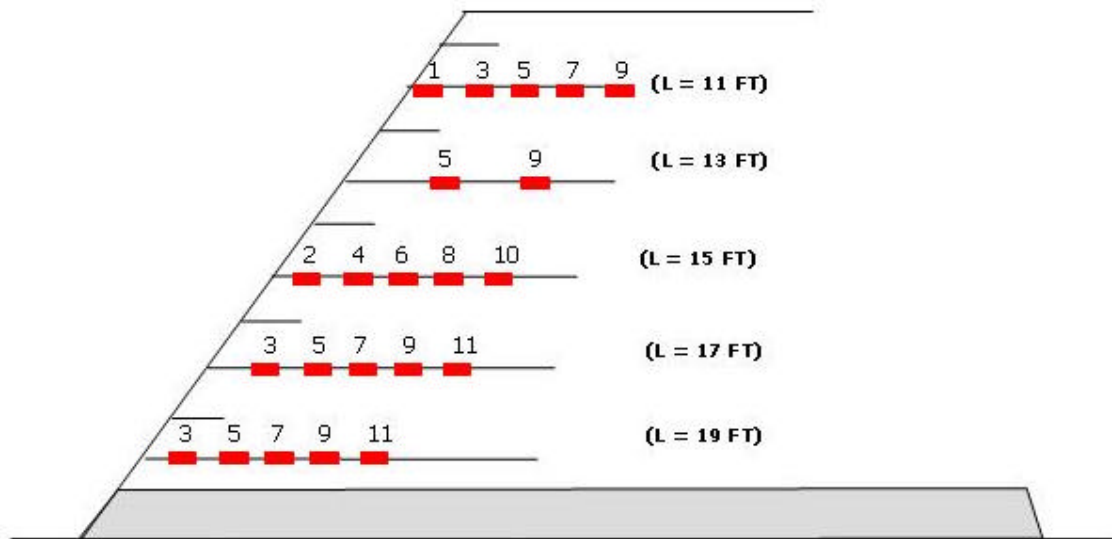
Figure 56
Locations of the strain gauges in the woven geotextile

Figure 57
Installation of the gauges in the woven geotextile

DISCUSSION

Instrumentation Measurements

Base Soil Reinforcement

Strain measurements along the geogrid UX-1600 at the base of the wall are shown in figures 58 and 59. The figures show the development of geogrid strains during the construction of the vertical wall side and slope side, respectively. Refer to figure 37 for the locations of the strain gauges along the geogrid. The results show an increase in strain of about 1.2 percent at the wall side and 2.5 percent at the slope side.

The distribution of strains along the wall cross-section is shown in figure 60. The lower strain values at the end of construction indicate strain relaxation, possibly due to wall settlement and redistribution of strains along the base reinforcement. The figure also shows that the maximum strains did not occur at the center of the wall, but rather suggests the locations of the slip circles in both sides of the wall as shown in figure 61.
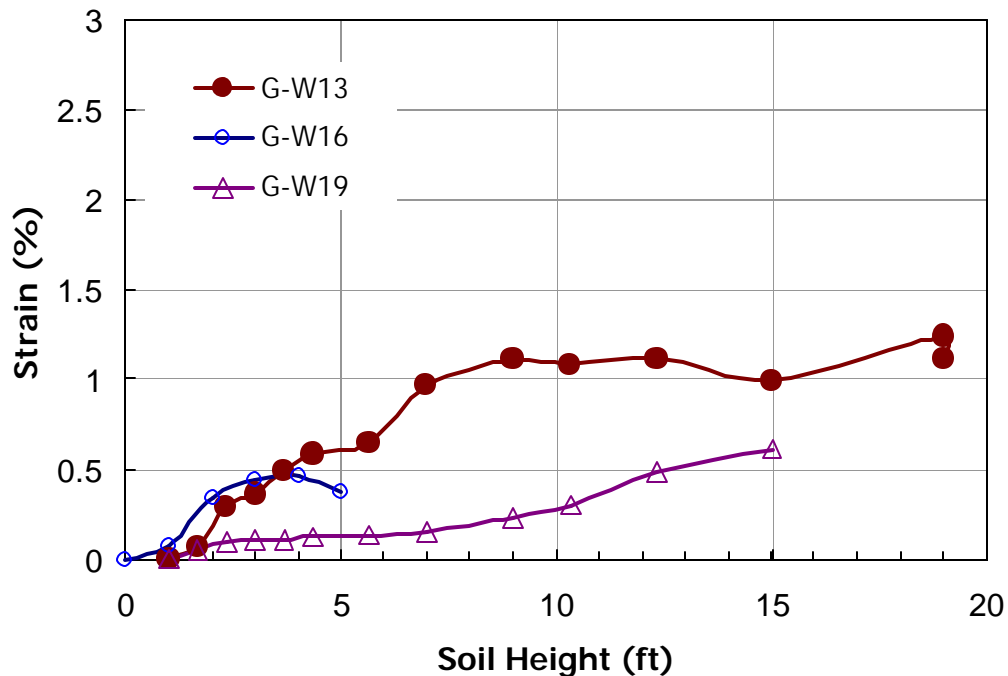
Figure 58
Strain measurements during construction of the vertical wall side
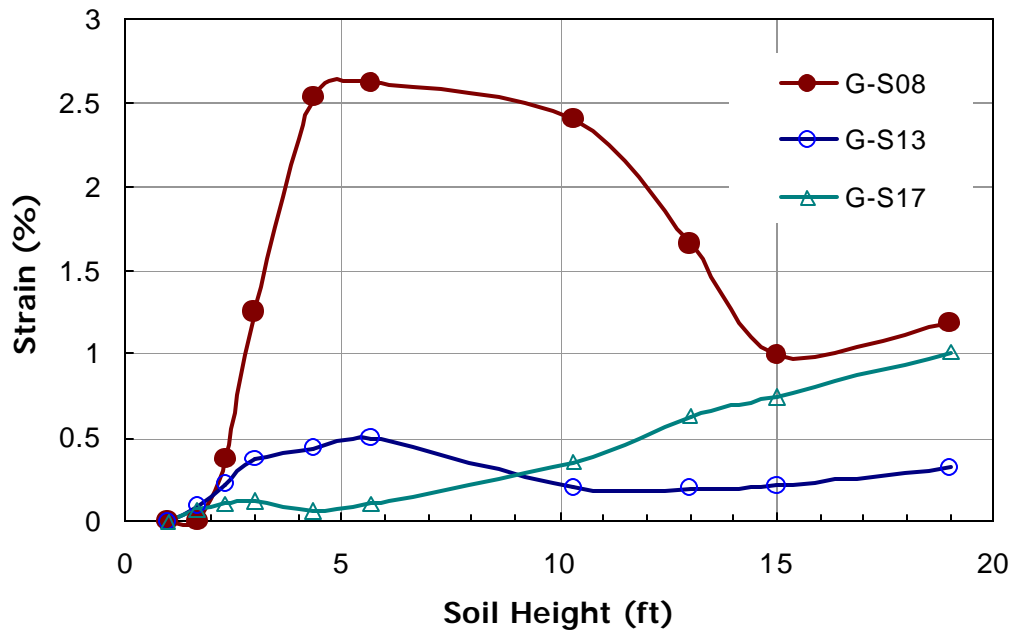
Figure 59
Strain measurements during construction of the slope side
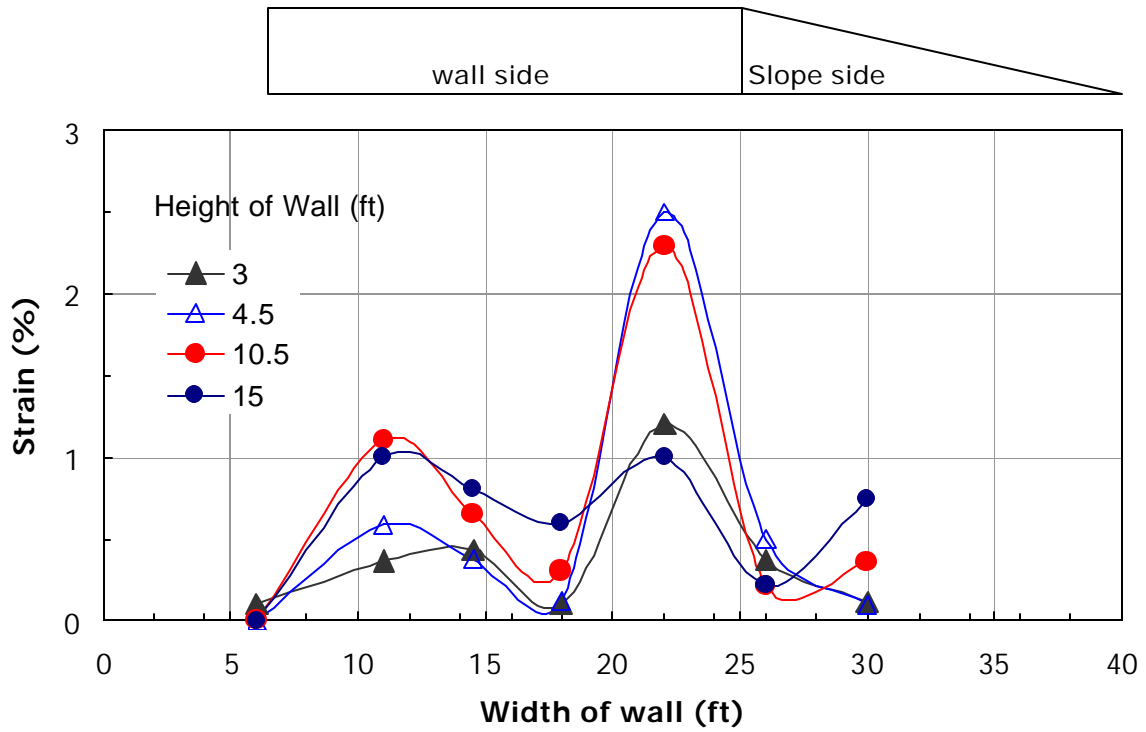
Figure 60
Strain distribution along the wall cross-section
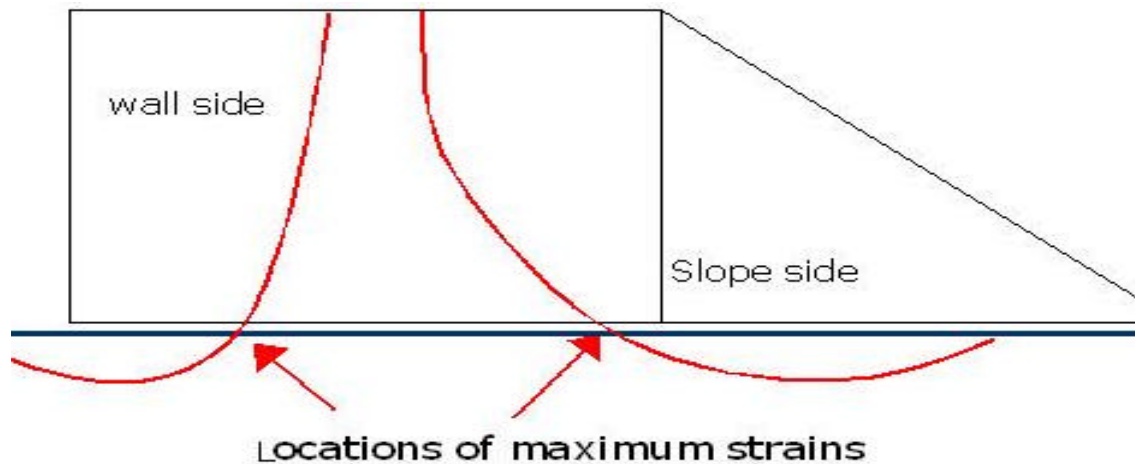
Figure 61
Prediction of the locations of slip circles from strain measurements

Measurements for Pore-Pressure during Construction

The duration of the test wall construction was about four months. With the exception of the first month, little rainfall occurred during construction, and the ground water level did not significantly change. The relatively long period of construction allowed for partial dissipation of the pore water pressure. The measurements, however, showed an increase in pore water pressure at the late stages of construction. This stage was characterized by faster construction activities of about one soil layer per day. Refer to figure 25 for the display of construction activity with time. Figure 62 shows the measurements of pore water pressure during and after construction. The change of pore pressure with respect to the total earth pressure above the piezometers is shown in figure 63.
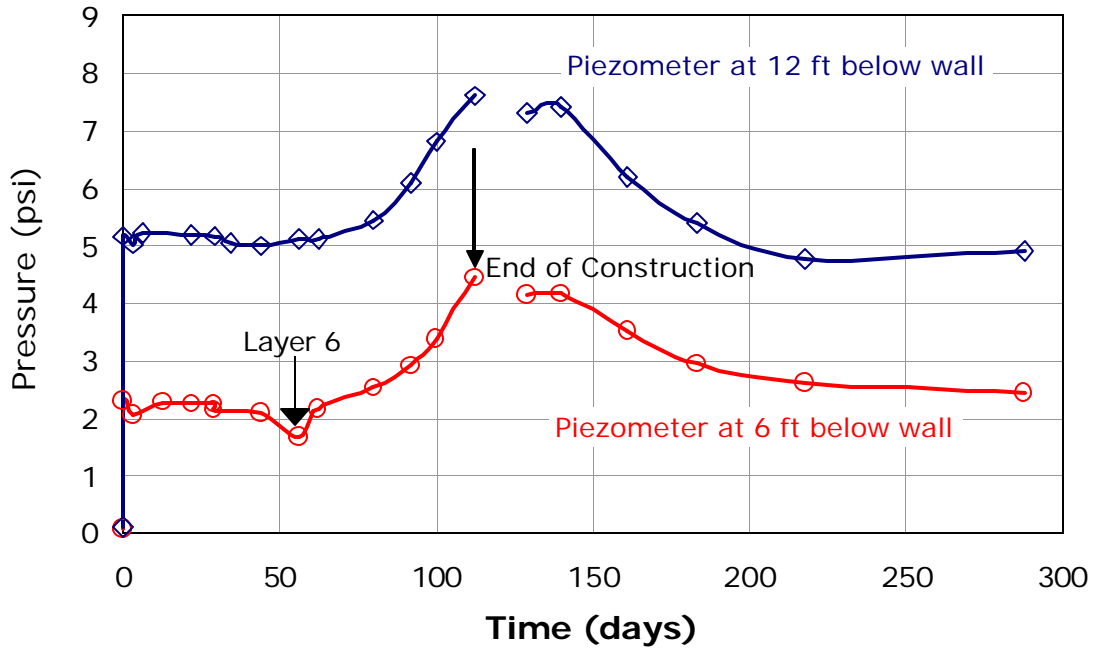
Figure 62
Piezometer readings during construction
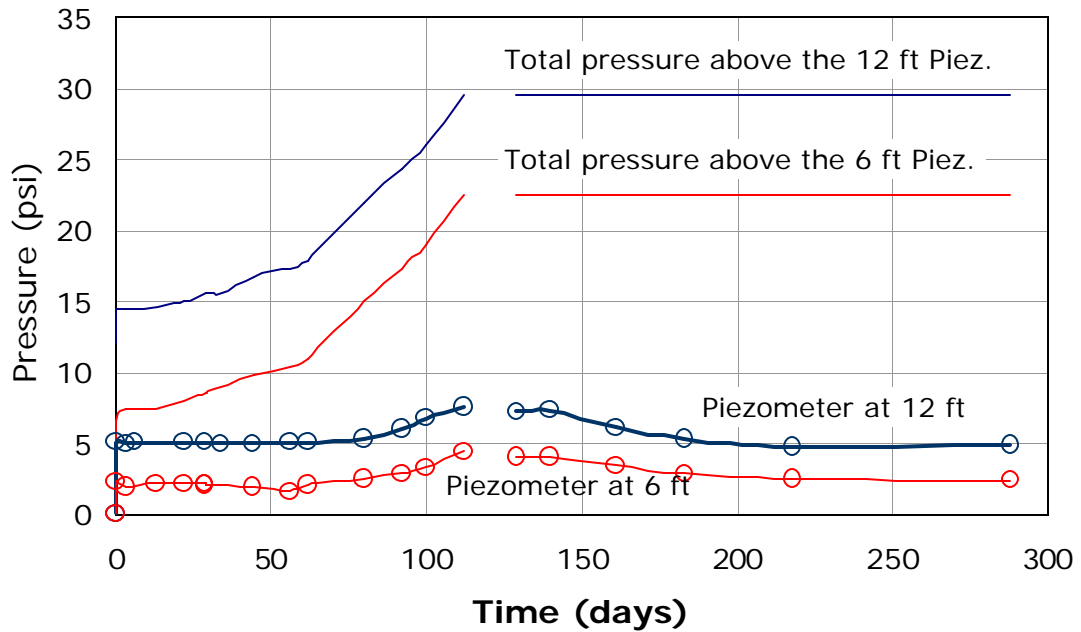
Figure 63
Development of total pressure and pore pressure during construction

In general, at each construction stage, pore water pressure dissipates until another layer is added to the wall. In order to monitor pore pressure dissipation after adding a new soil lift, measurements were taken during the six hours after the completion of layer 6 of the wall. Figure 66 shows the readings of the top piezometer during this period. The readings of the bottom piezometer did not show change in pore pressure during the same period.
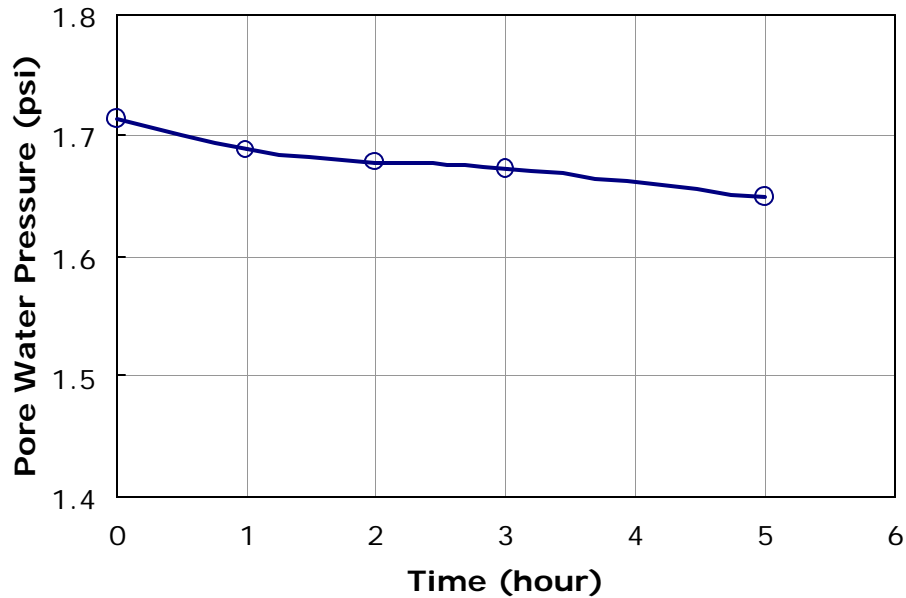
Figure 64
Dissipation of pore pressure after construction of layer 6

Wall Settlement

Facing Survey

The results of the survey of the levels at the base of the vertical modular block facing are shown in Figure 65. The initial zero readings were taken on March 10, 1998, after the placement of the 2-ft. stone base layer and the first soil layer of the wall. The facing settlement was approximately uniform along the constant height of the wall and it linearly decreased to zero along the 3:1 slope at the side of the wall. A maximum settlement of about 8.5 in. was measured at the middle of the facing at the end of construction. It should be noted that this value is at the facing and it is not the maximum settlement under the wall.
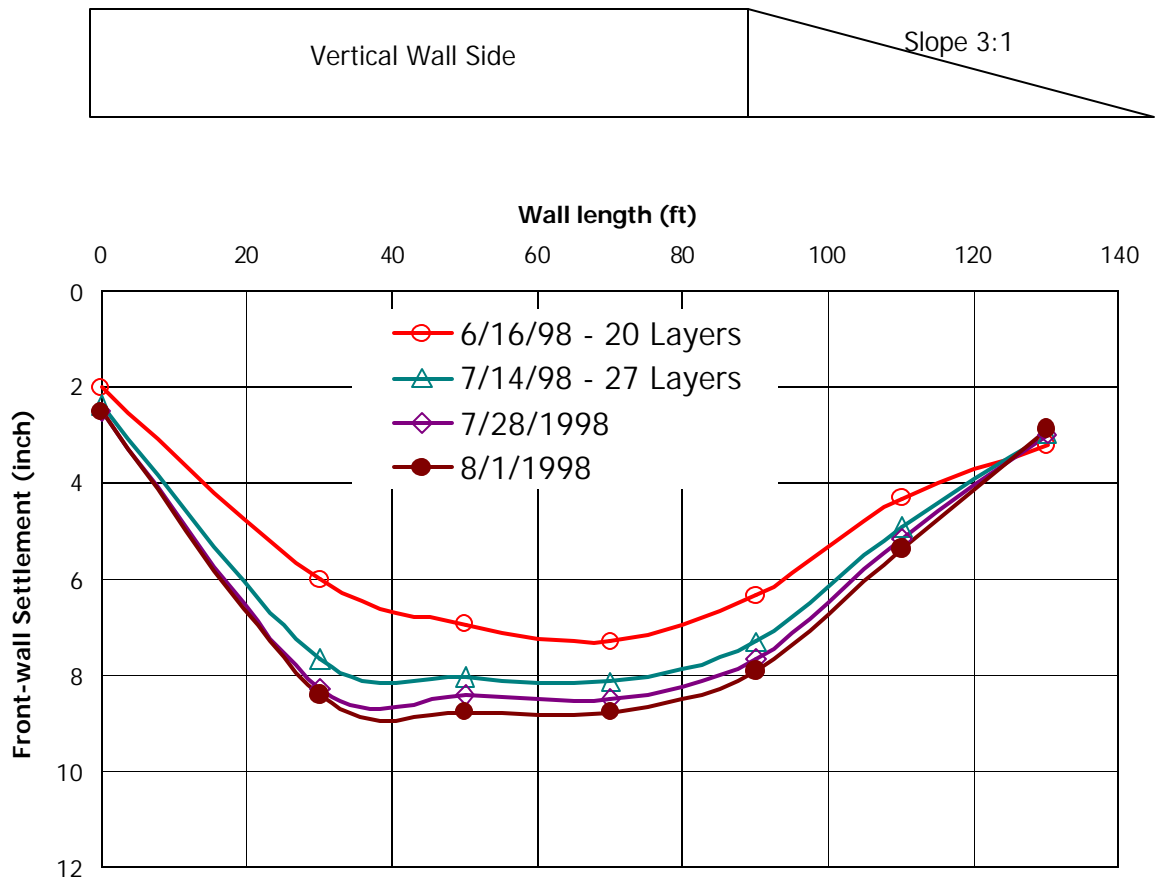
Figure 65
Settlement of the modular block facing of the wall

Settlement Plates

The survey results of the settlement plates are shown in figure 66. The figure shows the measurements in the four plates during the four-month construction period. Refer to figure 41 for the locations of the settlement plates. The measurements show a maximum settlement of about 9.5 in. near the vertical wall facing, which compares well with the survey measurements at the facing. The measurements at the other plates show a uniform wall settlement of about 8.5 in. at the end of construction. It should be noted that figure 66 shows settlement measurements until one month after the completion of construction. Consolidation settlement continued to increase during the three-month post-construction monitoring period.
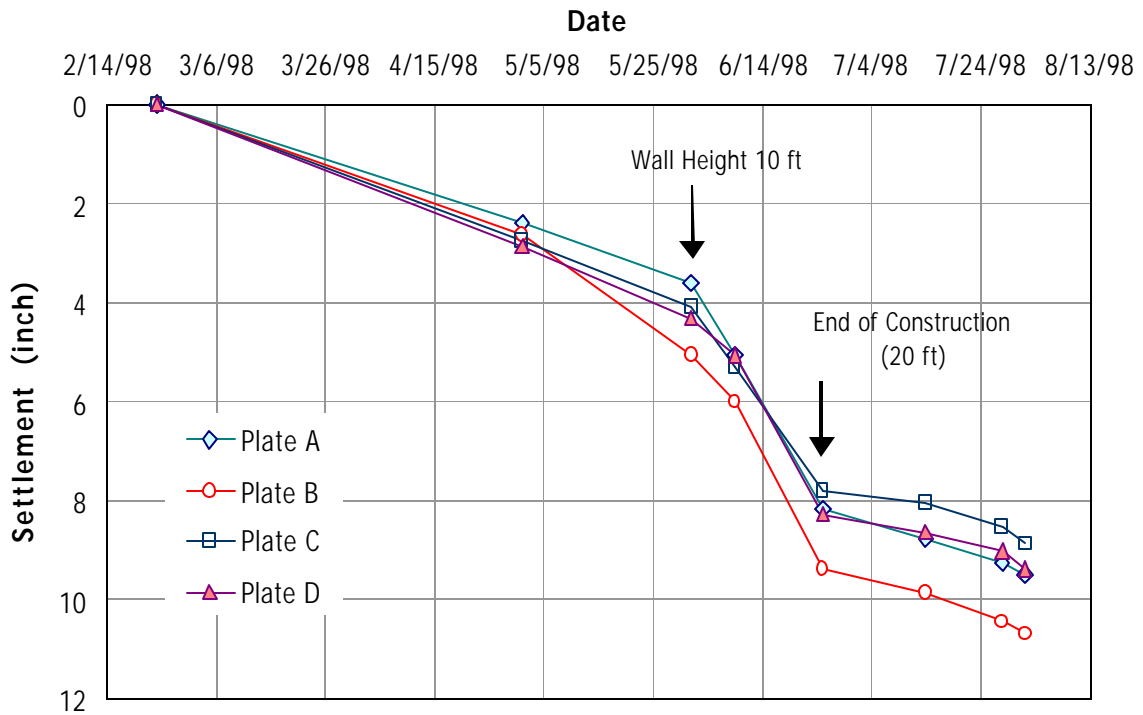
Figure 66
Measurements of the settlement plates at the base

Horizontal Inclinometers

Settlement measurements from the cross and longitudinal horizontal inclinometers are shown in figures 67 and 68, respectively. Refer to the locations of the inclinometers in figure 41. The results of the cross-inclinometer showed a maximum settlement of about 10 in. near the wall facing at the end of construction. The longitudinal inclinometer readings were taken only for 40 ft. along the length of the wall since the remaining part of the inclinometer pipe was damaged during construction. The results of the inclinometers compared well with each other and with the settlement plates and survey measurements.
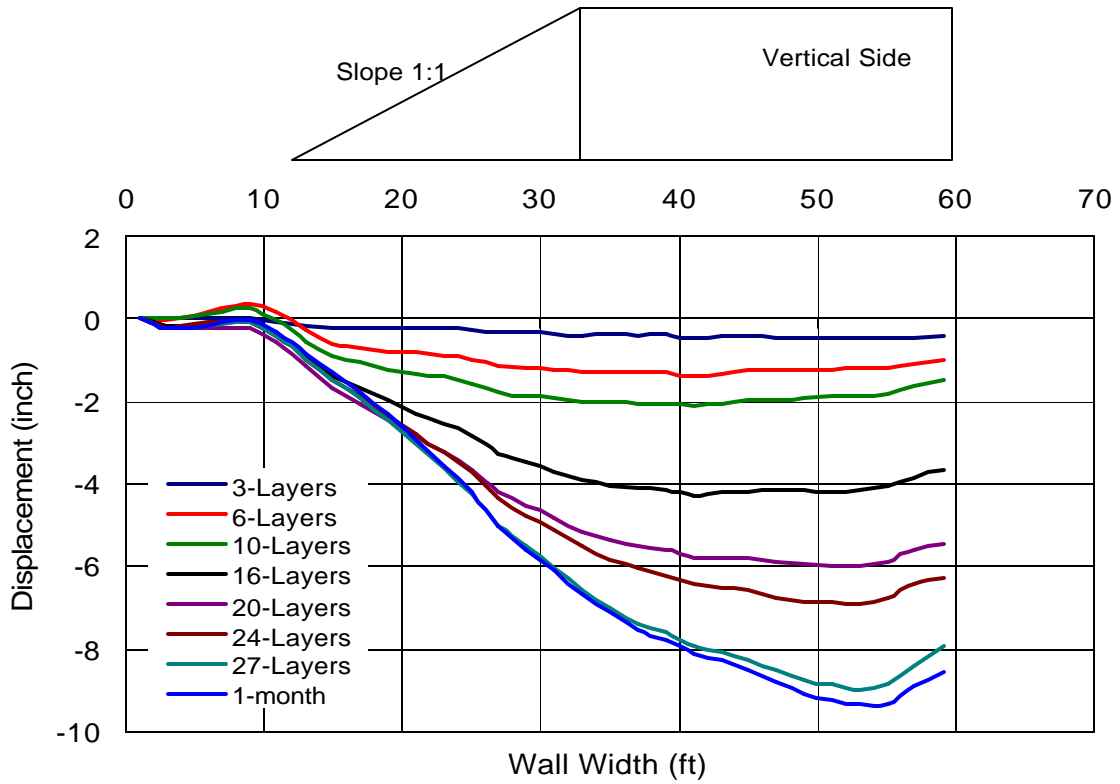
Figure 67
Settlement profile from cross-inclinometer
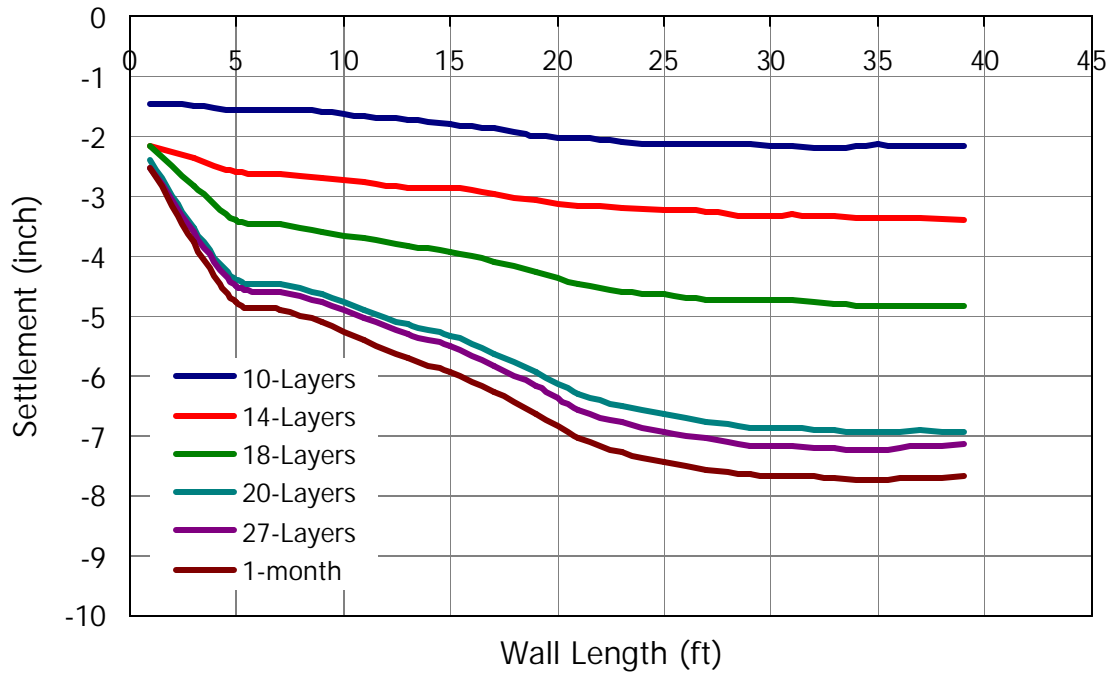
Figure 68 Settlement profile from longitudinal-inclinometer

66

Measurements of Horizontal Deformation

Survey of the wall facing

The horizontal movement of the vertical wall facing was surveyed at 3 elevations; namely at 2.7 ft. (soil layer 4), 9.3 ft. (soil layer 14), and 10 ft. (soil layer 24). The measurements are shown in figures 69, 70, and 71 for the mid-points of sections 1, 2 and 3, respectively. The results in the figures show that:

- The maximum deformation of wall section-1 (UX-750 geogrid) occurred at the top of the wall. Maximum deformations in sections 2 (UX-1400) and 3 (UX-1500) were comparable and occurred at mid-height. The deformations at the top layer of wall are plotted along the wall length and are shown in figure 72.

- At the end of construction, deformations of sections 1 and 2 were comparable at 0.5 inches. The deformation in section 3 was lower at 0.35 inches.

- Post-construction deformations were higher in section 1 (1.15 inches) than in sections 2 (1 inch) and section 3 (0.85 inches).

It should be noted that the first survey measurement was always taken after the completion of the layer above the survey point. Accordingly, the measurements did not account for the deformations that may have occurred during the compaction of that layer.

Most of the deformations occurred during construction and during the first 3 months after the completion of the wall. Smaller deformations were monitored in the period from 3 months (9/1998) to one year (6/1999) after construction.

UX750_Section
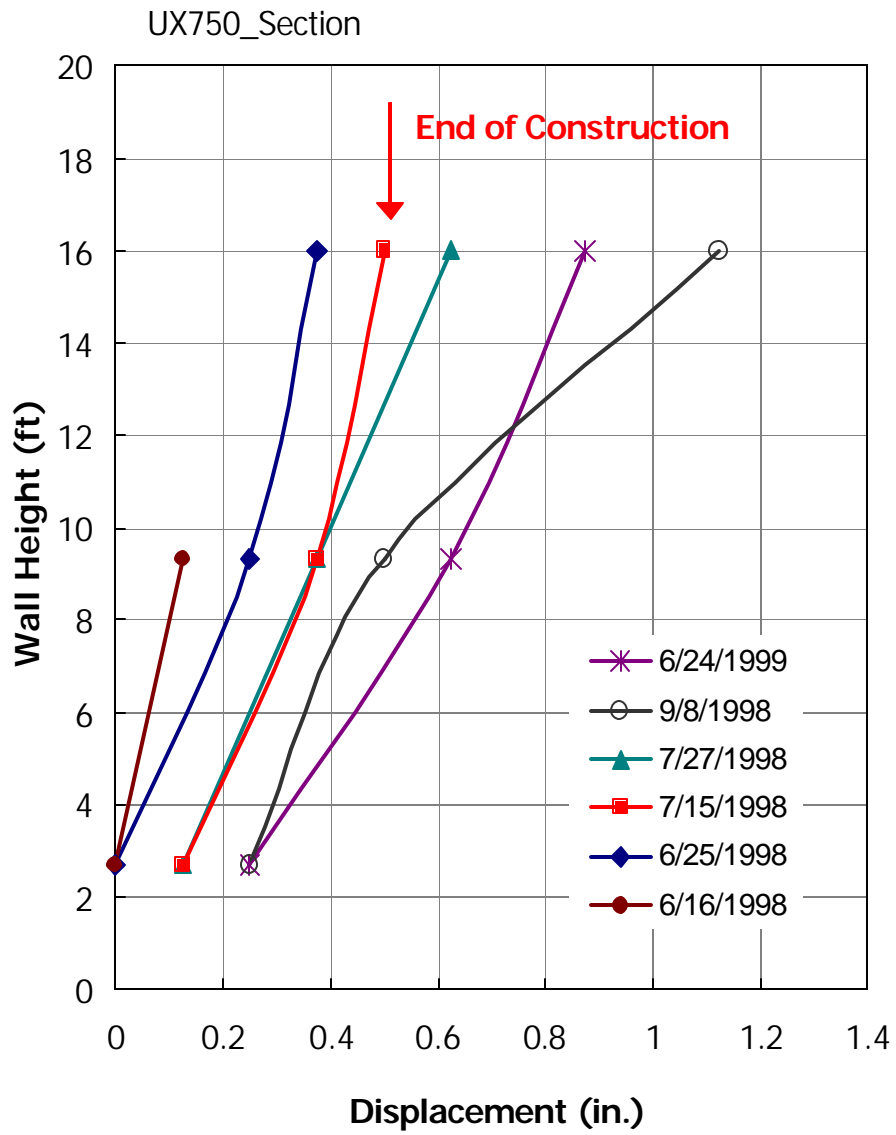
Figure 69
Deformations at the facing of wall section 1

UX1400_Section
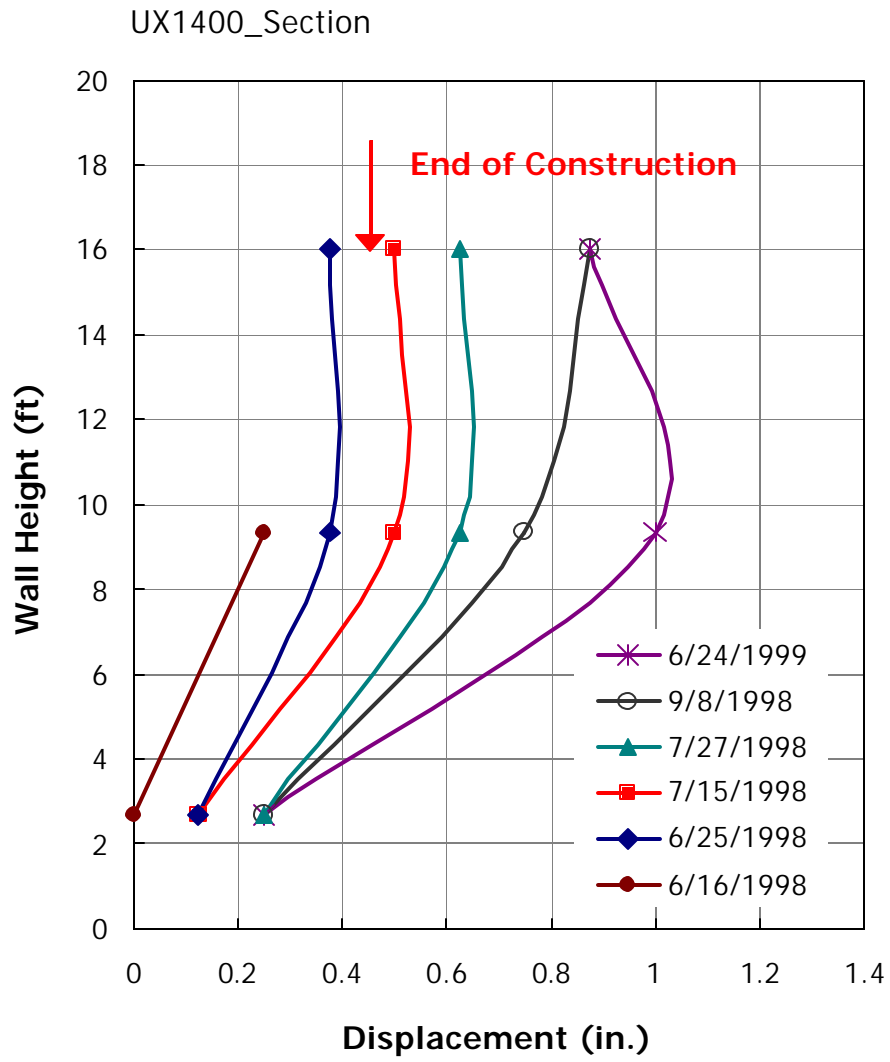
Figure 70
Deformations at the facing of wall section 2

UX1500_Section
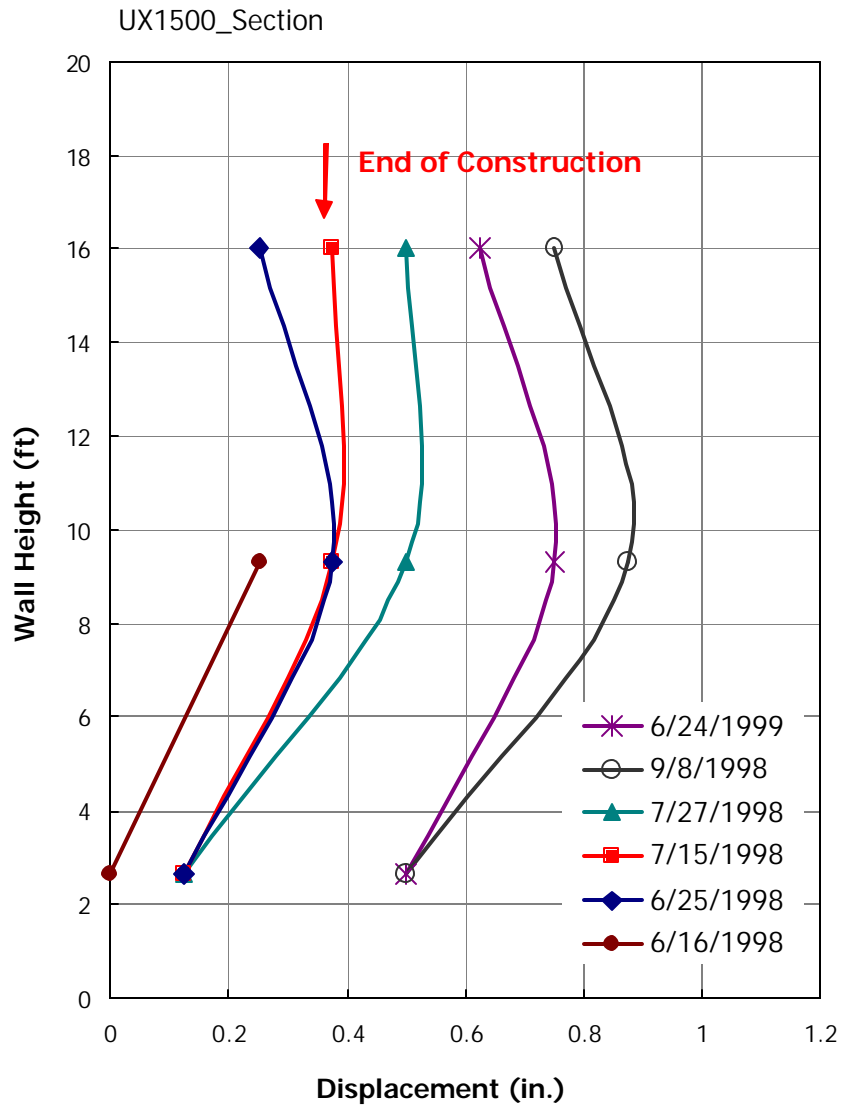
Figure 71
Deformations at the facing of wall section 3
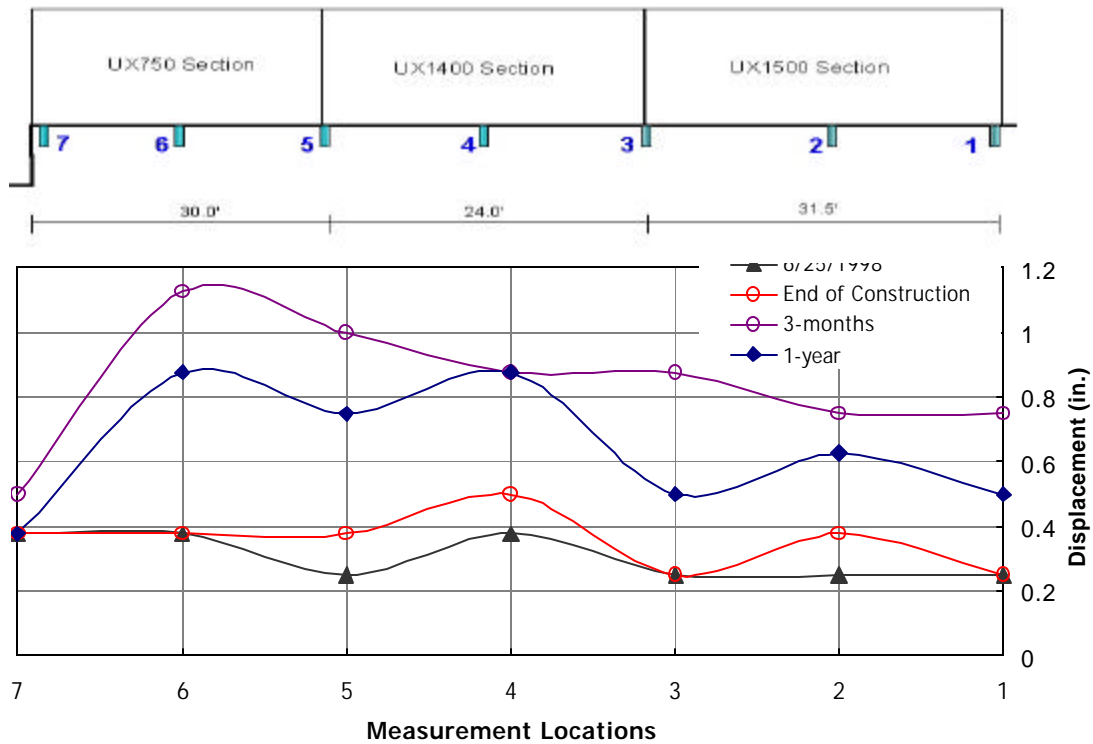
Figure 72
Longitudinal profile of displacement at top level of wall

Measurements of Vertical Inclinometers

The measurements of the vertical inclinometers in sections 1 and 2 of the vertical wall are shown in Figures 73 and 74, respectively. The figures show the readings incurred since June 9, 1998 (the initial reading of the inclinometers) at a wall height of 21 layers. Accordingly, the measurements represent the deformations during the late stages of wall construction and for a period of about four months after completion of the wall. Measurements of the inclinometers during early stages of construction were not successful due to the movement of the inclinometer pipes during backfilling the compaction.

The measurements in figure 73 of section 1 show:
- Most of the deformations occurred at the top part of the section, which is similar to the results obtained from the wall survey.

71

- The maximum deformations were relatively in the same order for both the front and back inclinometers (0.65 in. and 0.8 in., respectively). The equal deformations of both inclinometers indicate low geogrid strains at the top half of the wall.
- The front deformation at a wall height of 16 ft. was in the order of 0.65 in. on July 29, 1998. The facing survey of the same elevation was 0.6 inches at the same period (figure 69).

The results of the vertical inclinometers of section 2 in figure 74 show that most of the deformations occurred at the front inclinometer with maximum deformations near to the mid-height of the wall, which correlates well with the survey results shown in figure 70. The maximum deformation of 0.7 in. on July 29 was slightly higher than the facing movement of about 0.5 during the same period.

The results of the vertical inclinometer at the top of the woven slope are shown in figure 75. The measurements of the inclinometer at the mid-height of the slope were not successful due to the damage of the inclinometer pipe during construction. The results show that the movement of the slope reached a maximum of 0.8 in. with the maximum deformation measured at the mid-height of the slope.

The results of the top and mid-height vertical inclinometers in the non-woven section are shown in figure 76. The figure shows a comparable magnitude of maximum deformation to the woven section with the maximum deformations measured near the top of the slope.

The results of the inclinometer readings in the vertical side of the Geoweb section are shown in figure 77, which show that the maximum deformation was 0.6 in. with most of this value occurring during the late stages of construction.

Horizonal Displacement (inch)   Horizonal Displacement (inch)

Back Inclinometer

6/17/98
7/17/98
7/29/98

Front Inclinometer

7/17/98
7/29/98
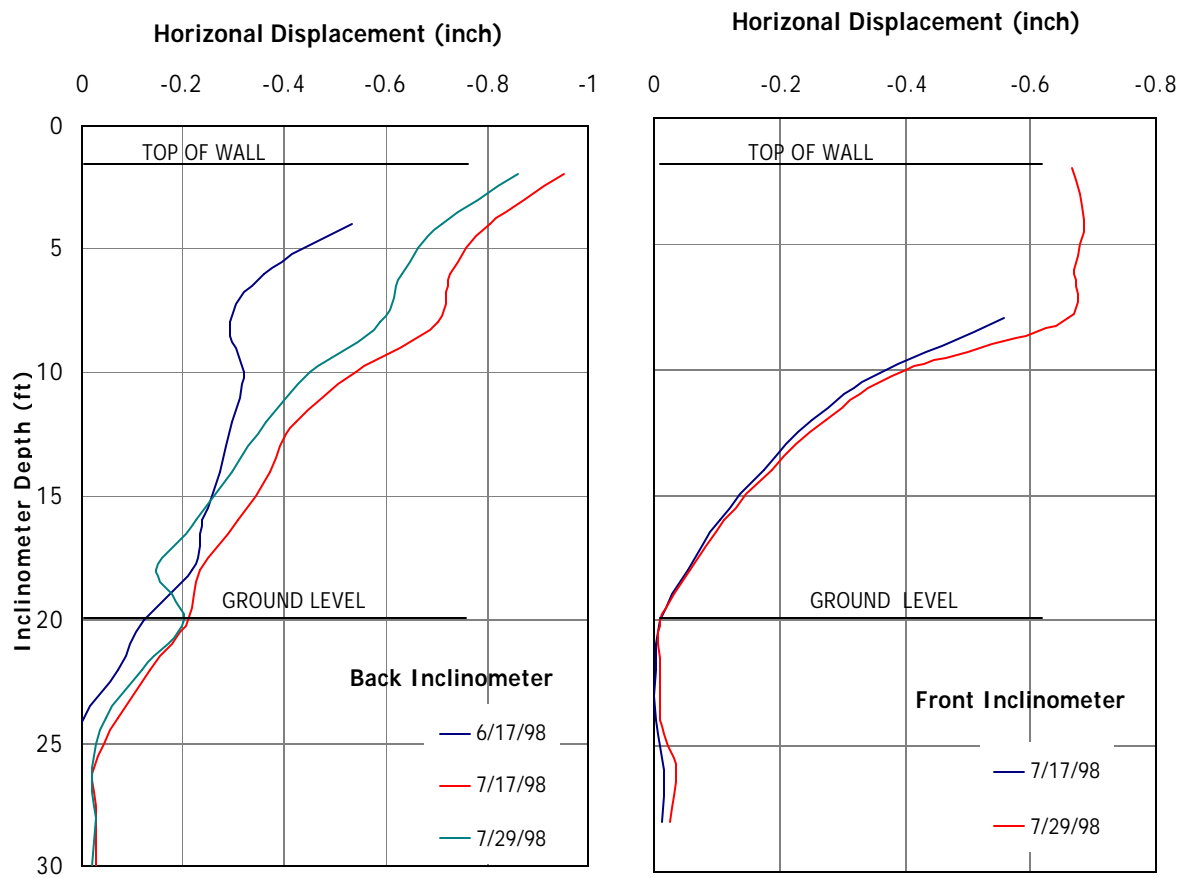
Figure 73
Vertical inclinometer measurements in wall section 1
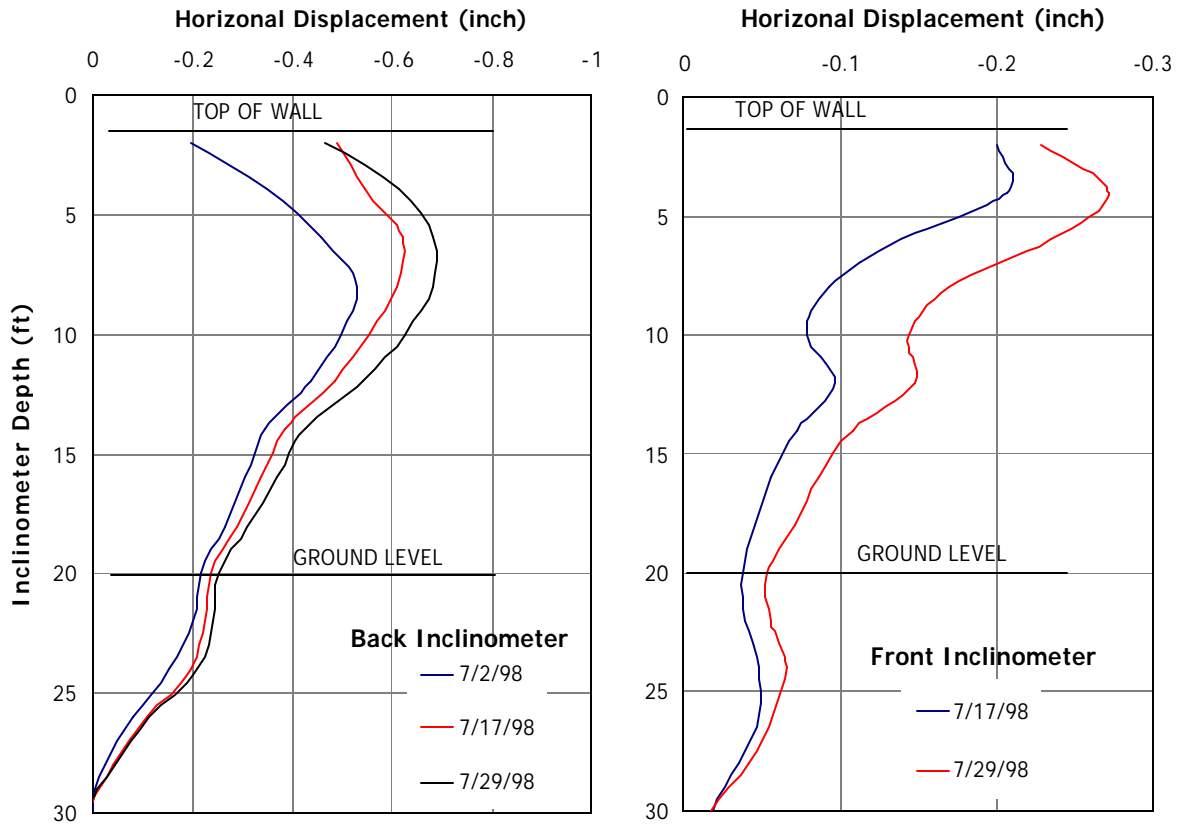
Figure 74
Vertical inclinometer measurements in wall section 2
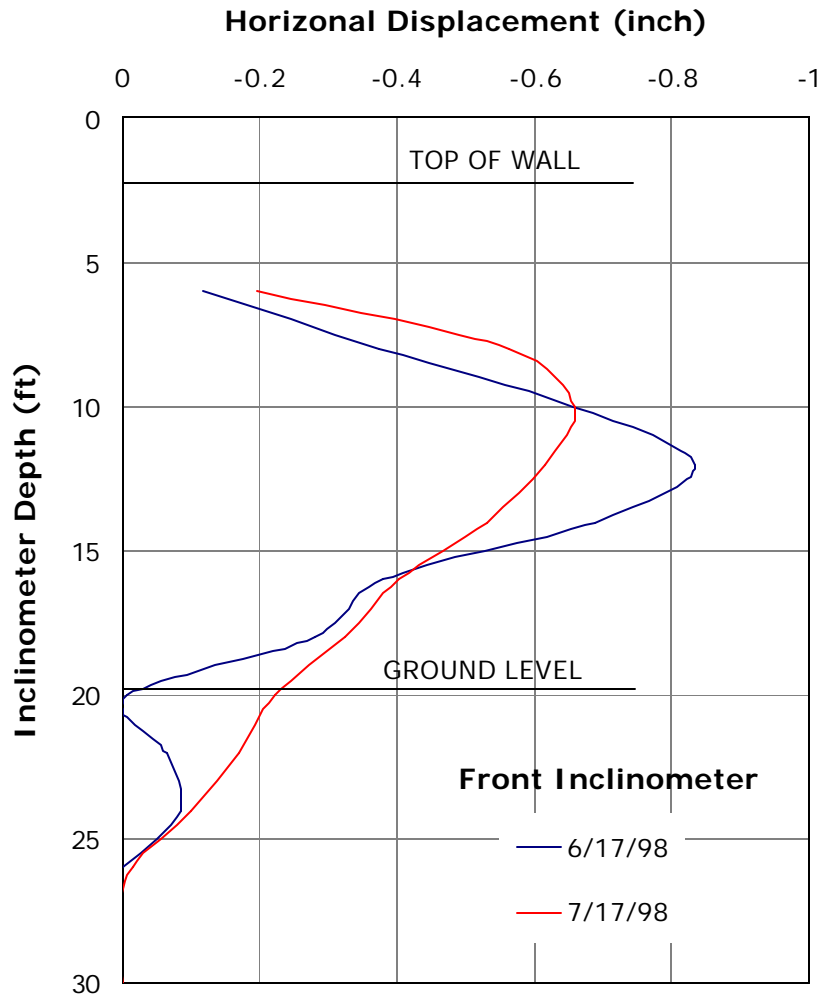
Figure 75
Measurements of front inclinometer in woven slope section
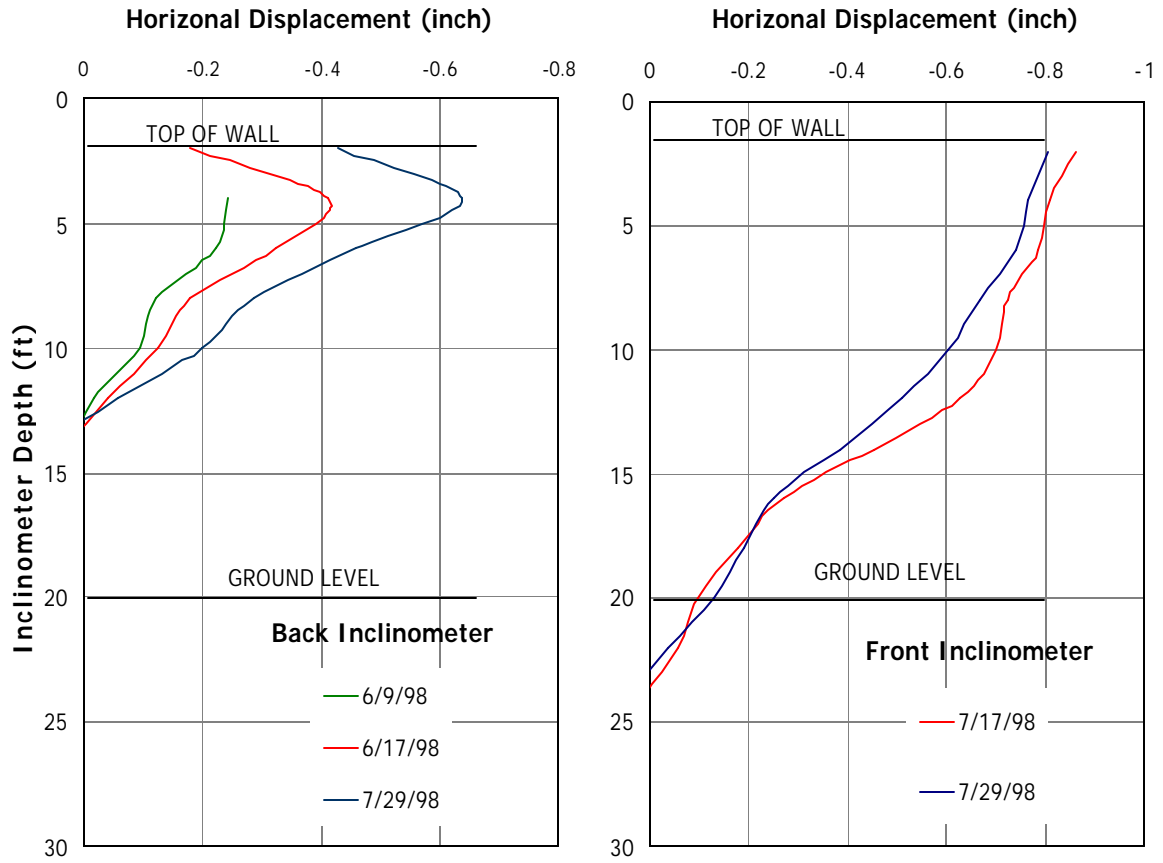
Figure 76
Vertical inclinometer measurements in the non-woven slope
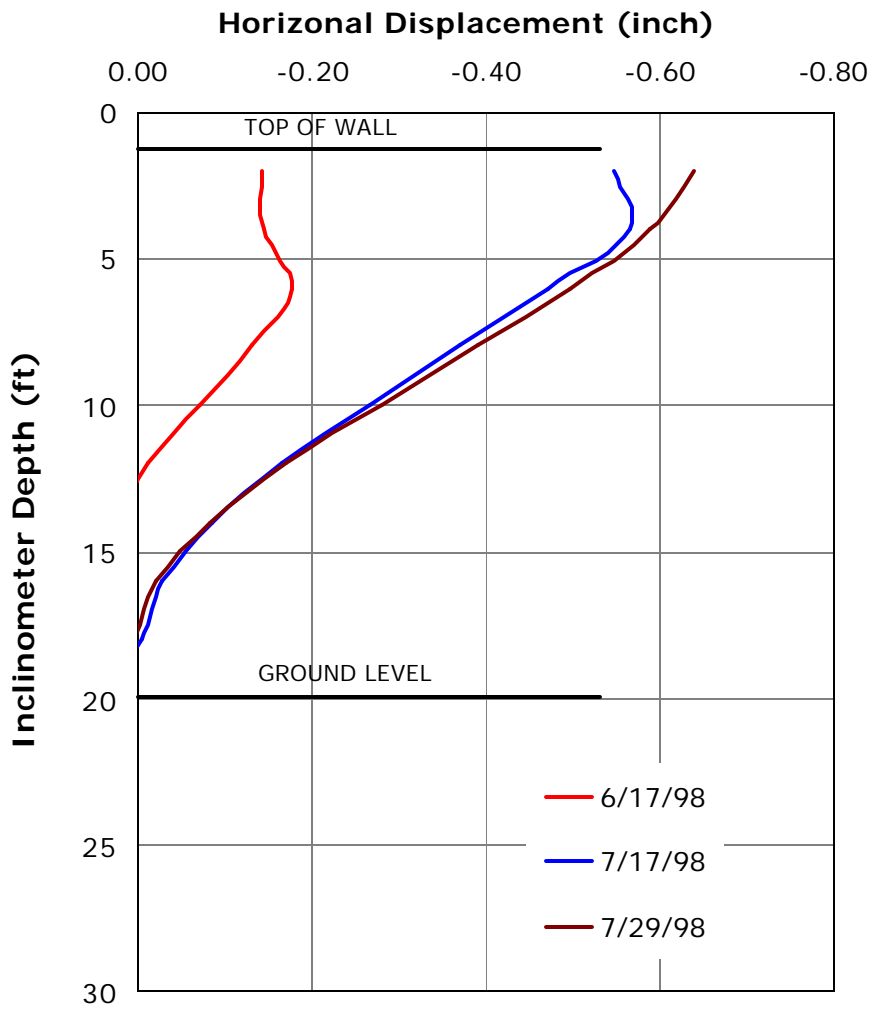
Figure 77
Vertical inclinometer measurements in the Geoweb section

Measurements of Earth Pressure

Base Pressure under Block Facing

Two earth pressure cells were placed on the leveling pad under the modular block facing. These cells were vibrating wire type of 9-in. diameter. One cell (cell 43-684) was placed under the compact block and the other cell (cell 43-685) was placed under the standard block. The results in figure 78 show the vertical pressures at the base of the wall facing. The results of base pressure are also plotted with the pressure calculated from the weight of the blocks and are shown in figure 79. The figure shows that the measured pressure was significantly lower than the theoretical weight of the facing blocks.

The pressures are characterized by a slow increase during the early stages of construction followed by a sharp increase during the faster construction period of the top half of the wall. The base pressure decreased with time after the completion of wall construction, possibly due to wall settlement.

Soil Pressure at the Wall Base

The horizontal earth pressure was monitored at the base of the wall by the earth pressure cell which was placed against the facing blocks. The measurement of the cell is shown in figure 80. The results show that horizontal earth pressure was not fully mobilized at the wall base and reached about one third of the expected theoretical value calculated using 0.3 as K_a.
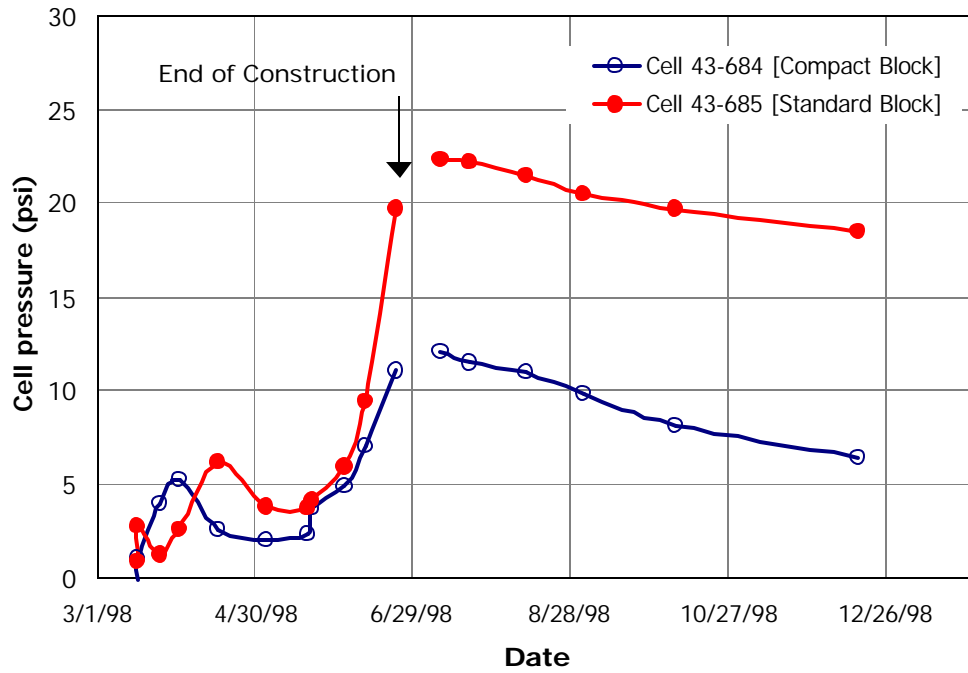
Figure 78
Measurement of base pressure under the facing blocks
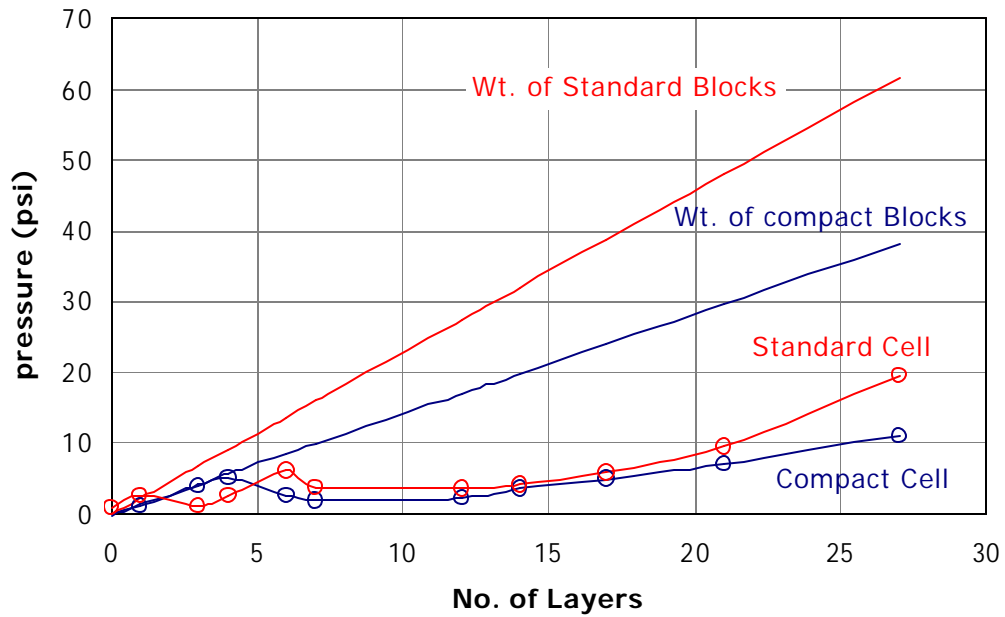
Figure 79
Measurement of base pressure relative to block weights
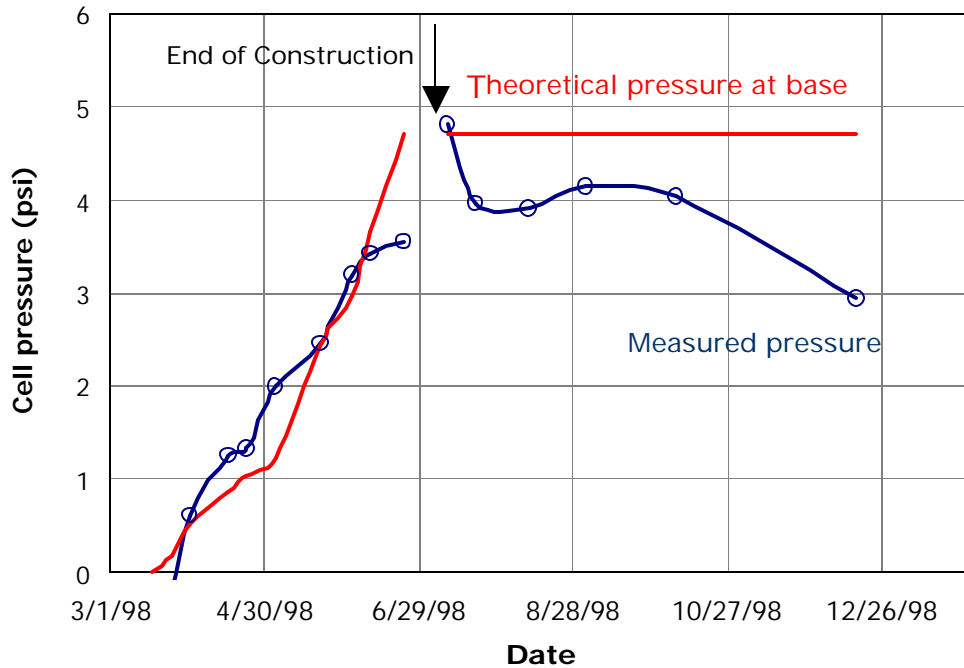
Figure 80
Measured and theoretical horizontal pressure at wall base

Earth Pressure in the Backfill

The development of vertical earth pressure during wall construction was monitored by load cells placed at layers 5 (4 ft. of wall height) and 17 (12 ft. of wall height). The cells were placed at about 3 ft. from the wall facing. Refer to figure 49 for the locations of the pressure cells. The results of earth pressure measurements and the theoretical pressured calculated from the weight of the soil above the cells are shown in figure 81. The results show that vertical earth pressure increased during early stages of construction at a rate equal to its theoretical values. At the end of construction, the pressure was only about 75 percent of the estimated soil weight. The results also show a reduction of soil pressure after the construction of the wall possibly due to wall settlement.

Similarly, the measurement of the horizontal earth pressures were measure by vertical pressure cells at the same locations. The results are shown in figure 82 along with theoretical earth pressure values (based on $K_a = 0.3$). The results show that horizontal earth pressure did not fully mobilize till the end of construction.

80
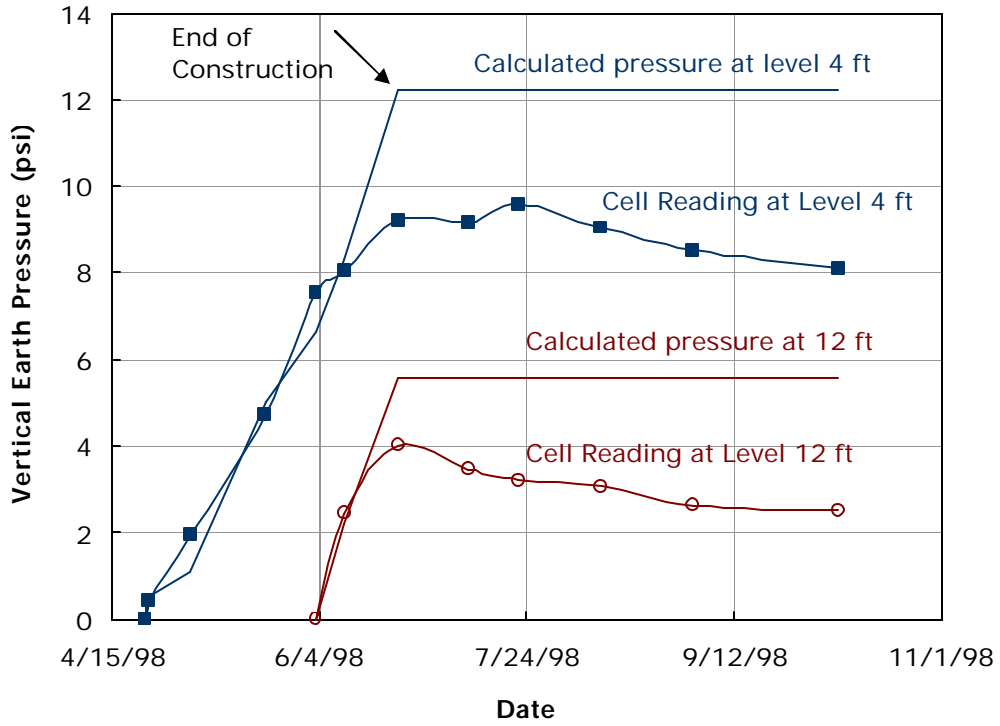
Figure 81
Measurements of vertical soil pressure
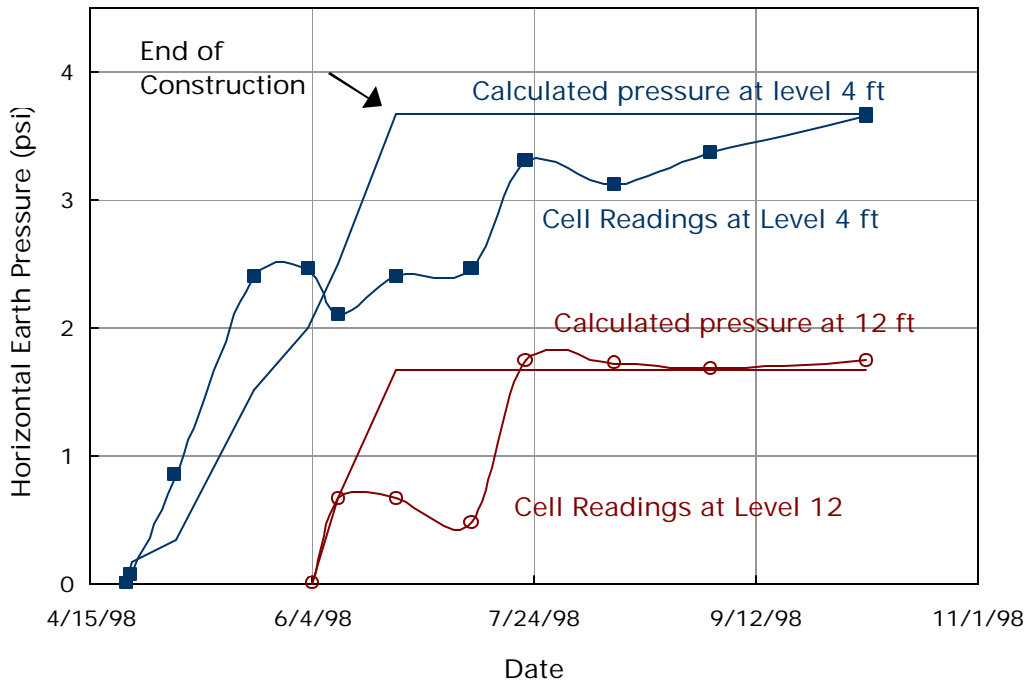
Figure 82
Measurements of horizontal soil pressure

Measurements of Reinforcement Strains

Strains in Section 1 (UX-750 Geogrid)

Figure 83 shows strain measurements during and after the construction of layer A of section 1. The rate of increase in strain corresponded to the rate of construction of the wall. The figure shows a reduction in strains after the wall's completion. Figure 84 shows the distribution of strain along the reinforcement. The figure shows the progressive increase of reinforcement strains with the increase of soil lifts during the construction of the wall. The horizontal axis in the figure shows the number of the ribs along the length of the geogrid.

Similarly, figures 85 to 100 show the measurements of the strains in the other reinforcement layers of section 1 of the wall. Refer to table 10 and figure 52 for the locations of the strain gauges in each layer. During the construction of the wall, strains were maximum at the bottom third of the wall and reached a value of about 3.5 percent in layer D.

Construction of the test wall was complete by the end of June 1998. After the completion of wall construction, the figures show strain relaxation of the reinforcement at the bottom layers of the wall and stain increase in the top layers.

The figures also show the distribution of the strains along the reinforcement. The trend of strain distribution is that maximum strains are well defined at the bottom layers of the wall and the strains were more uniform at the top layers of the wall. A discussion of strain distribution of the three wall test sections is presented at the end of this chapter.
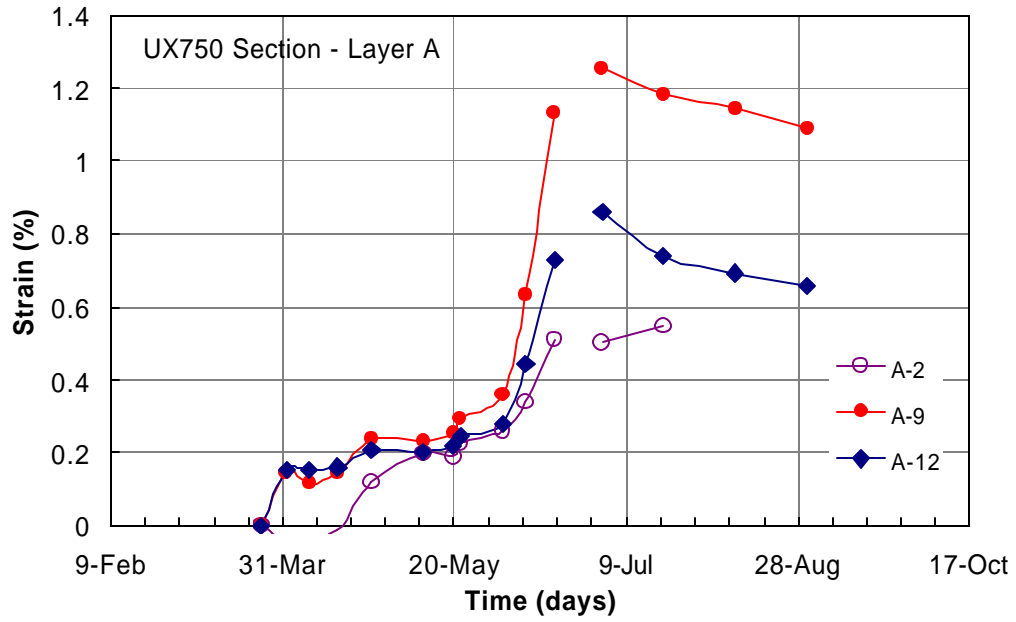
Figure 83
Strain measure ments of layer A in test section 1
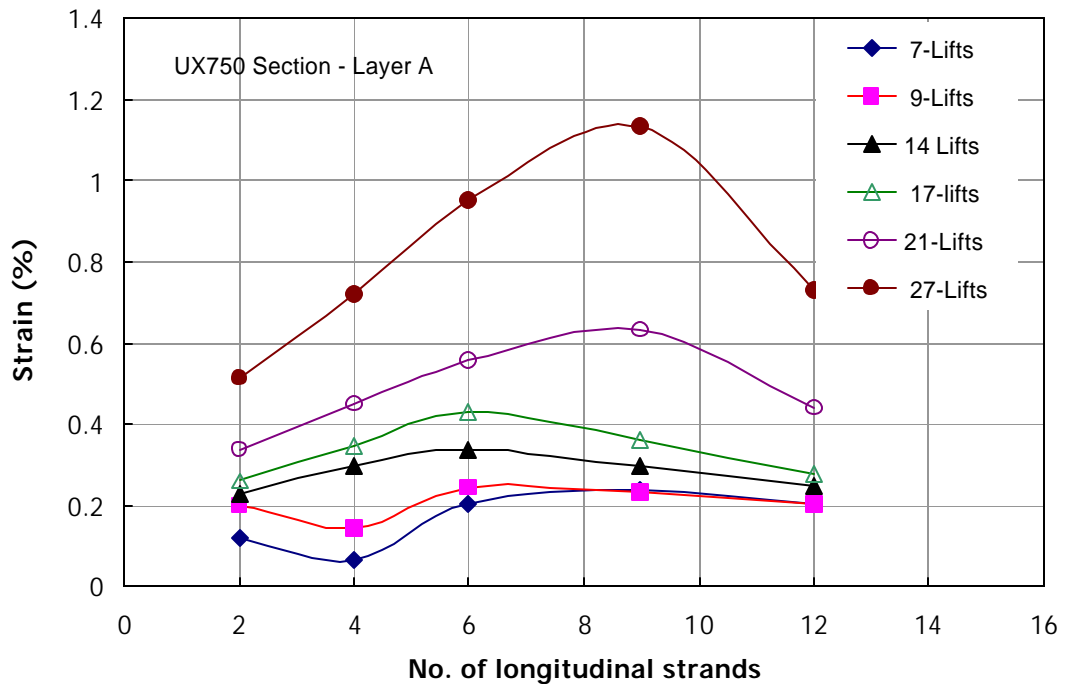
Figure 84
Distribution of strains along the reinforcement in layer A
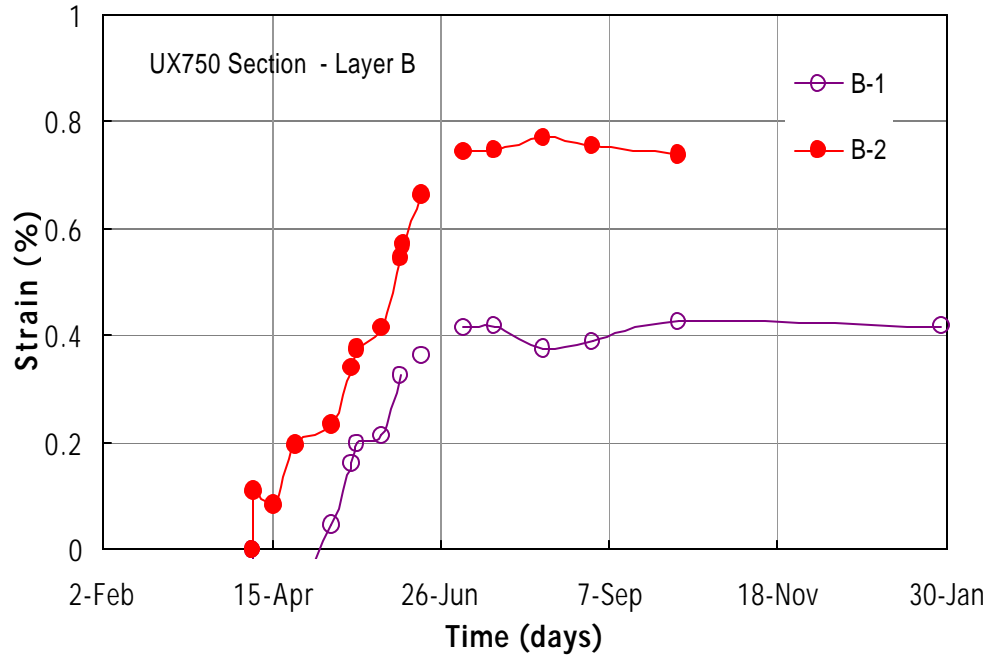
Figure 85
Strain measurements of layer B in test section 1
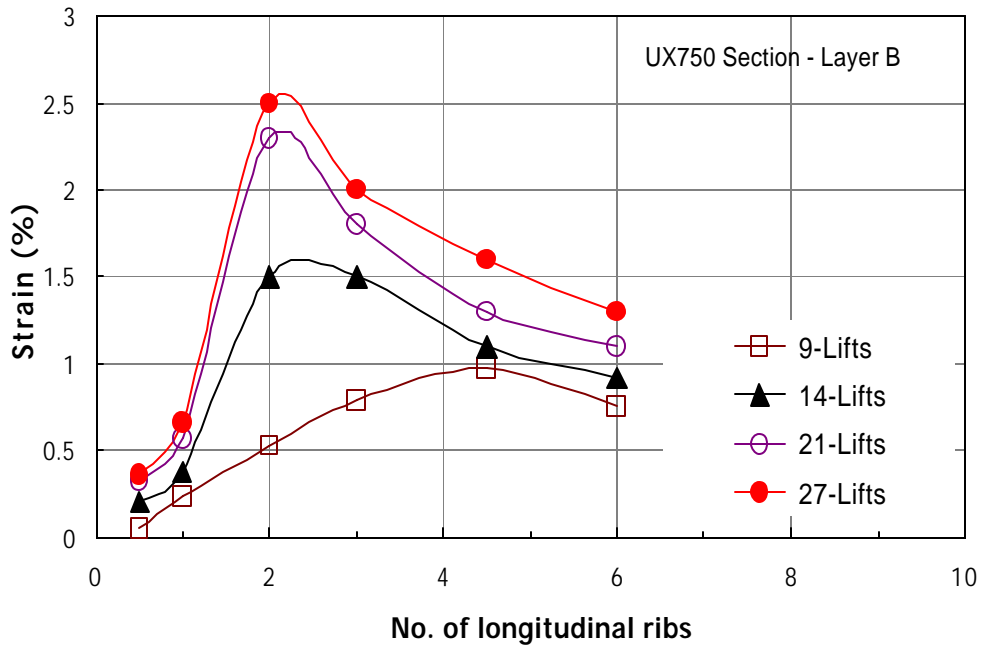
Figure 86
Distribution of strains along the reinforcement in layer B
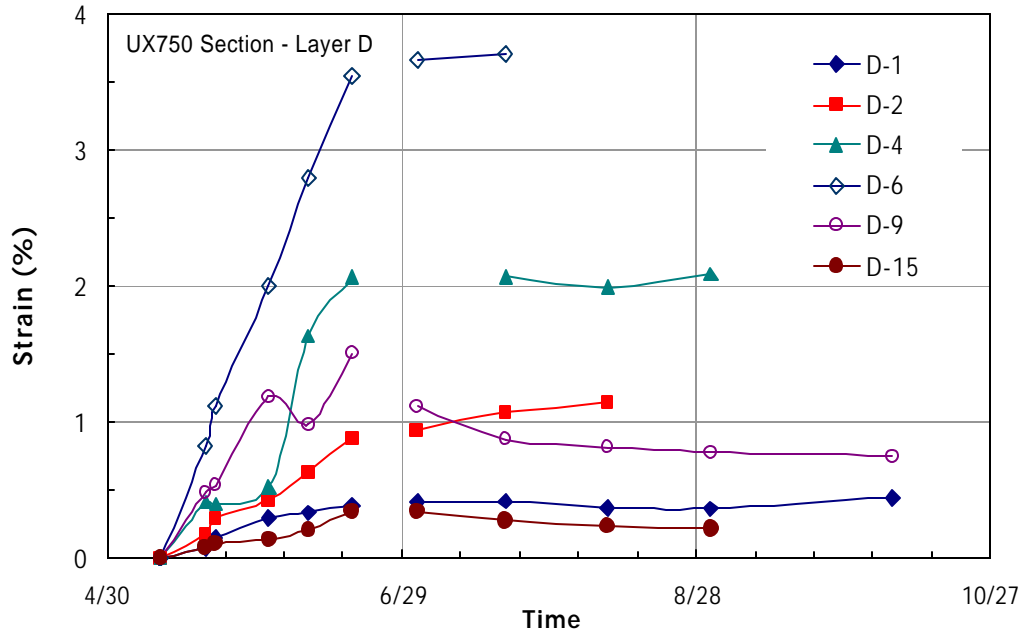
Figure 87
Strain measurements of layer D in test section 1
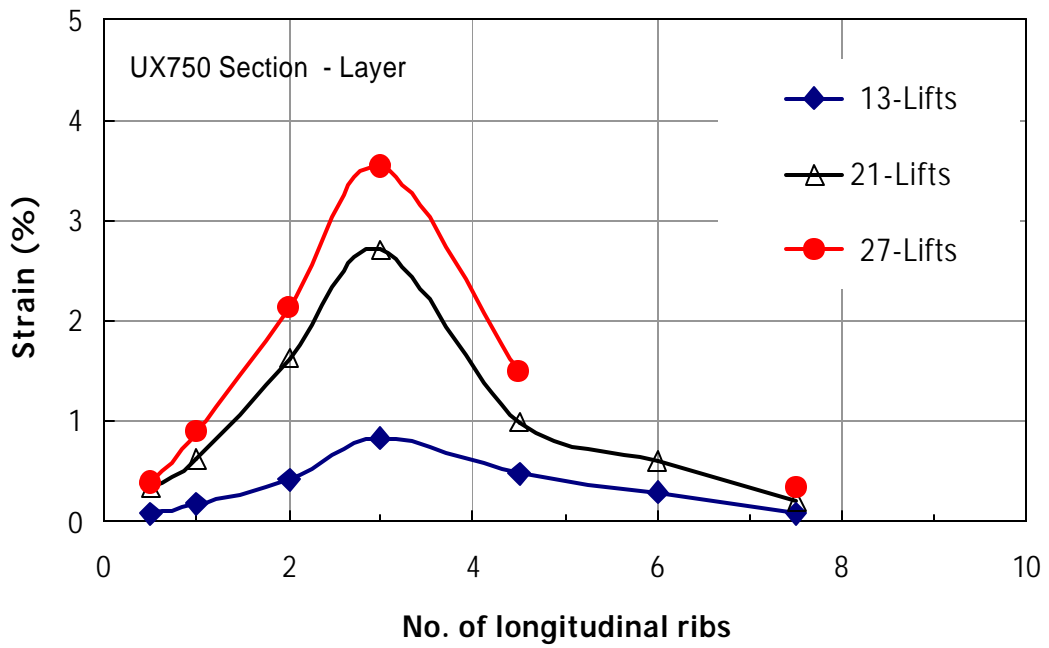
Figure 88
Distribution of strains along the reinforcement in layer D
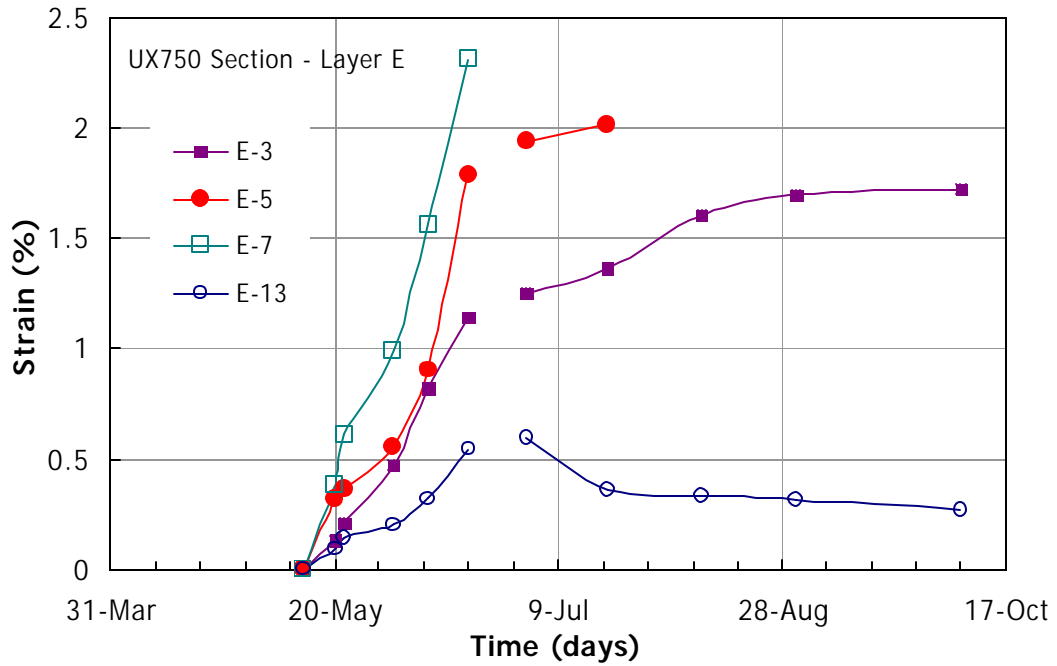
Figure 89
Strain measurements of layer E in test section 1
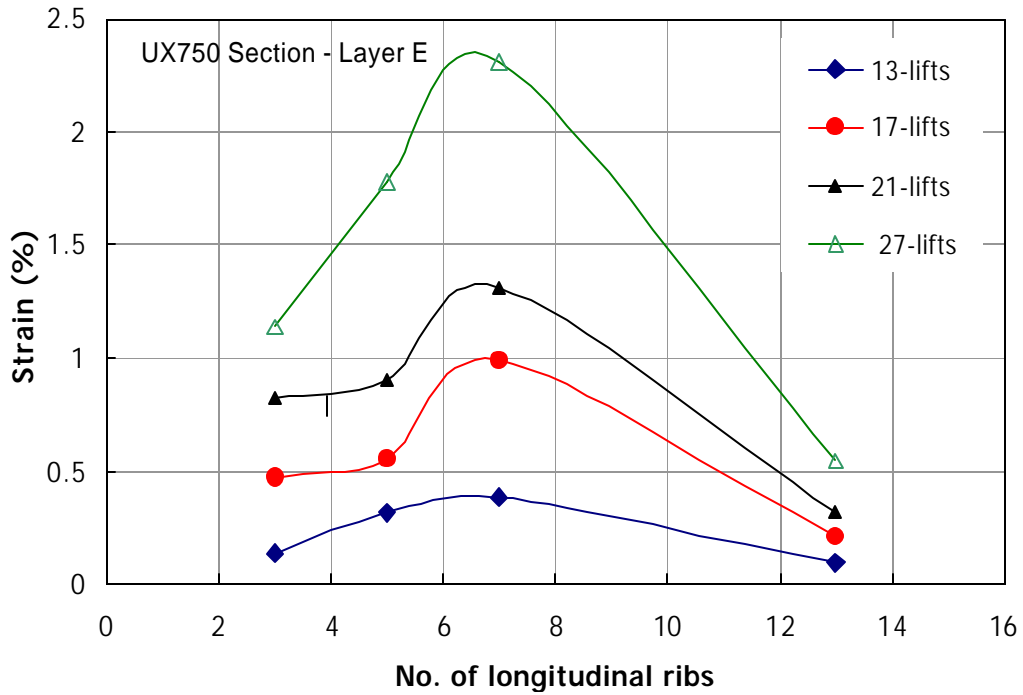
Figure 90
Distribution of strains along the reinforcement in layer E
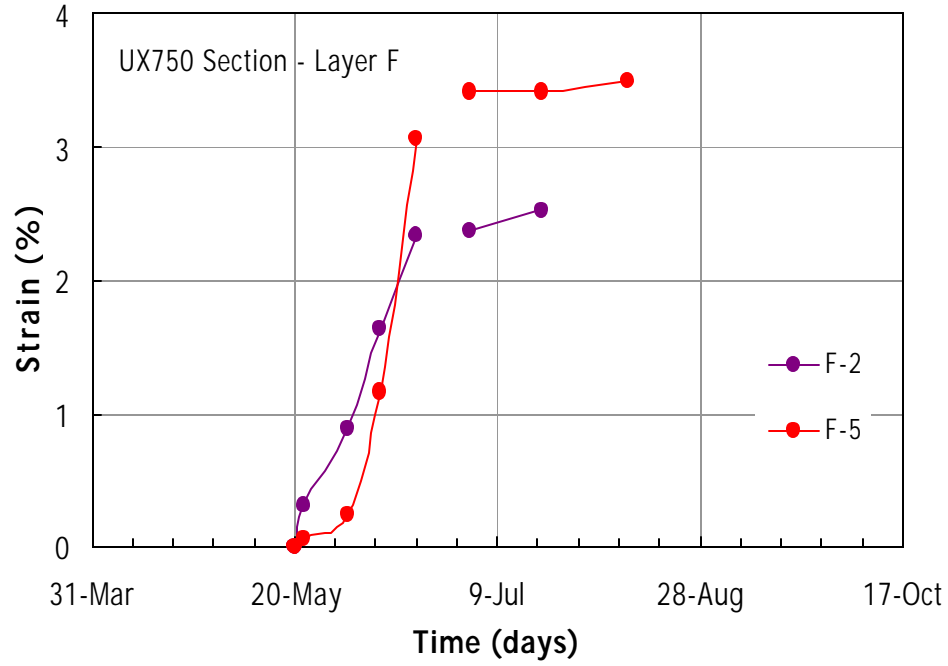
Figure 91
Strain measurements of layer F in test section 1
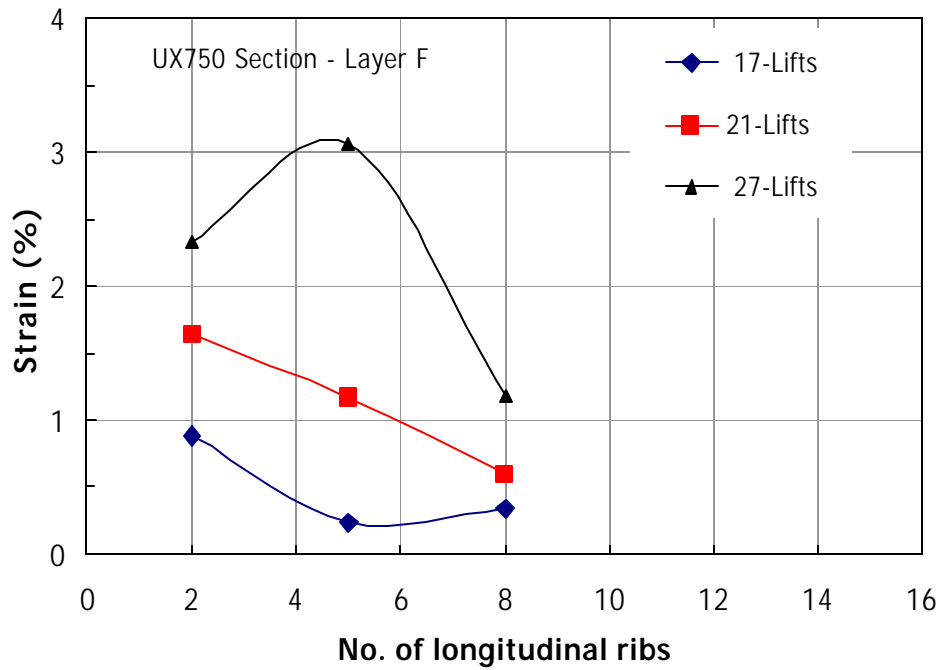
Figure 92
Distribution of strains along the reinforcement in layer F
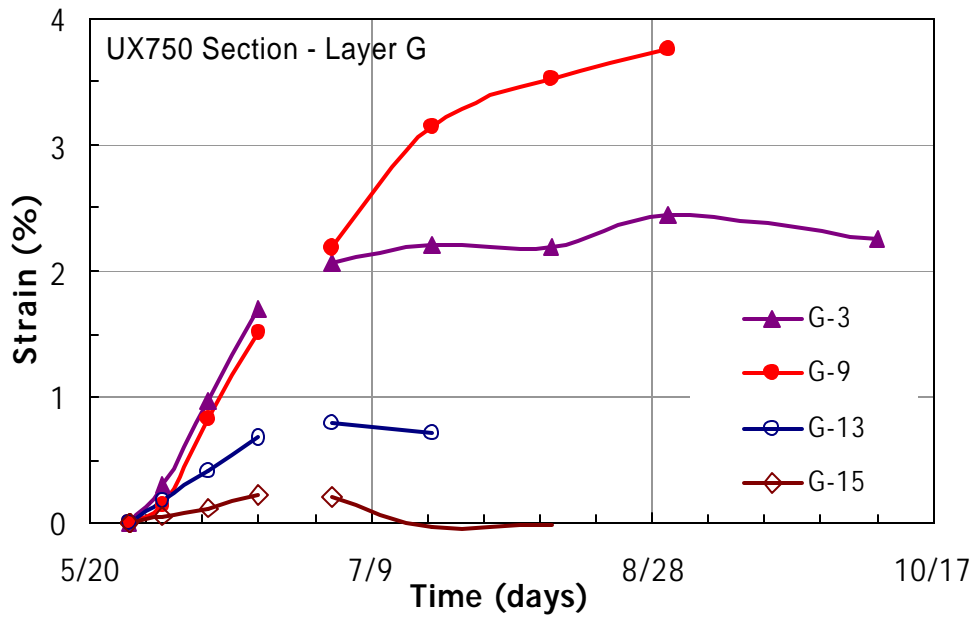
Figure 93
Strain measurements of layer G in test section 1
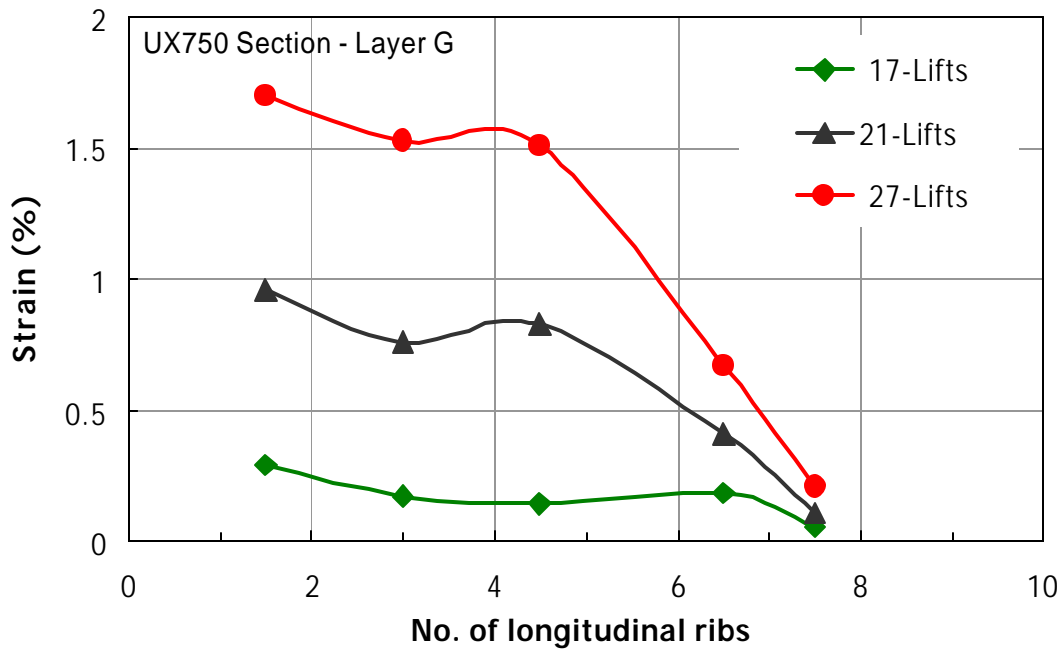
Figure 94
Distribution of strains along the reinforcement in layer G

88
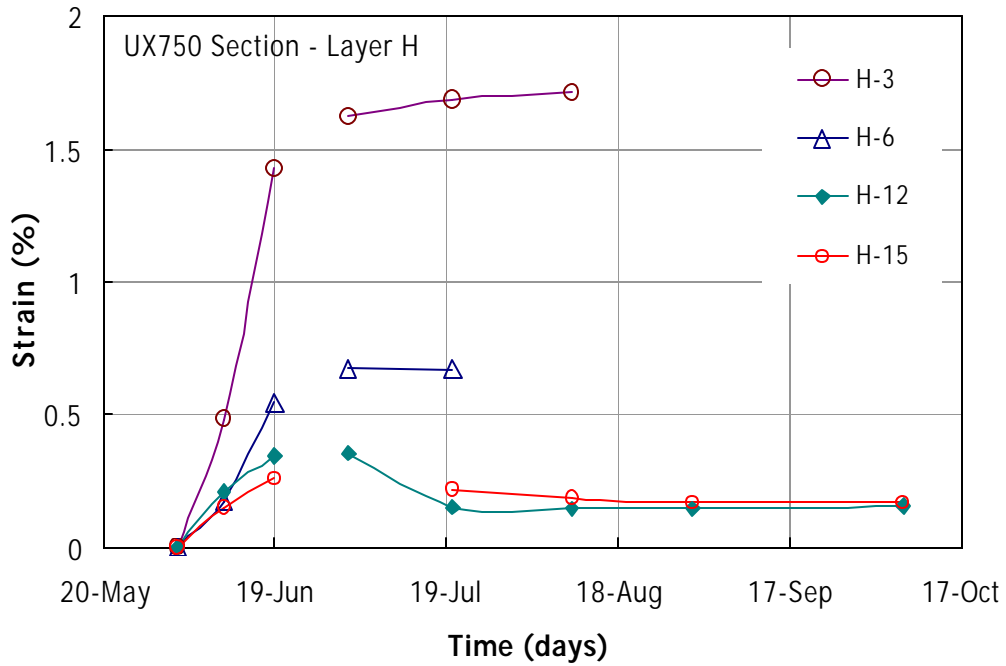
Figure 95
Strain measurements of layer H in test section 1
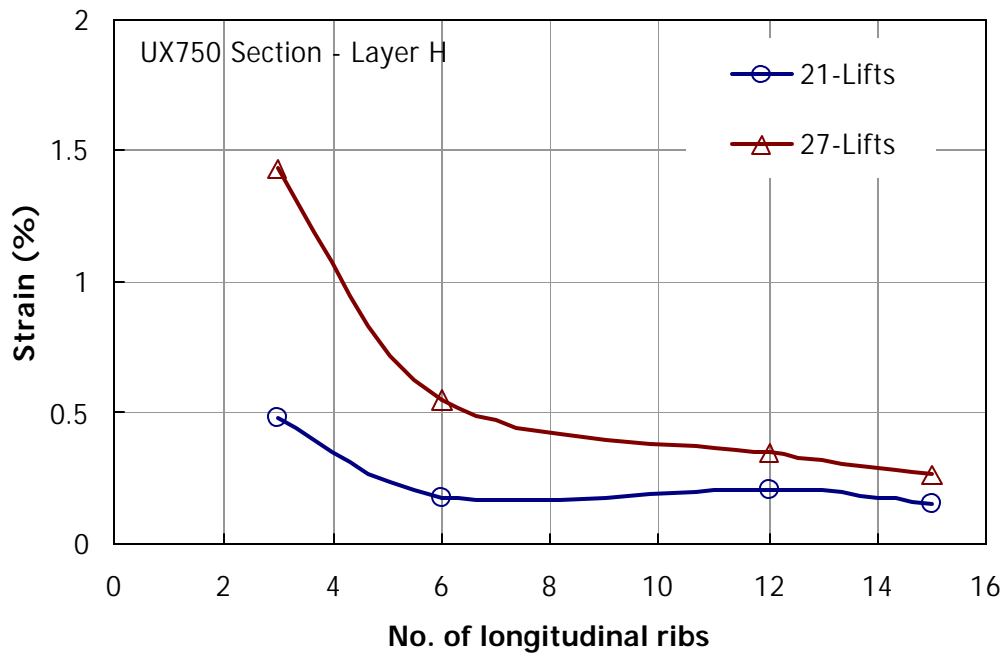
Figure 96
Distribution of strains along the reinforcement in layer H
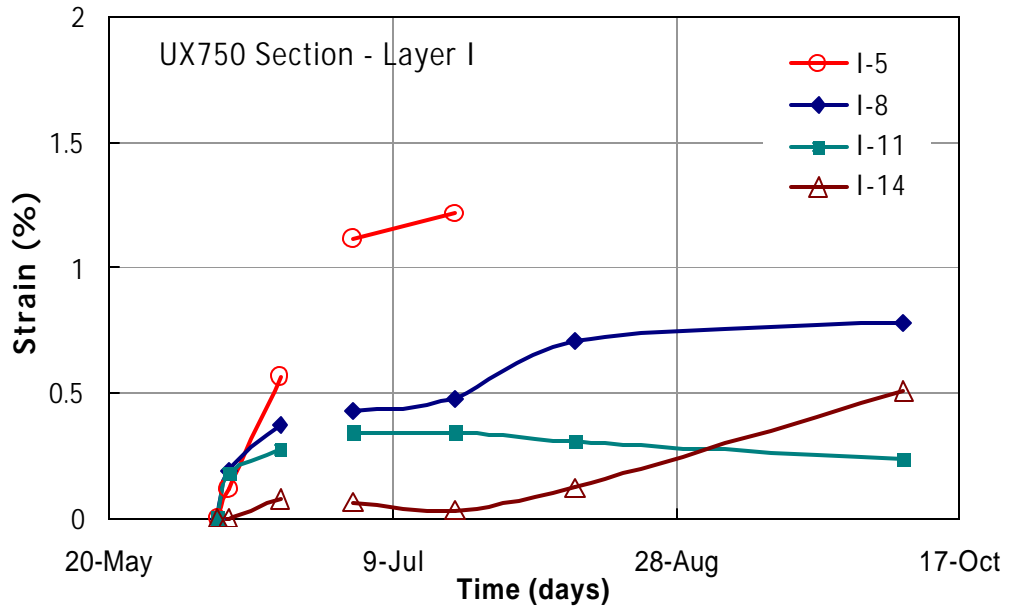
Figure 97
Strain measurements of layer I in test section 1
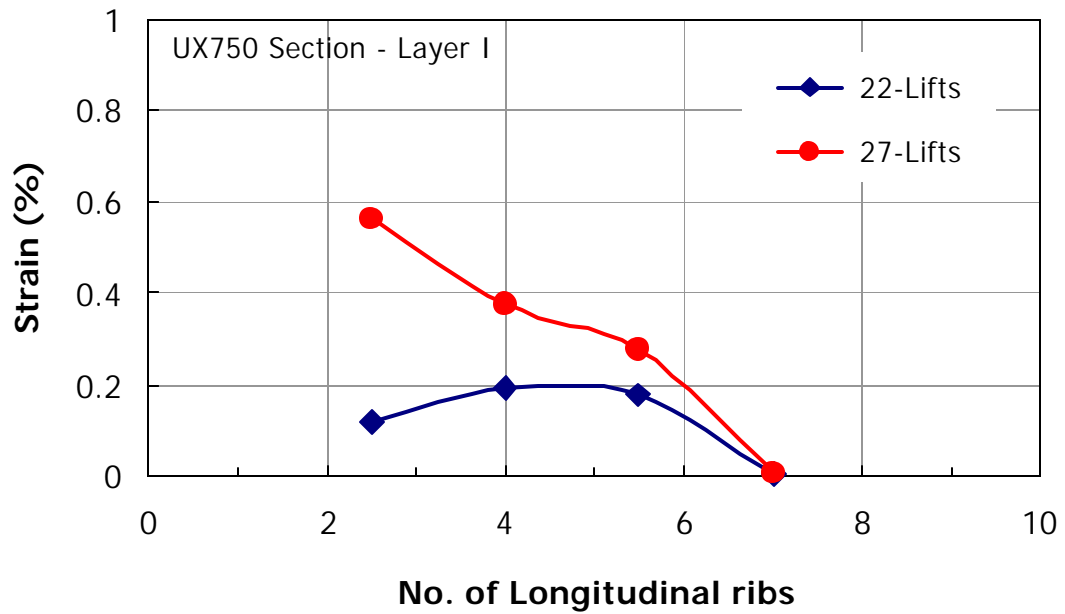
Figure 98
Distribution of strains along the reinforcement in layer I

90
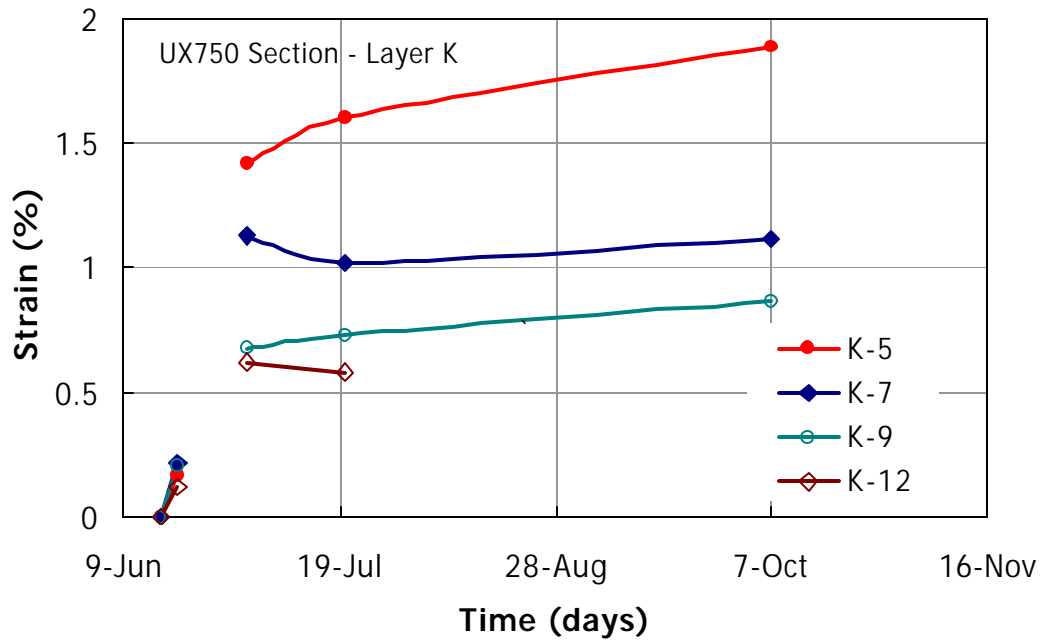
Figure 99
Strain measurements of layer K in test section 1
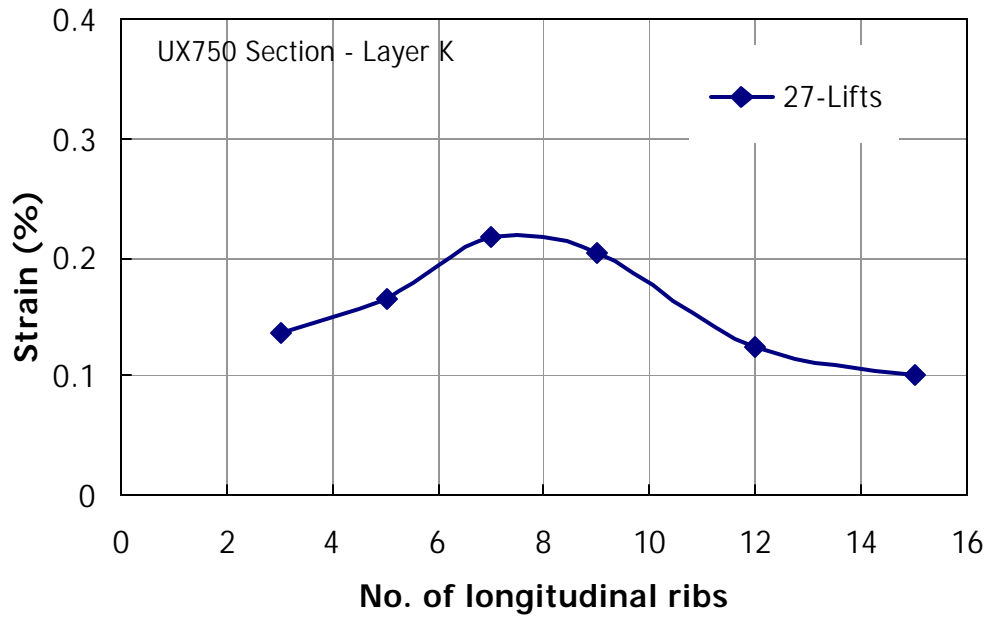
Figure 100
Distribution of strains along the reinforcement in layer K

91

Strains in Section 2 (UX-1400 Geogrid)

The measurements of the strains in the reinforcement layers of section 2 are shown in figures 101 through 112. Refer to table 11 and figure 53 for the locations of the strain gauges on the geogrids. The results show that the maximum strains in the layers at the bottom half of the wall were close and were about 1.5 percent. The locations of the maximum strains in these layers were measured in the third and fourth longitudinal ribs (about 4 to 4.5 ft. from the wall facing). At the top half of the wall, the maximum strains were in the range of 0.4 percent. The figures also show the same trend of strain relaxation at the bottom layers of the wall and strain increase in the top layers after the completion of the wall.

Several strain gauges were installed at the same longitudinal ribs in layer F of the section in order to evaluate the repeatability of the measurements at identical locations. The measurements of the gauges were relatively comparable and are shown in table 13.

Table 13
Results of strain gauges at identical locations

Layer	Location	Strain (%)
F	Rib No. 3	0.16 0.23
	Rib No. 6	0.2 0.19
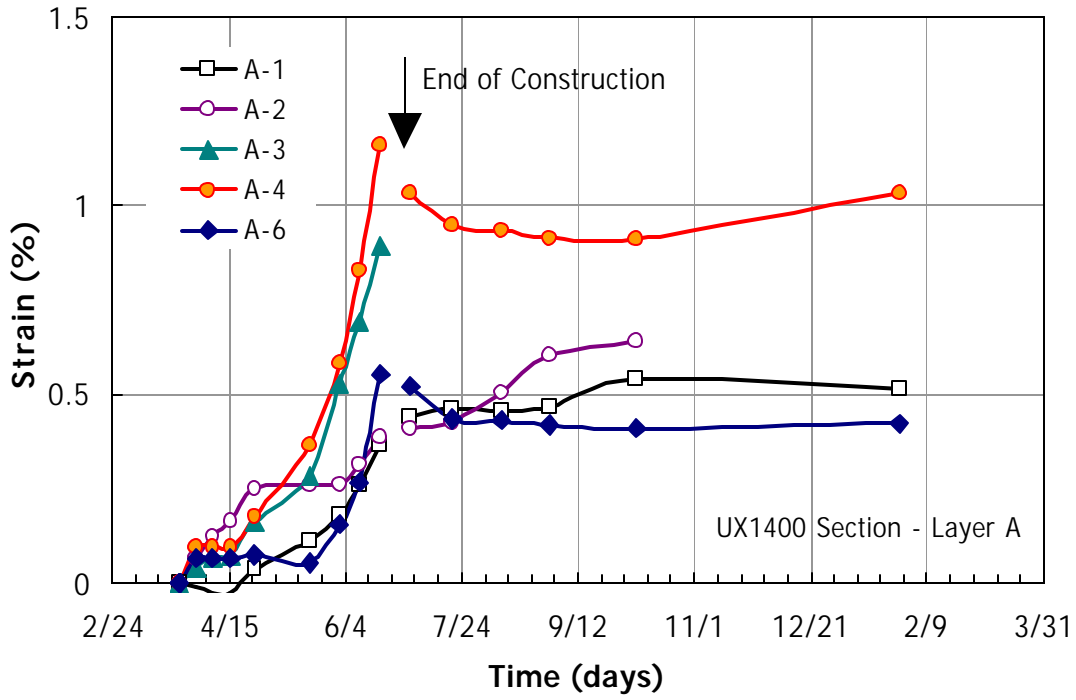
Figure 101
Strain measurements of layer A in test section 2
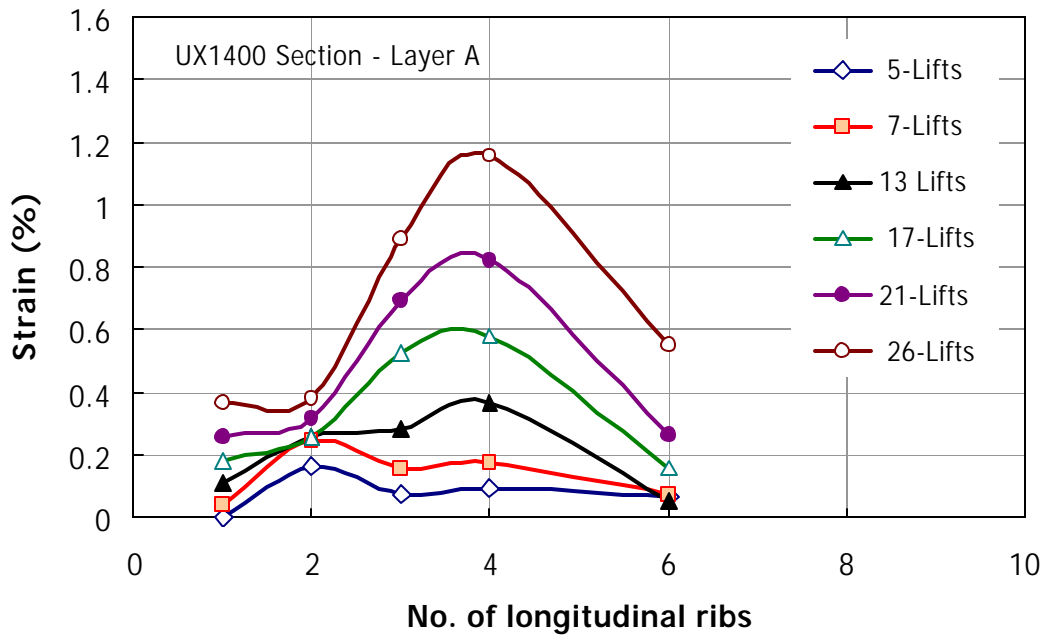
Figure 102
Distribution of strains along the reinforcement in layer A
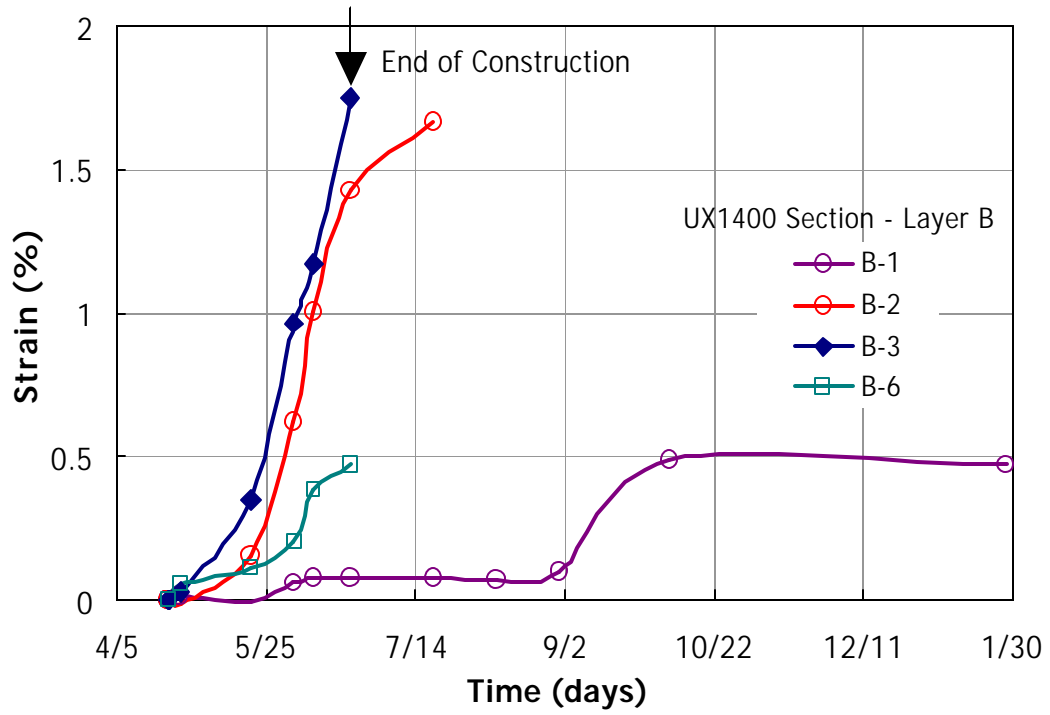
Figure 103
Strain measurements of layer B in test section 2
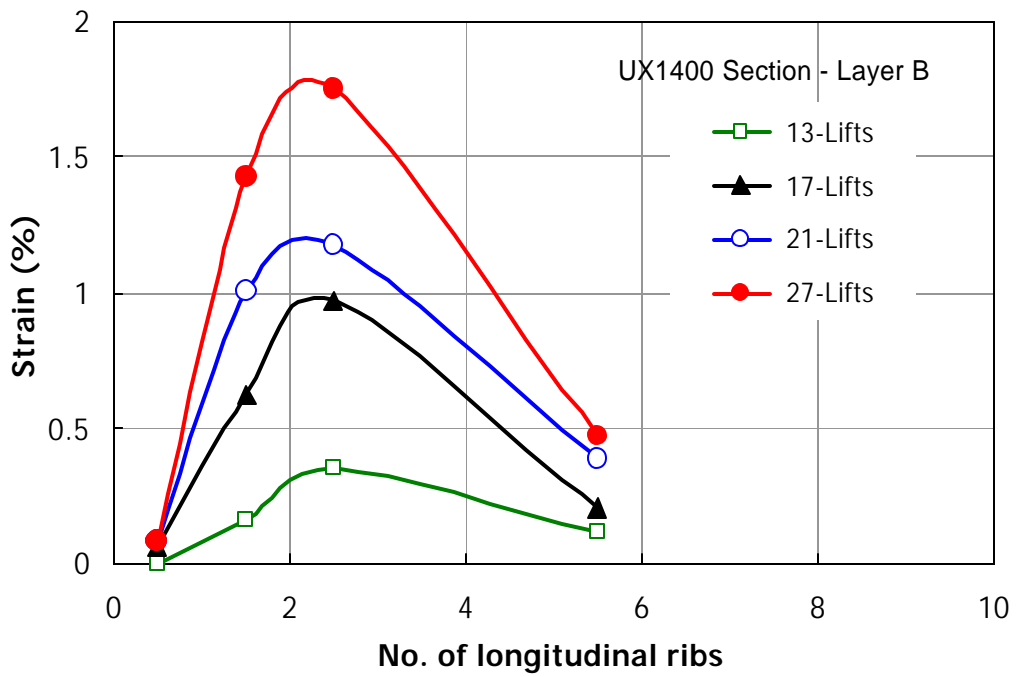
Figure 104
Distribution of strains along the reinforcement in layer B
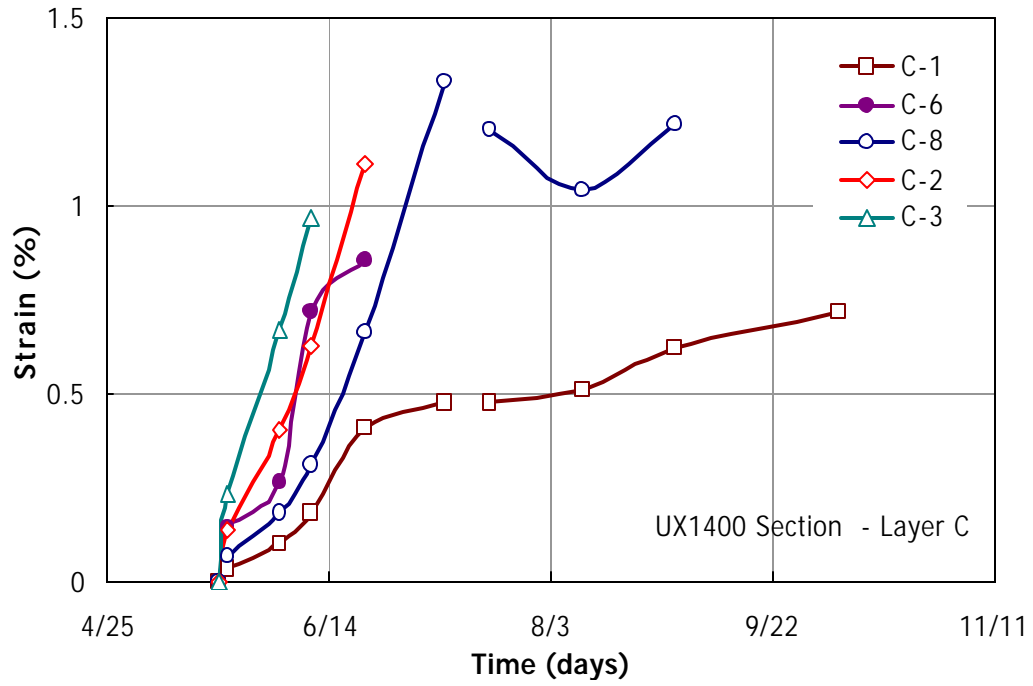
Figure 105
Strain measurements of layer C in test section 2
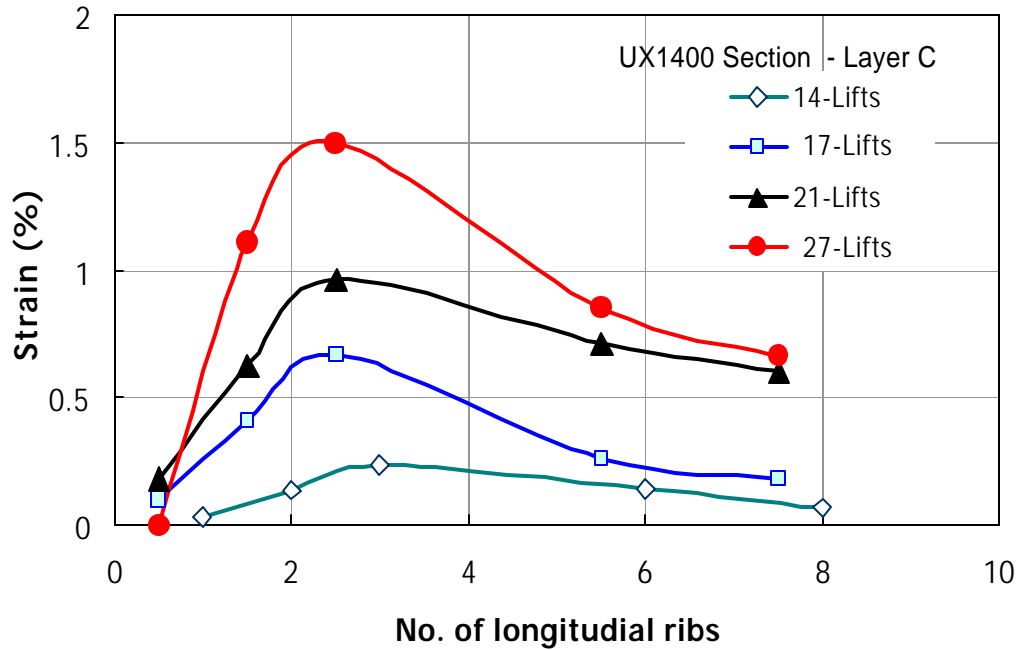
Figure 106
Distribution of strains along the reinforcement in layer C
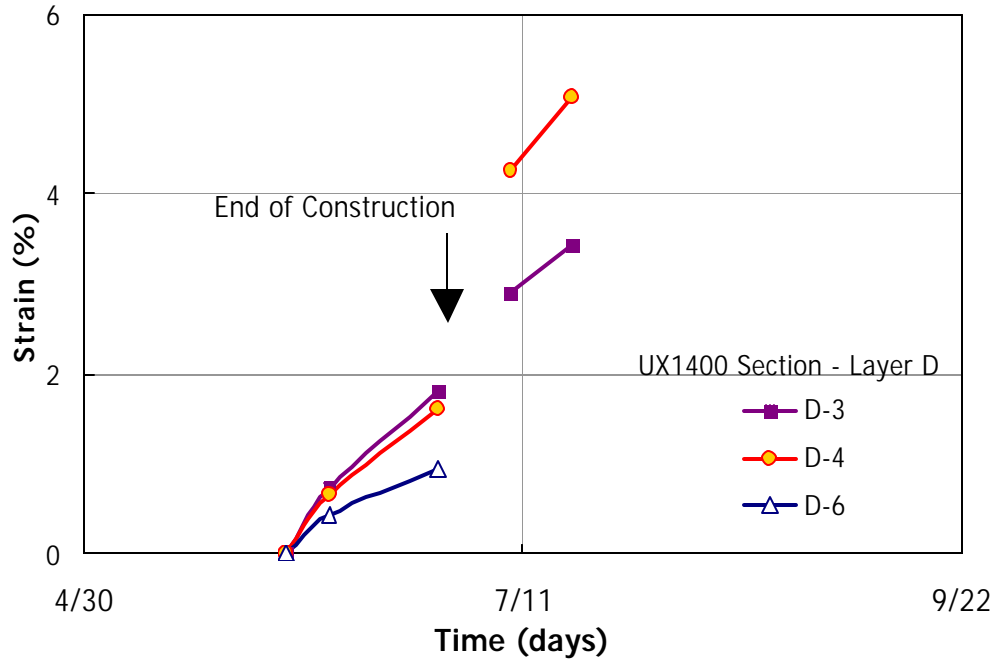
Figure 107
Strain measurements of layer D in test section 2
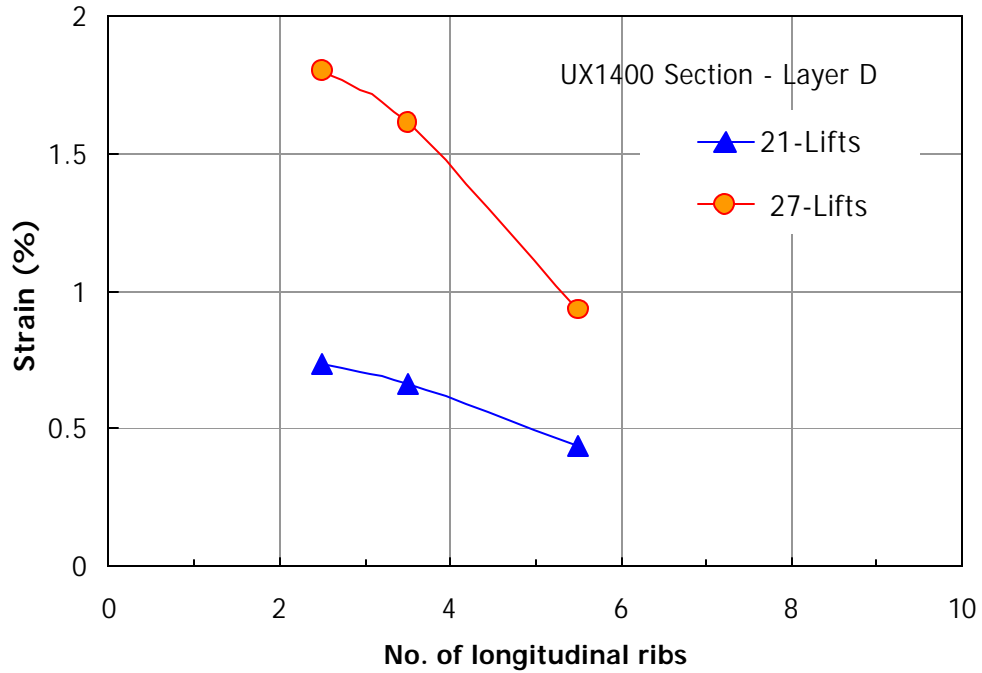
Figure 108
Distribution of strains along the reinforcement in layer D

96
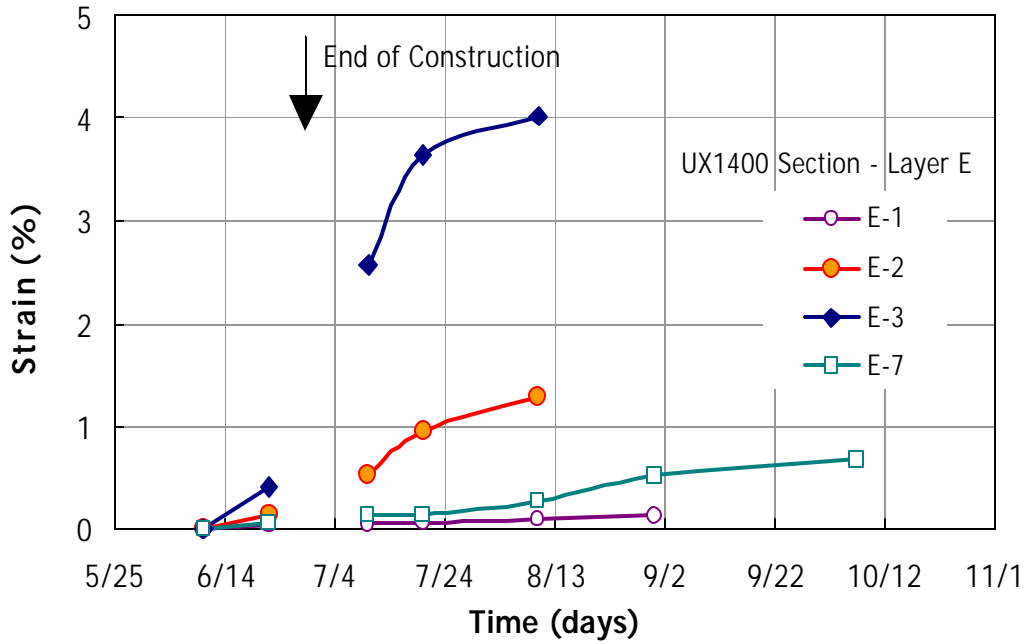
Figure 109
Strain measurements of layer E in test section 2
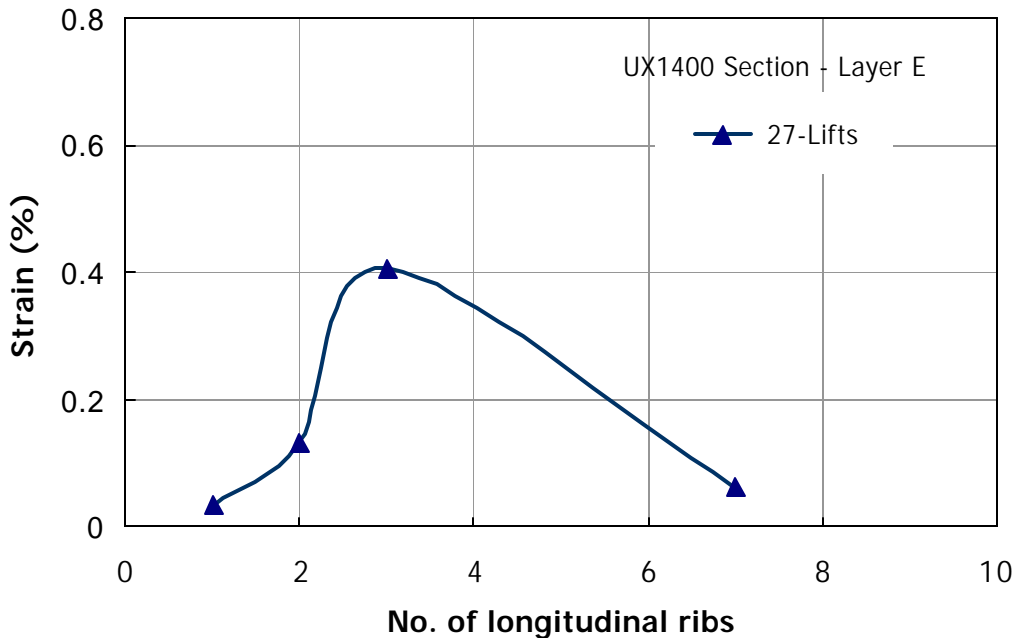
Figure 110
Distribution of strains along the reinforcement in layer E
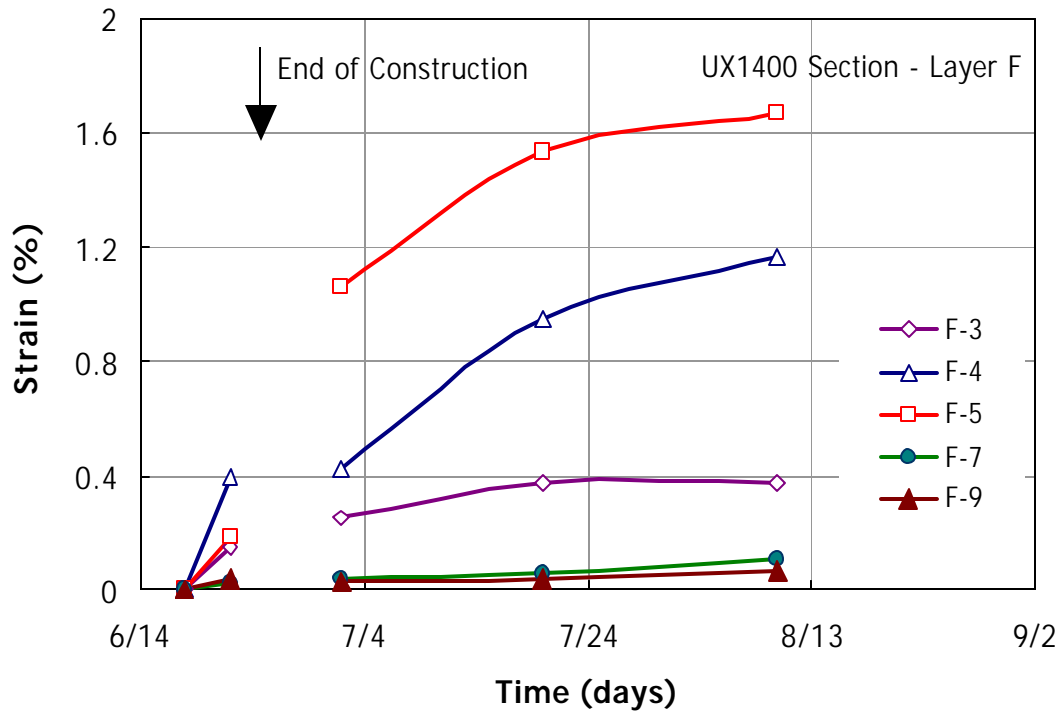
Figure 111
Strain measurements of layer F in test section 2
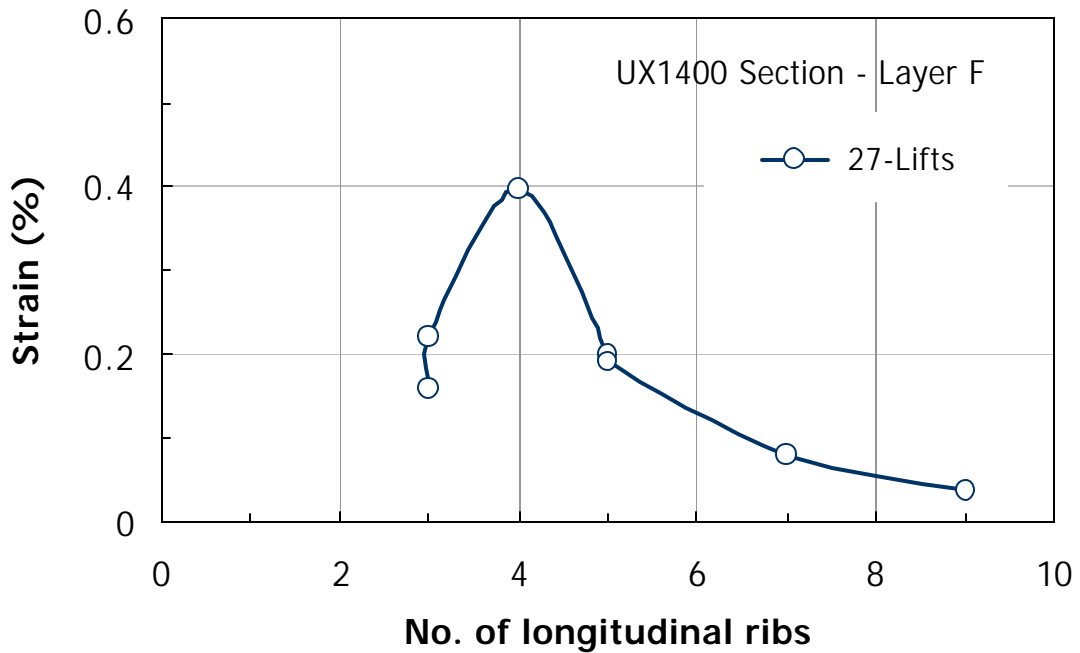
Figure 112
Distribution of strains along the reinforcement in layer F

Strains in Section 3 (UX-1500 Geogrid)

Figures 113 through 120 show the measurements of strains along the geogrids in section 3. Refer to table 12 and figure 55 for the locations of the strain gauges in this section. The locations of maximum strains were closer to the wall facing at the bottom of the wall and were moving further from the facing at the top reinforcement layers. The maximum strain in this section was 1.5 percent and it was measured in the bottom half of the wall.

Strains in Woven Slope

Figures 121 through 129 show the strain measurement at the reinforcement layers of the woven slope section. The strains in the slope section were small compared to the vertical side and reached a maximum value of 0.5 percent at the completion of construction. Most of the strains were reduced in the three-month period after construction with the exception of the top layer E, which showed an increase of strain with time.
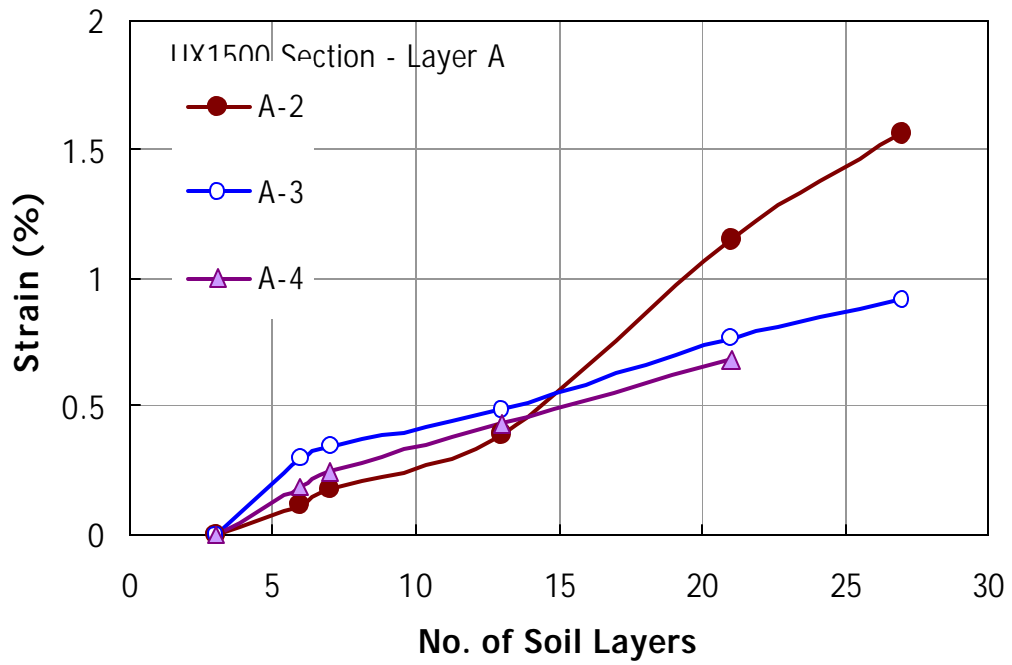
Figure 113
Strain measurements of layer A in test section 3
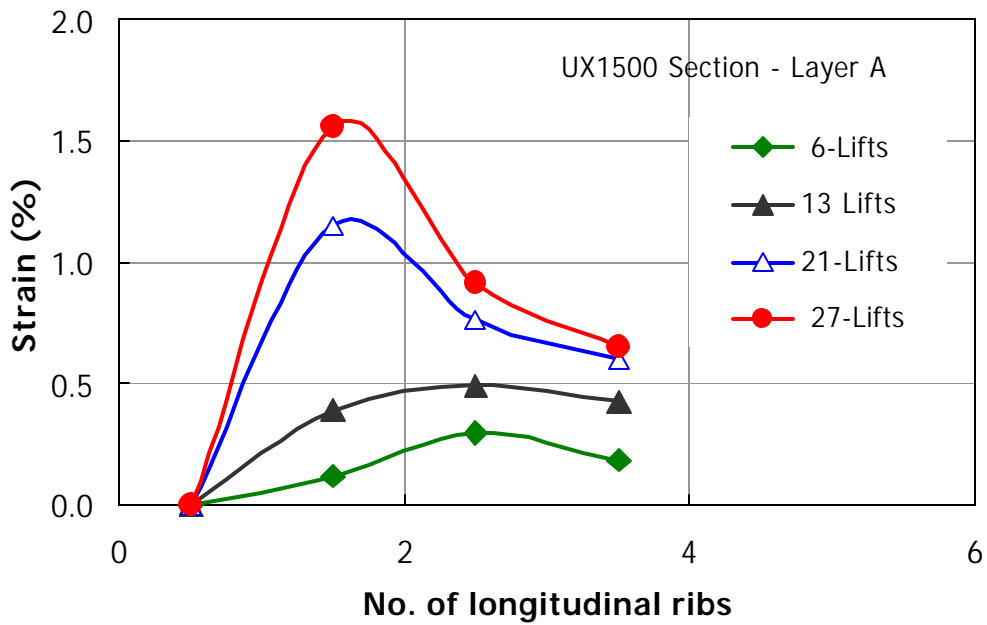
Figure 114
Distribution of strains along the reinforcement in layer A

`

100
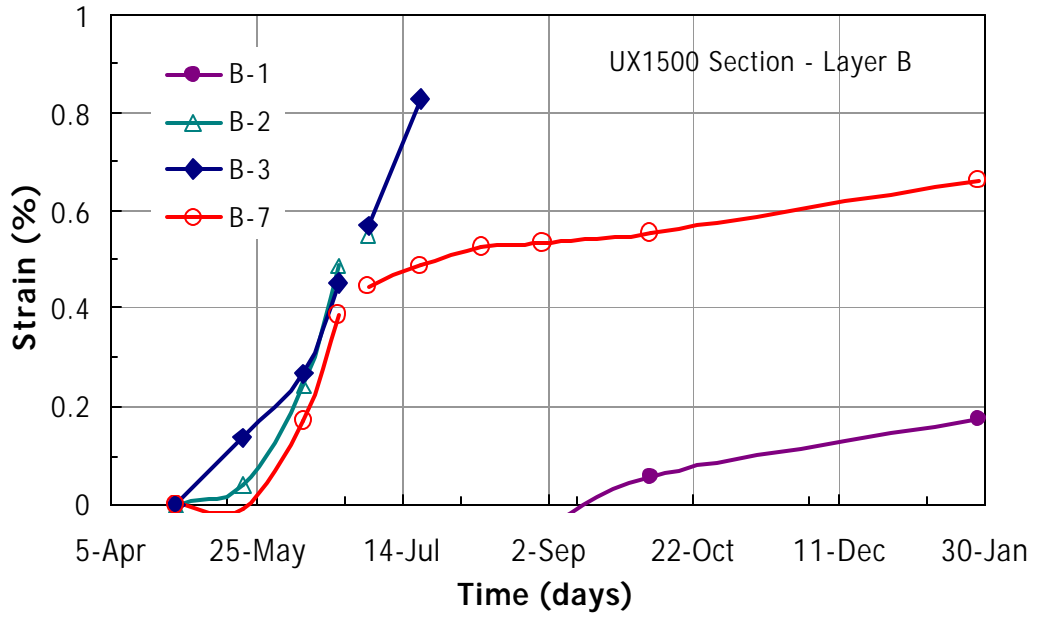
Figure 115
Strain measurements of layer B in test section 3
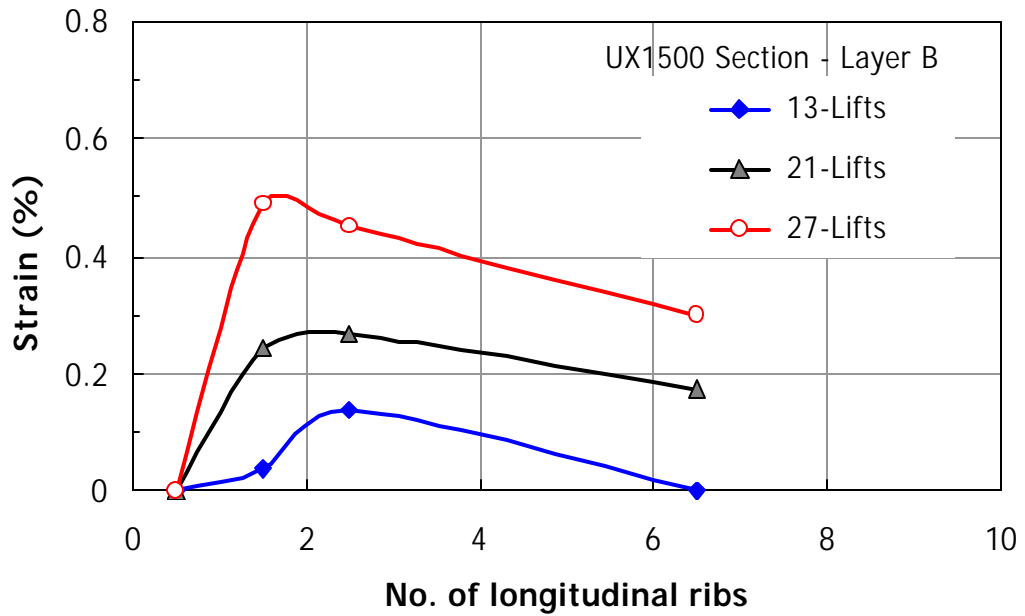
Figure 116
Distribution of strains along the reinforcement in layer B
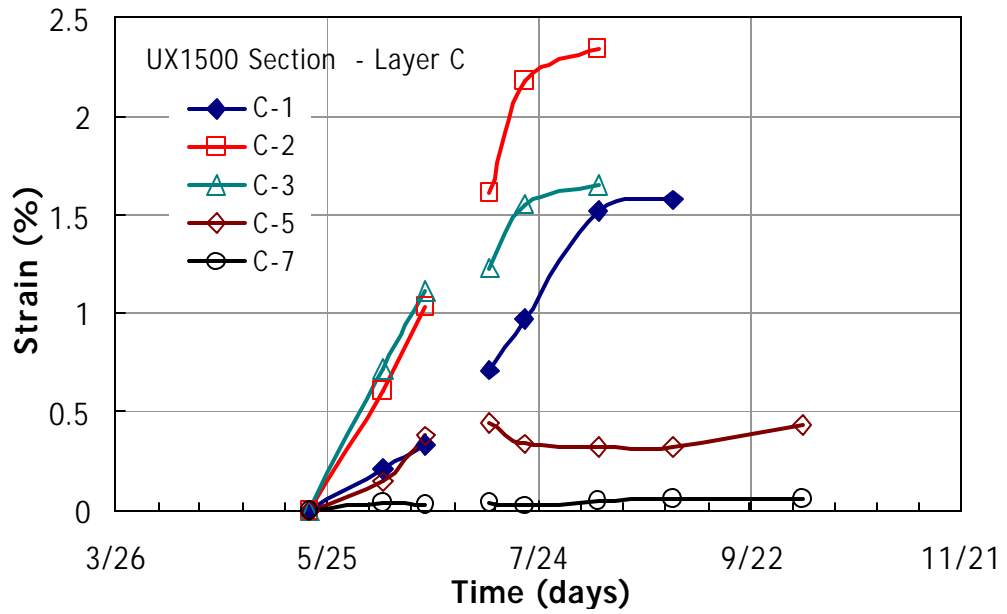
Figure 117
Strain measurements of layer C in test section 3
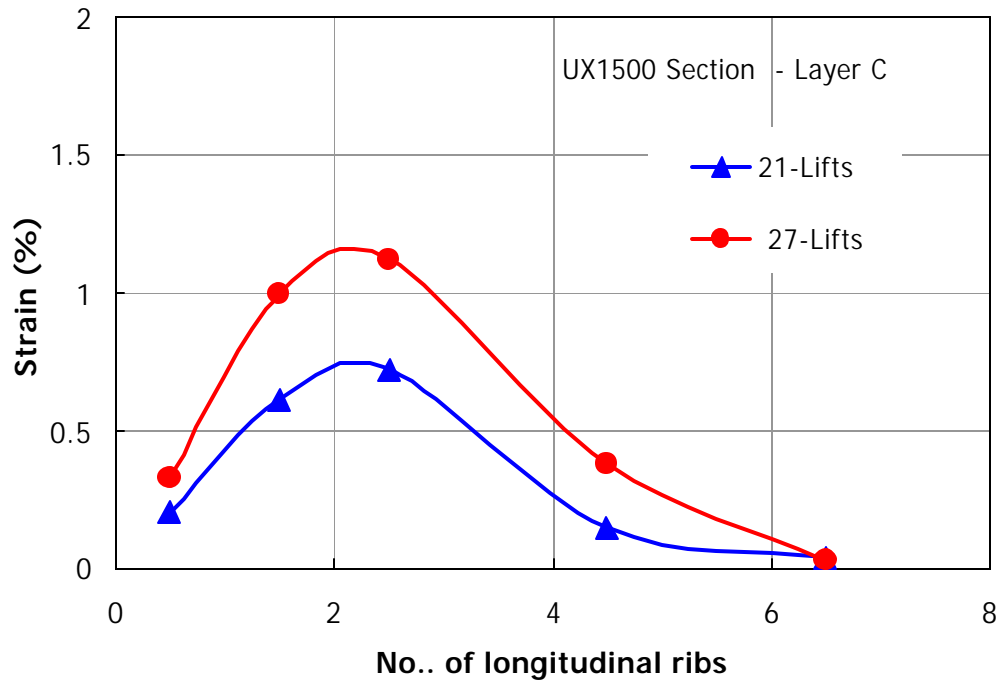
Figure 118
Distribution of strains along the reinforcement in layer C
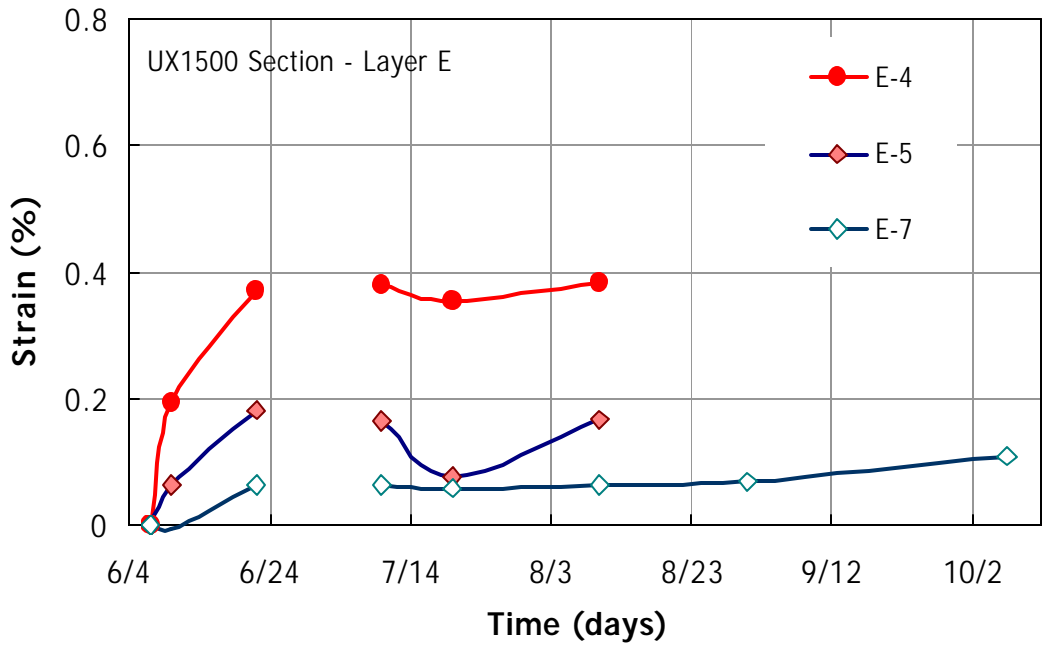
Figure 119
Strain measurements of layer E in test section 3
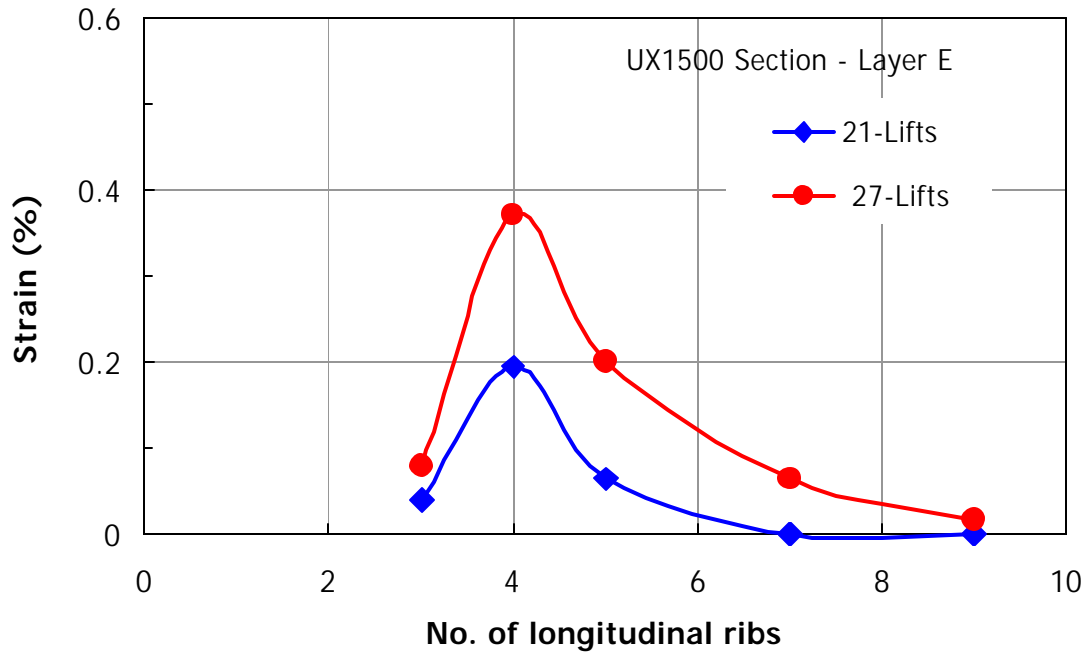
Figure 120
Distribution of strains along the reinforcement in layer E
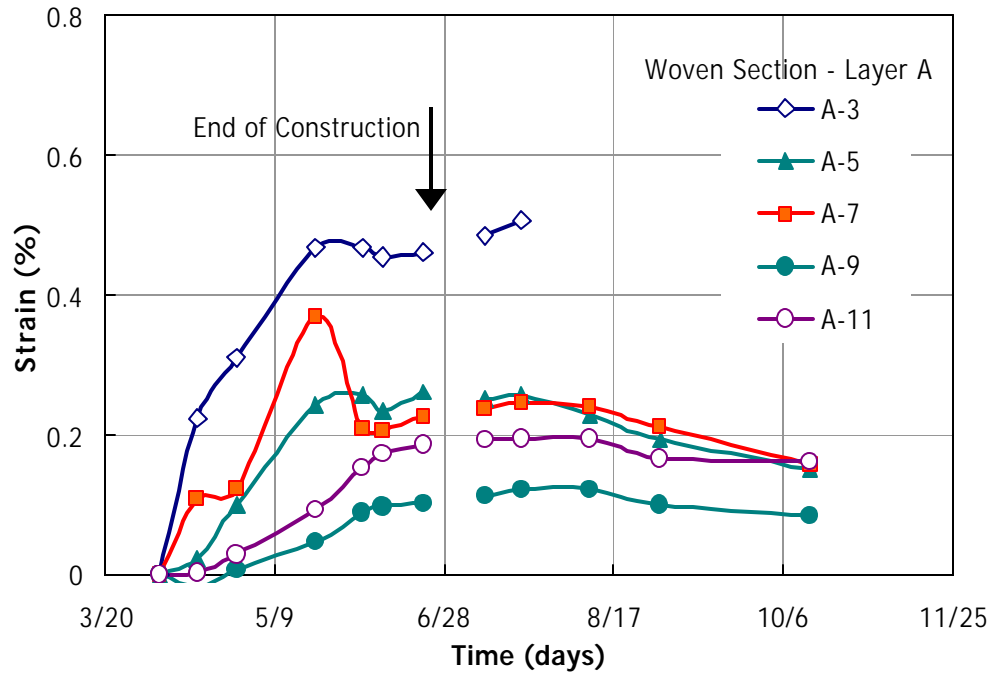
Figure 121
Strain measurements of layer A in woven section
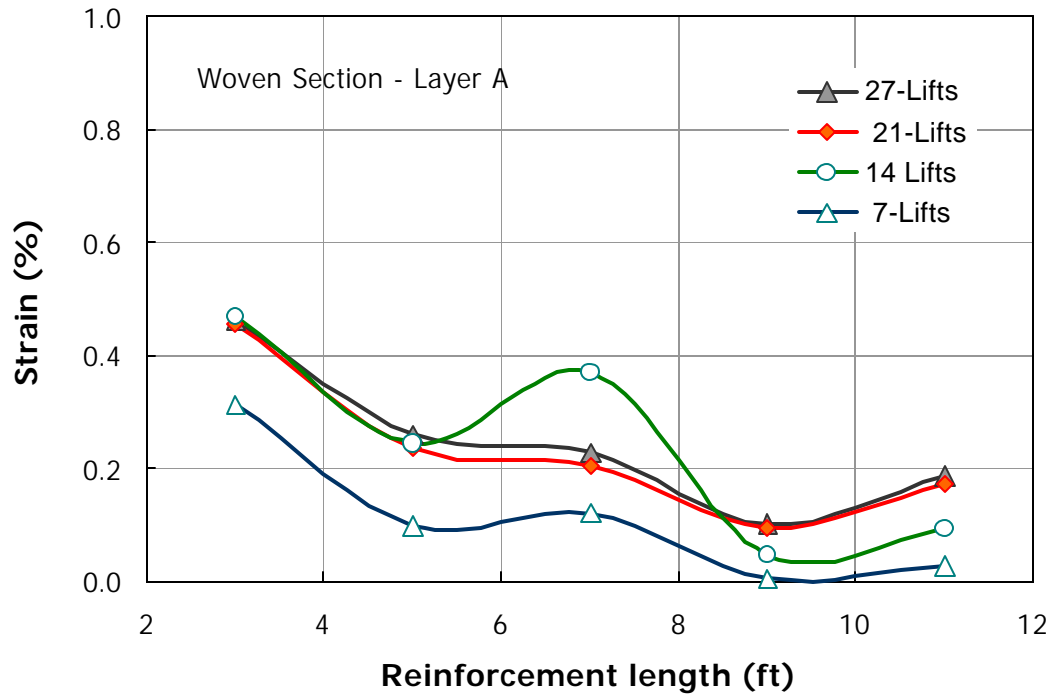
Figure 122
Distribution of strains along the reinforcement in layer A
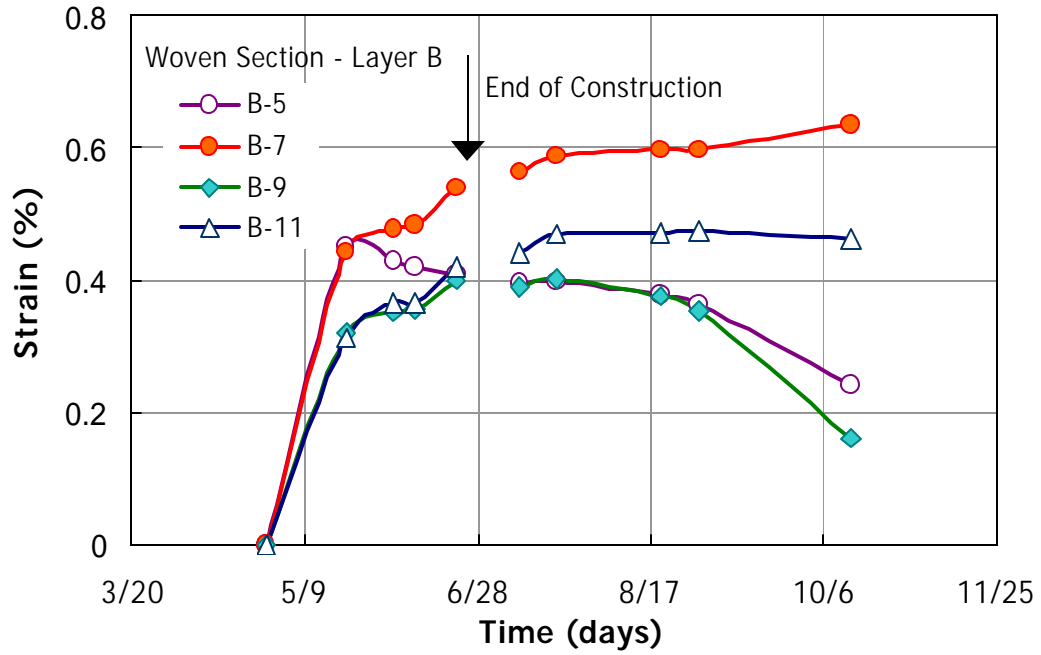
Figure 123
Strain measurements of layer B in woven section
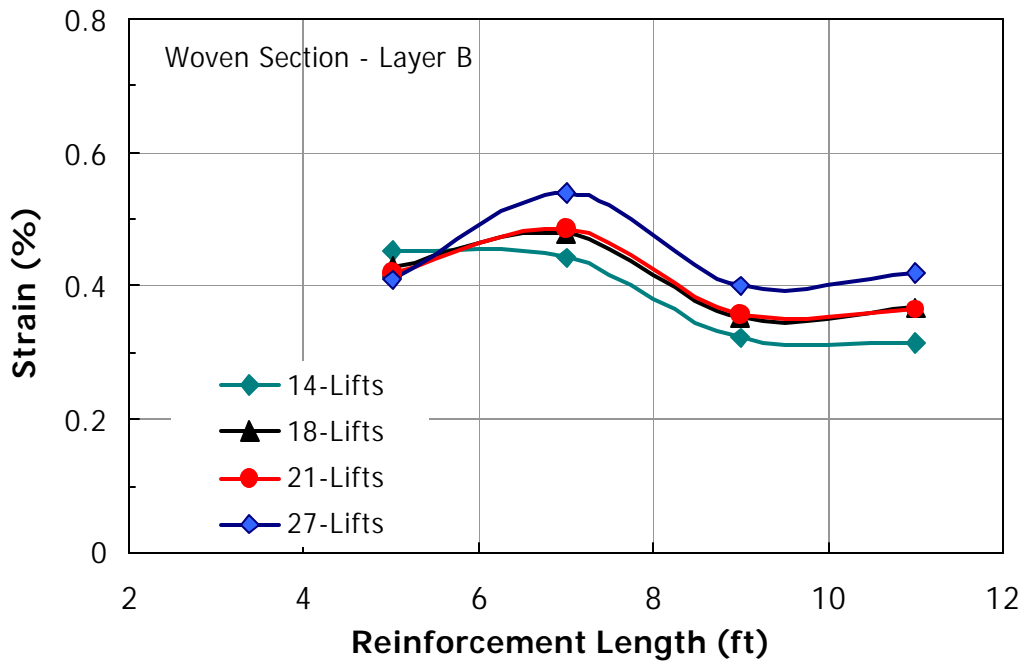
Figure 124
Distribution of strains along the reinforcement in layer B

105
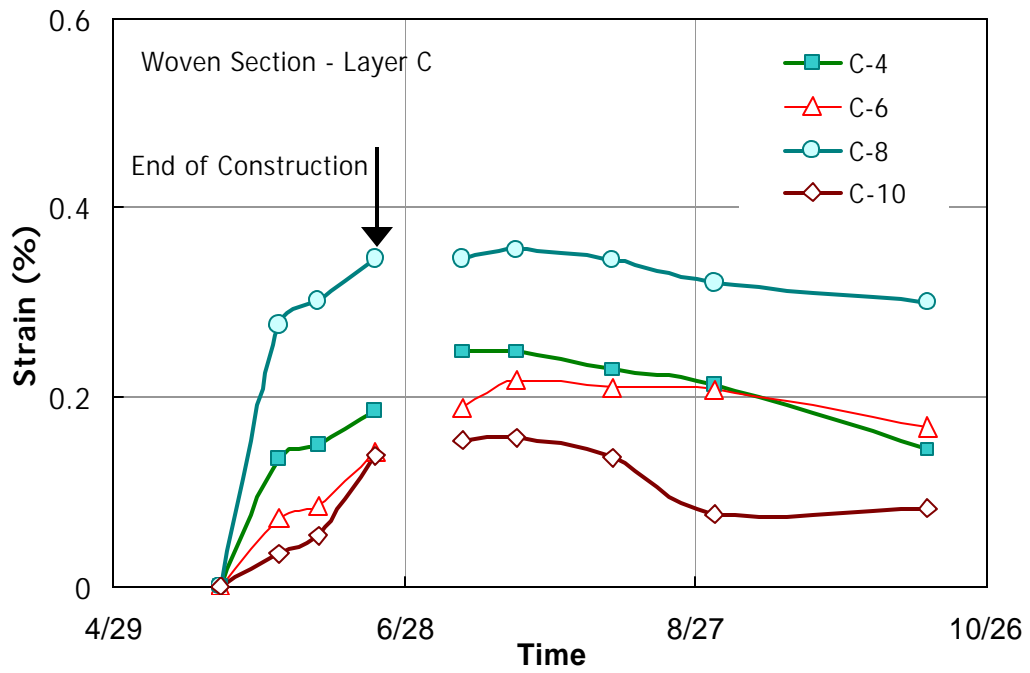
Figure 125
Strain measurements of layer C in woven section
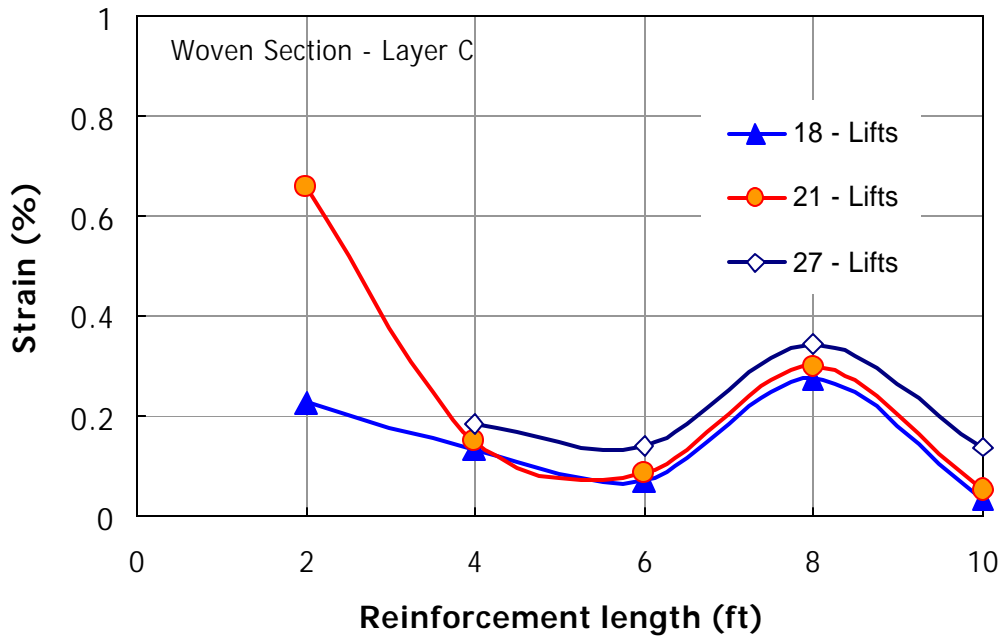
Figure 126
Distribution of strains along the reinforcement in layer C
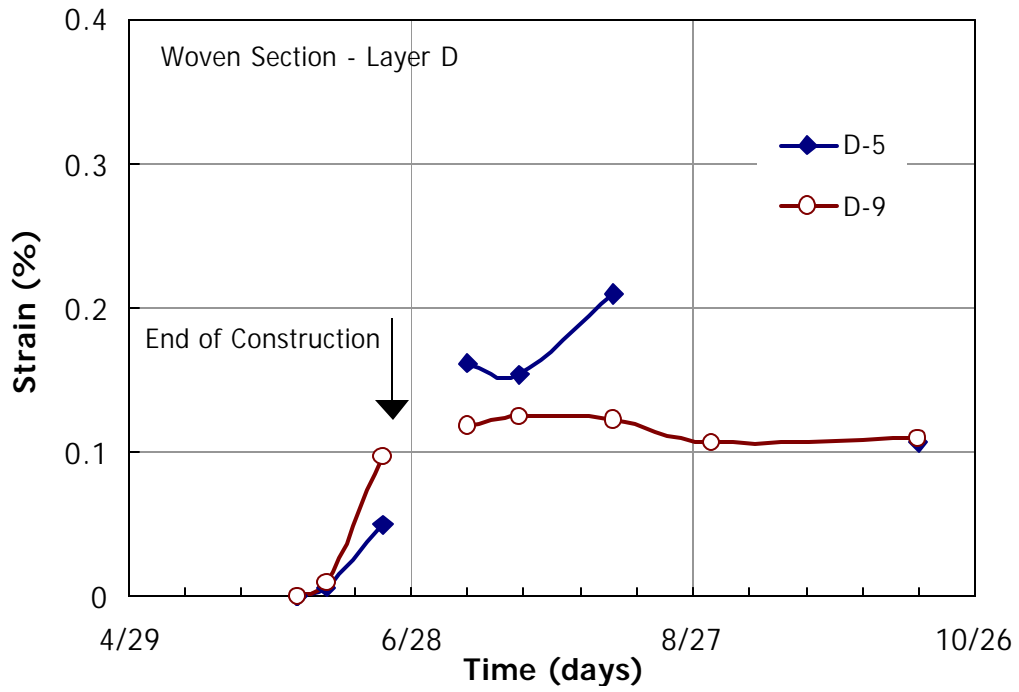
Figure 127
Strain measurements of layer D in woven section
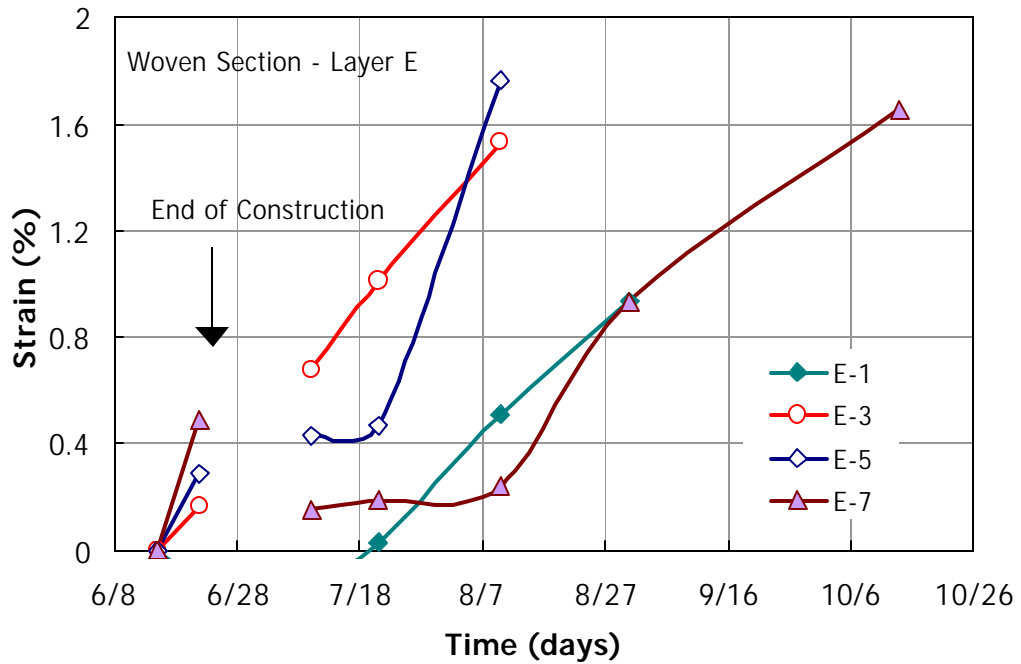
Figure 128
Strain measurements of layer E in woven section
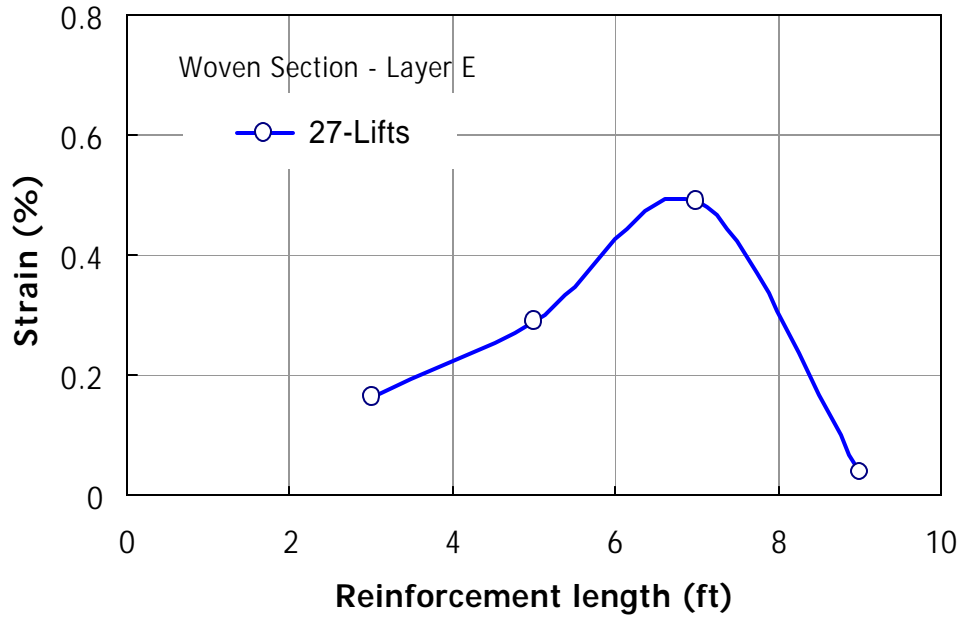
Figure 129
Distribution of strains along the reinforcement in layer E

Performance of the Geoweb Section

The measurements of the vertical inclinometer in the Geoweb section (figure 77) showed maximum deformation of 0.6 in. at the top of the wall during construction and negligible movement after construction of the section.

A 5-ft. diameter corrugated drainage pipe was installed in the section to evaluate the effect of wall settlement on the deformation of the pipe. The Geoweb cells formed a gravity type wall that did not provide the horizontal pressure required to resist the horizontal deformation of the pipe. Furthermore, it was difficult to compact the soil inside the Geoweb cells. Accordingly, excessive horizontal deformation occurred in the pipe during construction due to the weight of the wall above the pipe. An additional support system was provided at the end of construction to restrain pipe deformation. Figure 130 shows pipe deformation at the late stage of wall construction.

108

Figure 130
Deformations of the circular pipe at the end of construction

Performance of the Test Wall

The measurements of strains during the construction of the vertical wall are shown in figures 131, 132, and 133 for the three test sections 1, 2, and 3, respectively. The figures show the strain distribution along the reinforcement at selected layers and the locus of maximum strains in the wall. The comparative performance of the three sections during constructions can be summarized as follows:

- Maximum reinforcement strains occurred in section 1 (weak geogrid – minimum spacing). Strain of 3.5 percent was mobilized in the bottom third of the section (layer D). In section 2 (strong geogrid – maximum spacing), the maximum strain of 2 percent was measured at mid-height of the wall (layer D). Maximum strain in section 3 was 1.2 percent and was at the bottom third of the wall height (layer C).

- The result of the inclinometer readings and survey of the wall facing also showed more deformations in section 1 and that it was more "flexible" system than sections 2 and 3.

- The strain curves along the reinforcement had a defined peak at the lower layers of the wall. Maximum strains at the top layers were spread over a wider length of the reinforcement.

- The locations of maximum strains were defined at early stages of construction. Maximum strains in section 1 occurred at the bottom third of the wall while maximum strains in section 2 were in the middle half of the wall. Figure 134 shows the distribution of strain along the height of the wall during construction.

- The locus of maximum strains in the three sections formed an angle less than the theoretical k_a failure surface of angle $(45 + \varphi/2)$.

- Measurements of strains near the facing show that the strains were mobilized at the connections between the reinforcement and the modular blocks only at the upper half of the wall.

- Sections 1 and 2 had higher strains at the facing than section 3. Moreover, the strains at the facing in section 1 were almost equal to the maximum strains in the reinforcement.

The strain measurements for the woven slope sections are shown in figure 135. The figure shows low strain levels in the reinforcement with a maximum value of 0.5 percent. The locus of maximum strains had almost equal distance from the facing in most layers, suggesting that a linear slip surface better represents the locus of maximum stresses. High strains were also measured at a distance of 2 ft. from the slope facing.

Estimation of Failure Surface

The critical failure surface is assumed to coincide with the locus of maximum strain in each reinforcement layer. The assumption of Rankine's failure surface of (45 + ϕ/2) with the horizontal is usually assumed for extensible reinforcement [1], [2]. Strain measurements show that the locus of the slip surface differed in the three test sections. The locations of maximum strains are plotted in figure 136. The figure shows that maximum strains coincided with the (45 + ϕ/2) line only at the bottom halves of the sections. A bilinear slip surface better represented the locus of maximum strains in the section 1 and a line at almost equal distance from the wall facing better represented the locus of maximum strains in section 2.
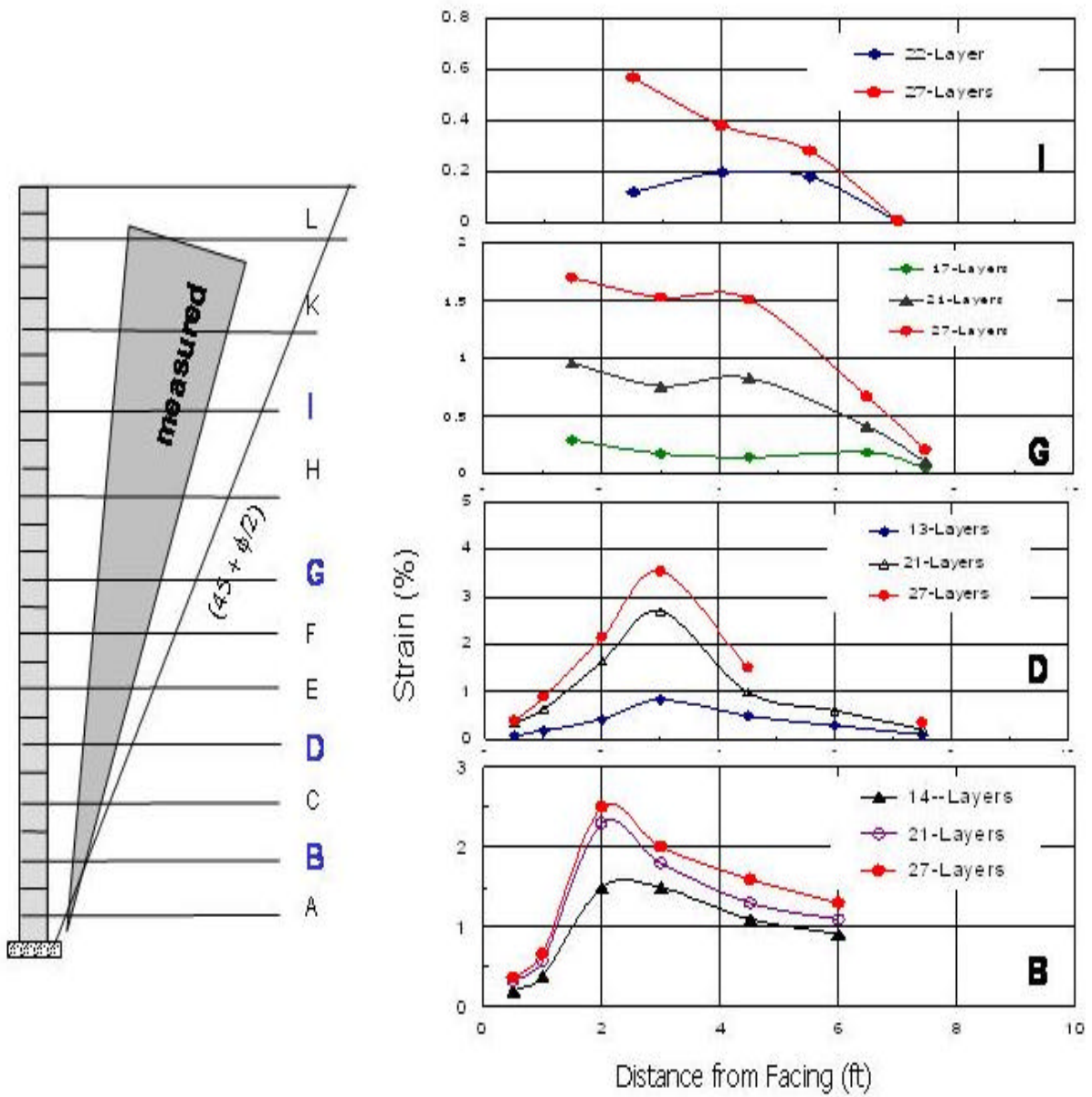
Figure 131
Mobilized strains in the reinforcement in section 1
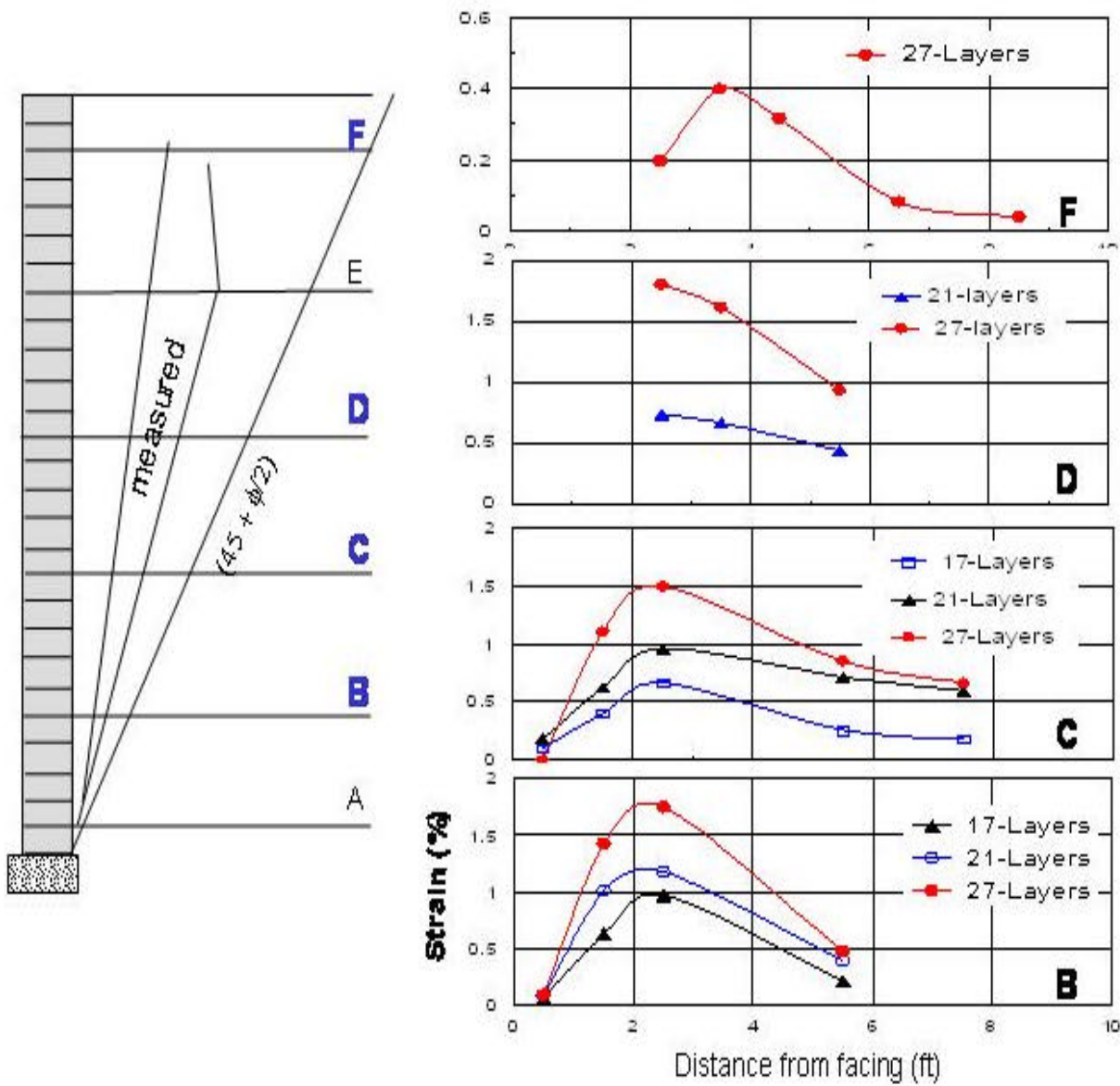
Figure 132
Mobilized strains in the reinforcement in section 2
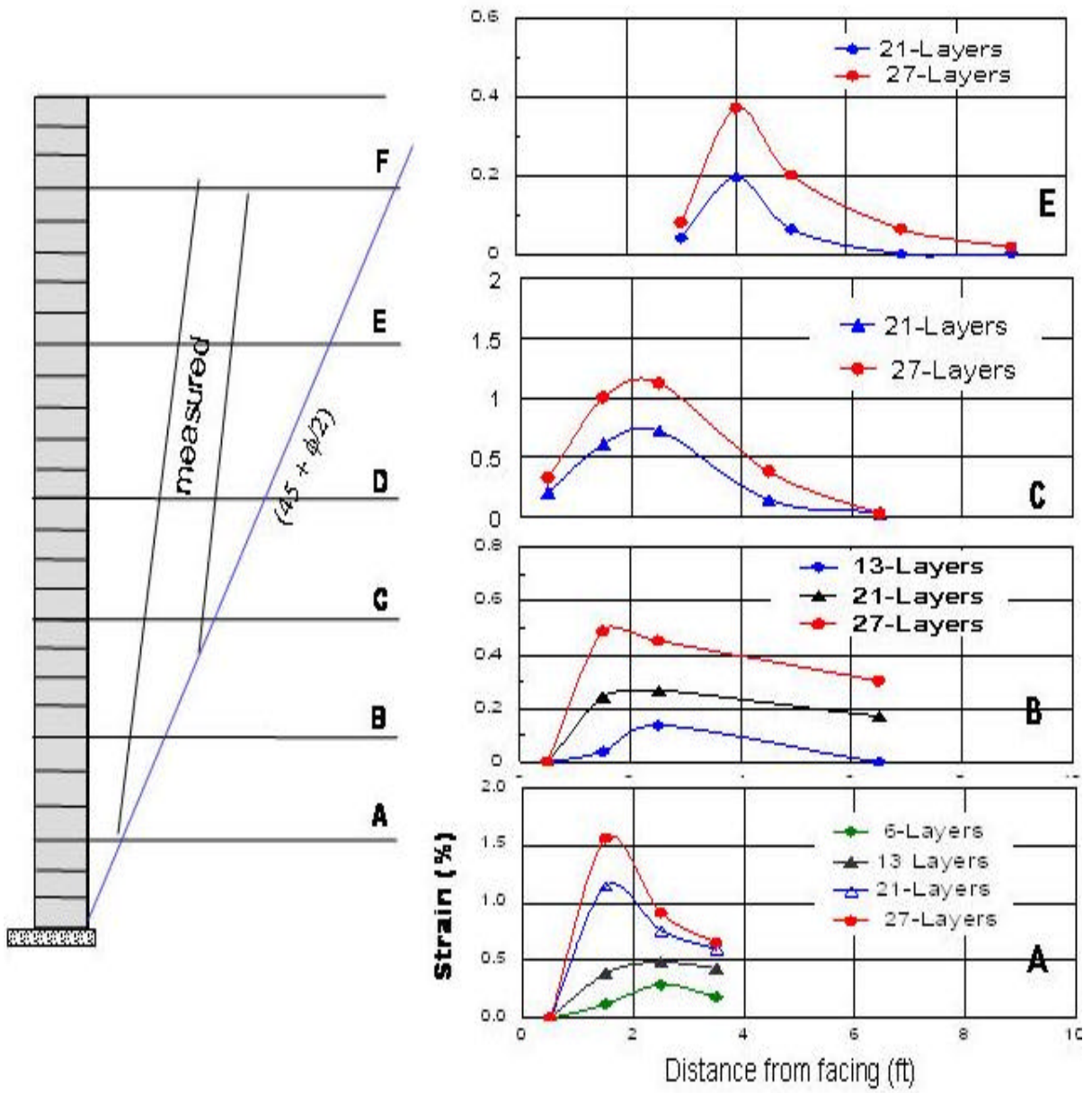
Figure 133
Mobilized strains in the reinforcement in section 3
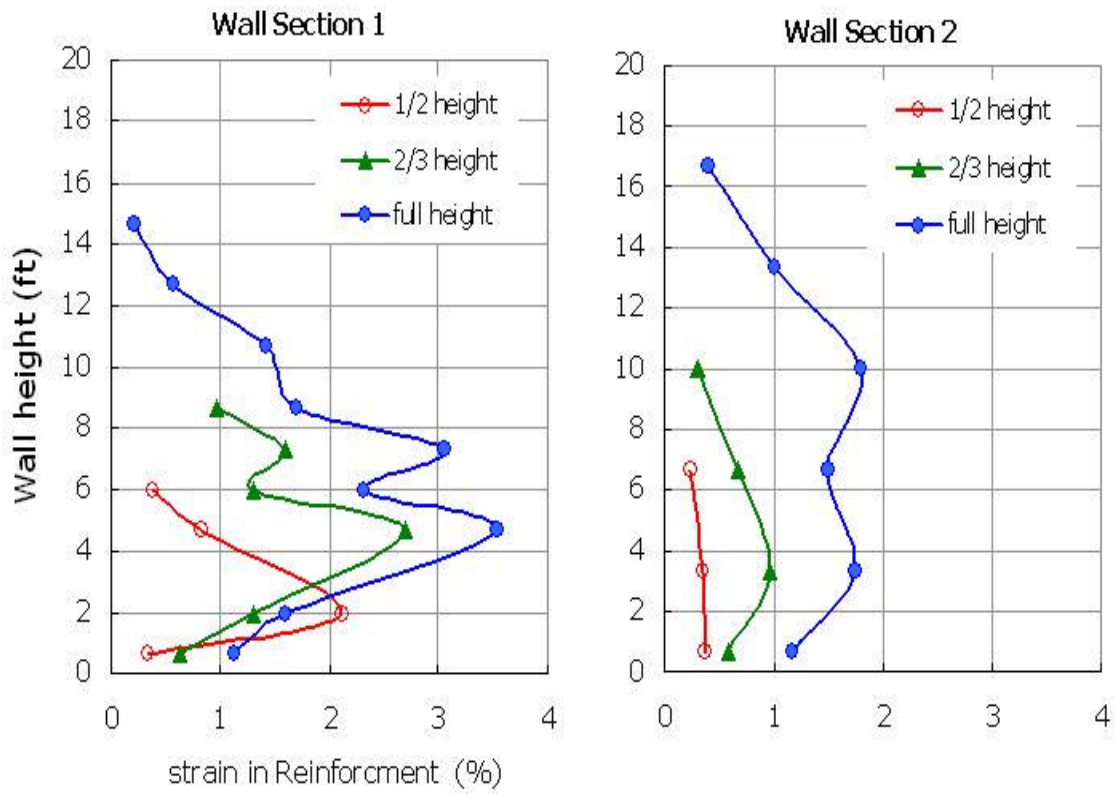
Figure 134
Profiles of maximum strains during construction
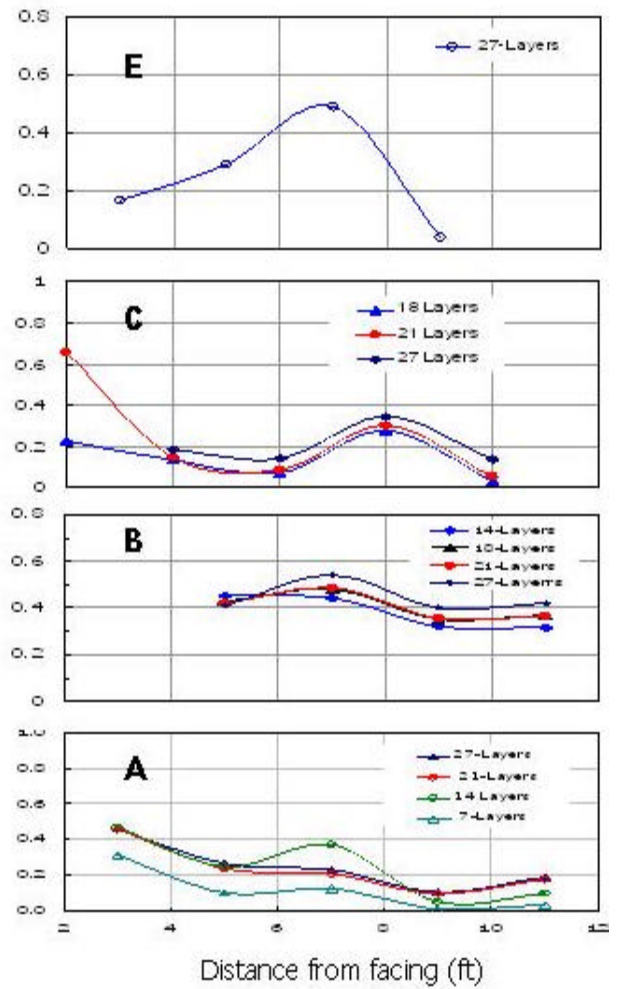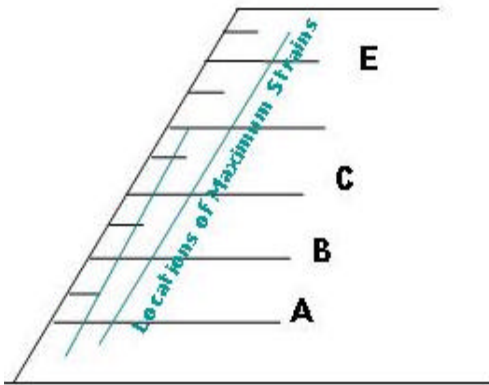
Figure 135
Mobilized strains in the woven slope section
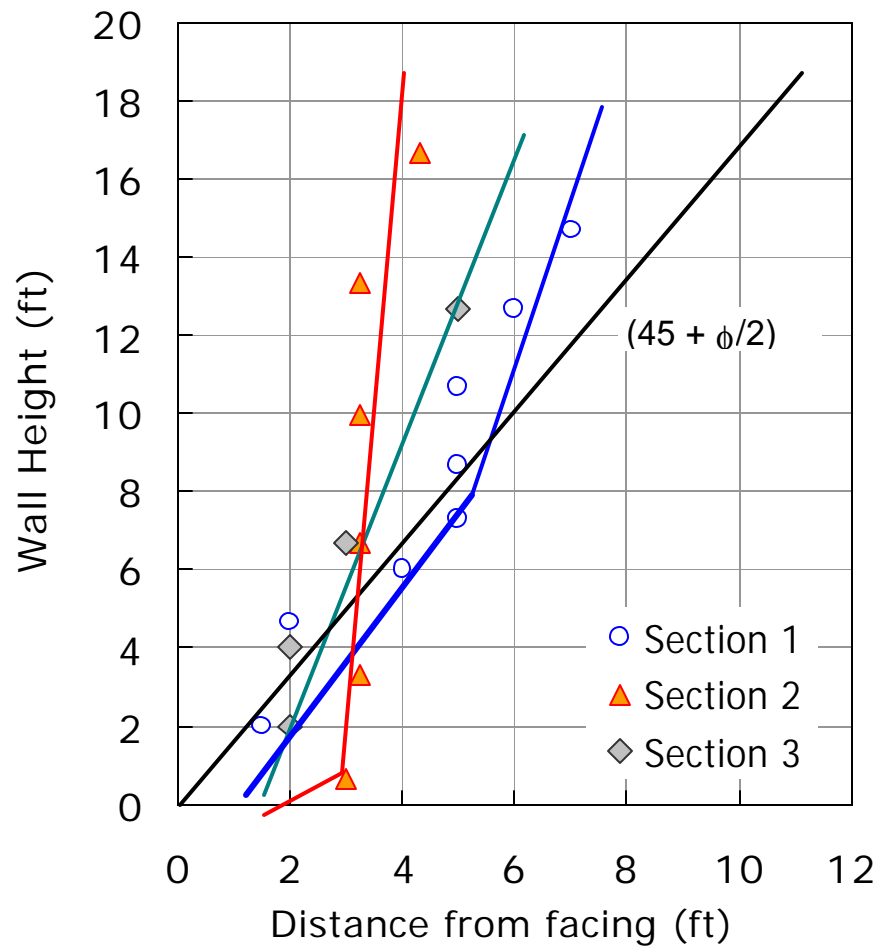
Figure 136
Locus of maximum strains in the test sections

Estimation of Reinforcement Stresses

The magnitude of the mobilized strains (and consequently, stresses) in the reinforcement depends mainly on reinforcement strength, its spacing, and soil-reinforcement interaction properties. This dependency is demonstrated in the relationship:

$$T_{max} = K \, (\gamma h) \, S_h \, S_v \tag{1}$$

Where T_{max} is the maximum tensile stress mobilized in the reinforcement layer, K is the coefficient of the horizontal stresses mobilized in the reinforcement level, γ is soil unit

weight, h is soil height above the reinforcement, S_h is the horizontal spacing (equals one unit length for the geogrid), and S_v is the vertical spacing.

The lateral earth pressure coefficient K is the challenging factor in estimating stresses in reinforced walls and it depends primarily on the soil-reinforcement interaction properties and the extensibility of the reinforcement. Based on measurements in reinforced walls, the state-of-practice design procedures assume K to be equal to the active earth pressure K_a for extensible reinforcement [1], [7]. By rearranging equation 1, the value of K can be evaluated by plotting the normalized tensile stresses ($T_{max} / \gamma h\ S_h\ S_v$) for each reinforcement layer as shown in figure 137. In the figure, the values of T_{max} were calculated from the measured strains and the stiffness modulus of the geogrids. The geogrid stiffness modulus was assumed to equal the initial slope of the stress-strain curves of the geogrids in confined extension tests. The distribution of normalized stresses in the figure shows that:

- Low tensile stresses are commonly developed at the first reinforcement layer near the wall base due to the effect of the rigid base soil, which restrains the horizontal deformation. This is consistent with many other measurements in the field and in model walls [8], [9].
- The lateral earth pressure coefficient K (and consequently the normalized stresses) in section 1 increased with depth till a maximum value near the bottom third of its height. For section 2, the stresses were approximately uniform throughout most of the wall height. The stresses in wall C increased linearly with depth with values less than K_a.

118
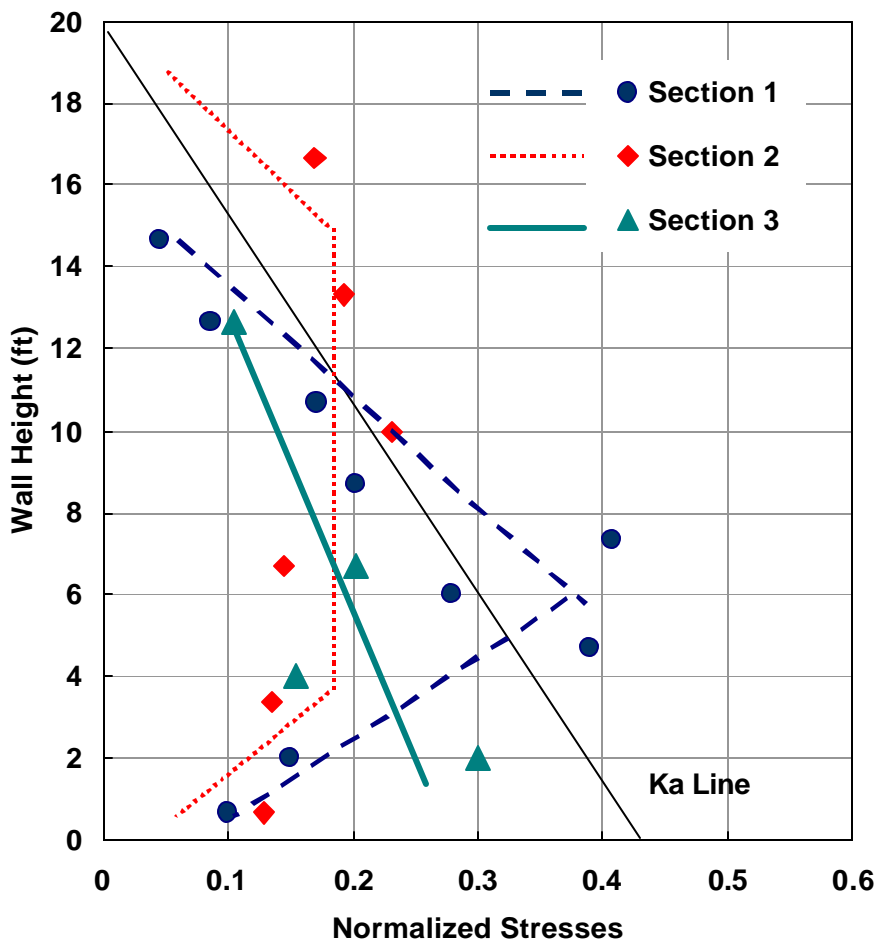
Figure 137
Variations of normalized stresses with wall height

CONCLUSIONS

The performance of the test wall was monitored to evaluate the use of low quality silty-clay soil as a backfill, to investigate the interaction mechanism between various geosynthetic materials and the soil, and to monitor the state of stresses and deformations of the wall test sections. The LTRC test wall was designed to produce measurable deformations in the test sections. Consequently, the results of the instrumentation program showed relatively higher deformations than in conventionally designed walls. The high deformations were mainly due to the design of the wall with low factors of safety and the high settlement of the base soil. The various configurations of the wall design, however, provided a flexible system that could stand the deformations.

The settlement of the wall was monitored using survey points at the wall facing, settlement plates, and horizontal inclinometers. The measurements of these instruments were comparable and showed a maximum settlement of 11 in. at the completion of construction. The maximum settlement occurred below the vertical wall and linearly decreased below the slope section. However, the measurements of the horizontal inclinometers showed that the settlement below the reinforced section of the wall (11 ft. length of reinforcement) was approximately uniform. Consequently, strain measurements of the reinforcement were not affected by the settlement of the wall.

The measurements of earth pressures near the wall facing displayed the slow increase of vertical earth pressure during the early stages of construction followed by a sharp increase during the later and faster construction period. However, the measurements were less than the theoretical values calculated from soil weight, and they decreased after the completion of construction due to wall settlement. The low values of vertical soil pressures near the facing are possibly due to the facing boundary effect as a portion of the vertical load is carried out by the frictional resistance of the modular blocks at the facing.

The results of the instrumentation of the test wall demonstrated the performance of various configurations of geometry and strength of geosynthetics in silty-clay soil. Section 1 of the

wall (weak geogrid – minimum spacing) had the highest deformations. At the completion of construction, section 1 had a maximum deformation of about one inch near the top of the wall. A maximum strain of 3.5 percent was monitored at the bottom third of the section. However, the strains in the reinforcement were reduced during the four-month monitoring period after the construction of the wall.

The maximum horizontal deformation of section 2 (stronger geogrid – maximum spacing) was 0.65 inches after construction. The maximum reinforcement strain was 2 percent and occurred at the mid-height of the wall. Section 3 demonstrated lower deformations and the maximum strain in the reinforcement was 1.2 percent near the mid-height of the wall.

Strain measurements were utilized to estimate the state of stresses in the reinforcement. The results showed that the distribution of reinforcement strength in the layers varied with the change of reinforcement stiffness modulus and its density in the wall sections. The assumption of Rankine's failure surface of slip angle $(45 + \phi/2)$ is usually assumed for extensible reinforcement. However, the results in Figure 135 showed that this assumption did not accurately represent the critical failure surface in the three wall sections.

The concept of normalizing reinforcement strength in the term ($K = T_{max} / \gamma h\ S_h\ S_v$) was used to define the relative "rigidity" of the wall and to determine the horizontal earth pressure coefficient of the wall (K). The results showed that the value of the coefficient K was less that the theoretical K_a value in the three wall sections. The values of K in figure 137 give more appropriate estimation of the lateral earth pressure coefficients for the three configurations of the test sections. The results suggest a bilinear stress distribution in section 1 (weak geogrid – minimum spacing) and a trapezoidal distribution in the strong-geogrid-maximum spacing surface. The stress distribution in section 3 was closer the surface than the Rankine's failure surface.

The performance of the reinforced slopes suggests the applicability of using woven and non-woven geotextiles in reinforcing steep one-to-one slopes. There were no results that

determine an advantage of using one type of geotextile over the others. The use of non-woven geotextiles as a drainage media between the soil layers was not investigated.

The measurements of the Geoweb sections showed negligible deformations after construction. The system, however, required additional efforts for aligning, backfilling, and compacting the soil inside the cells. The system was flexible to stand the high settlement of the foundation soils but it did not provide the required horizontal support for the embedded pipe. Consequently, large deformations were monitored in the corrugated steel pipe.

REFERENCES

1. *Mechanically Stabilized Earth Walls and Reinforced Soil Slopes, Design and Construction Guidelines*, Federal Highway Administration, Report No. FHWA-SA-96-071, 1998.

2. *Standard Specifications of Highway Bridges*, AASHTO, 1992.

3. K. Farrag, and M. Morvant, *Evaluation of Interaction Properties of Geosynthetics in Cohesive Soils: Laboratory and Field Pullout Test*, Louisiana Transportation Research Center, Report Number 380, 2003.

4. Measurement Group, "High Elongation Strain Measurements," Technical Note No. TT-605, 1983.

5. Measurements Group, "Strain Gauge Measurements on Plastics and Components," Technical Note, 1988.

6. Measurements Group, "Surface Preparation for Strain Gauge Bonding," Technical Note No. B-129.

7. *Geosynthetics Design and Construction Guidelines*, Federal Highway Administration, Report No. FHWA-HI-95-038, 1998.

8. Allen, T., Christopher, B., and Holtz, R., "Performance of a 12.6 m High Geotextile Wall in Seattle, Washington," Proceedings, *International Symposium on Geosynthetic-Reinforced Soil Retaining Walls*, Denver, 1991, pp. 81-100.

9. Wu, J. T., "Measured Behavior of Denver Wall," Proceedings, *International Symposium on Geosynthetic-Reinforced Soil Retaining Walls*, 1991, pp. 31-41.

APPENDIX A

Table A
List of instrumented reinforced-soil walls and slopes from the literature

Ref.	Wall Description	Wall Geometry	Soil-Reinf. System	Measurements	Instrumentation
[1]	- Reinforced wall - Location: Tucson, AZ - Year: 1984	- 15.5 ft high - Facing: full height pre-cast concrete panels	- Geogrid Tensar-SR2 - Granular backfill $(\varphi = 30^o)$	- Movement of front wall - Reinforcement strain - Horizontal and vertical strains in soil - Lateral and vertical earth pressure - Temperature	- Surveying of front panels - Resistance strain gauges - inductance coils - Inductance coils - Pressure cells - Resistance thermometers
[2]	- Model test wall - Location: Royal Military College, Canada	- 6 m long, 2.4 m wide - 3.6 m high - Facing: full height wooden propped panels	- Geogrid Tensar SS1 - Uniform sand $(\varphi = 56^o$ at 10 Kpa)	- Horizontal movement of central panels - Reinf. displacement and strains - Loads at toe and facing connections - Vertical pressure at base and layers	See reference [5]
[3]	- Reinforced Levee - Location: LA - Year: 1987	- Embankment test section 350 long, 10 ft high, slope 1:4	- Two layers of geogrid Tensar-SR2 - Soft-very soft clay	- Horizontal movement - Settlement - Pore pressure - Reinf. strain	- 3 inclinometers - 2 settlement plates - 4 piezometers - 34 strain gauges (MM CEA -13-250UM-350)

Ref.	Wall Description	Wall Geometry	Soil- Reinf. System	Measurements	Instrumentation
[4]	- Reinforced Levee - Location: Plaquemines, LA - Year: 1986	- Embankment 20 ft high	- Geotextile fabric - Soft-very soft clay	- Horizontal movement - Settlement - Pore pressure - Reinf. strain	- 6 inclinometers - 4 settlement plates - 8 piezometers - Strain gauges and LVDT's
[5]	- Model test wall - Location: Royal Military College, Canada - Same as wall in Ref. 5, different facing & instrumentation	- 6 m long, 2.4 m wide – 3.6 m high - Facing: incremental panels	- Geogrid Tensar SR2- and SS1 - uniform sand ($\varphi = 56^o$ at 10 Kpa)	- Horizontal and vertical movement of central panel - Reinf. displacement - Reinf. strain - Loads at toe and facing connections - Vertical pressure at base and layers - Soil strain	- Hybrid track recliner, HTR potentiometer - Extensometer wires attached at the back - Foil type gauges "Showa Measurements" – type Y11-FA-5-120 - Proving rings at the facing - "Geokon EP3500" cells & "Glotzel" cells -'Bison' inductance coil
[6]	- Reinforced earth wall - Location: Highway 101-Cloverdale, CA - Year: 1988	- Wall 62 ft high - Facing: hexagonal concrete face panels	- Steel wire bar mats - Sand-gravel backfill ($\varphi = 34^o$)	- front wall movement - Horizontal movement - Reinf. strain - Earth pressure	- Slope indicators - 4 horizontal settlement indicators - Resistance strain gauges - Earth pressure cells

130

Ref.	Wall Description	Wall Geometry	Soil-Reinf. System	Measurements	Instrumentation
[7]	- Embankment - Location: Mohicanville, OH. - Year: 1984-1985	- Embankment 28 ft high, 1800 ft long	- Welded wire mesh - CL soil	- Pore pressure - Horizontal & Vertical movement - Reinf. strains - Settlement	- 9 open tube, 7 electric and 23 pneumatic piezometers - 9 vertical and 4 horizontal inclinometers - 76 strain gauges - 12 settlement plates
[8]	- Reinforced earth wall - Location: I-80, Baxter, CA.	- 2 instrumented stations, 14-16 ft high - Facing: concrete panels	- Welded wire mesh - Sandy silt SM, and ML soil	- Wall movement - Water table - Reinf. strain - Vertical pressure at base and layers	- Reference points on top, face and toe of wall - Open standpipe piezometers - Strain gauges - Pressure cells, Carlson stress meters
[9]	- 2 Reinforced earth walls - Location: I-5, Dunsmuir, CA. - Year: 1976	- MSE wall: upper wall 20 ft high, lower wall 18 ft (Location A) - RE wall: 20 ft high (location B) - Facing: concrete panels	- MS wall: Steel wire bar mats - RE wall: Steel strips - Aggregate, $(\varphi = 34^o)$	- Wall movement - settlement - Soil pressure - Reinf. Strain - Corrosion - Vibration	- Reference monuments and plump points - Mercury-pneumatic sensors & settlement plates - Concrete, hydraulic & pneumatic pressure cells - Welded strain gauges - 'Magna' corrosmeter probes - Statham accelerometer

Ref.	Wall Description	Wall Geometry	Soil- Reinf. System	Measurements	Instrumentation
[10]	- Reinforced Earth wall - Location: Cal-39, L.A., CA. - Year: 1974	- 55 ft high, 528 ft long	- Steel strips - granular soil	- Wall movement - Soil settlement - Reinf. strain - Soil pressure	- Gauge points at facing, slope indicators - Settlement plate - Extensometers, strain gauges - Pressure cells
[11]	- Field test wall - Location: Glenwood Canyon, CO.	- 15 ft high, 350 ft long, 10 segments with different fabrics - Facing: gunnite	- Geotextiles - Well graded sandy gravel	- Wall movement and settlement	- Survey points on top, face and toe of wall, 5 vertical inclinometers, 5 manometers, 30 horizontal Inclinometers & extensometer casings.
[12]	- Reinforced wall - Location: Cascade Dam MI.	- 10 ft high wall	- Geogrid Signode TNX 250 - Sandy gravel fill	- Tension in geogrids - Lateral displacement - Lateral pressure	- Strain gauge MM-EP-08-250BG-120, and Bison type 4101-A - Wire extensometers - Load cells 'Sinco'.
[13]	- Model test wall	- 1.9 m wide and 1.44 m high model wall - Facing: wood plackets	- Woven polyester - Medium-fine sand	- Wall movement - Soil pressure - Reinf. strain	- Dial indicators at facing - 2 'Glozel' earth pressure cells - magnets

132

Ref.	Wall Description	Wall Geometry	Soil-Reinf. System	Measurements	Instrumentation
[14] [15]	- Reinf. embankment - Location: Devon, Alberta - Year: 1986	- 12 m high, 1:1 slope	- Mirafi paragrid 50s/50s, Signode TNX 5001, Tensar SR2 - Silty clay, 25% clay	- Pore pressure - Soil deformation - Reinf. strain	- 36 "Sinco" pneumatic piezometers - Vertical and horizontal "Sinco" inclinometers, multipoint magnetic extensometers - Resistance strain gauges, Bison sensors and thermocouples.
[16]	- Reinforced test embankment - Location: I-76, Denver, CO.	- 4 test cells 100 ft length each and 30 ft high, 1:1.25 slope, and 45 ft wide at top	- Supac, Tensar SS2, Mirafi 5T and Typar 3601. - Clay shale over flyash	- Wall movement and settlement - Reinf. strain	- 8 vertical inclinometers, 4 horizontal Inclinometers - 41 strain gauges
[17]	- Reinforced test wall - Location: Oslo, Norway - Year: 1987	- Sloped (2V:1H) wall, 4.8 m high	- Geogrid - Medium coarse sand	- Tension in geogrids - Reinf. strain - Earth pressure - Temperature	- Vibrating wire load cells - 'Bison' inductance coils
[18]	- Reinf. Embankment - Location: Highway 16, AR. - Year: 1988	- 2:1 embankment 40-80 ft high	- Tensar UX1400-1600 - Highly plastic clay	- Soil movement - Reinf. strain - Pore pressure and moisture content	- 3 extensometers, 3 inclinometers, settlement stakes - 67 strain gauges - 2 tensiometers, 3 pneumatic piezometers, 5 potential sensors

Ref.	Wall Description	Wall Geometry	Soil- Reinf. System	Measurements	Instrumentation
[19]	- Reinforced wall - Location: New Brunswick, Canada - Year: 1990	- Vertical wall 2.65 to 6.97 m high - Facing: pre-cast concrete panels 2.6 m wide	- Reinf.: Tensar SR2 - Soil: Granular backfill	- Wall movement - Reinf. strain - Total stress - Pore pressure - temperature	- Survey Targets - MM 125BT-12 strain gages - Petur pneumatic cells model EPC-9P - 1 Petur Piezometer model P106-1 - 2 copper constant thermocouples
[20]	- Full scale test wall - Location: Algonquin, IL	- Vertical wall 6.1 m high, 15 m wide - Facing: 20 cm high facing blocks.	- Reinf.: Mirafi polyester geogrid, Miragrid 5T - Soil: SW-GP fine to coarse sand	- Wall movement - Reinf. strain - Horizontal and vertical earth pressure	- 2 inclinometers - Glotzl extensometers - 42 Strain gages type KFE-5-C1 Kyowa Dengyo - Glotzl earth pressure cells

References of Table-A

1. Fishman, K.L., Desai, C.S., and Berg, R.R., "Geosynthetic-Reinforced Soil Wall: 4 Year History," *Transportation Research Record 1330*, 1991, pp. 30-39.

2. Bathurst, R.J., and Benjamin, D.J., "Failure of a Geogrid-Reinforced Soil Wall," *Transportation Research Record 1288*, 1990, pp. 109-116.

3. Hadj-Hamou, T., Bakeer, R.M., and Gwyn, W., "Field Performance of a Geogrid-Reinforced Embankment," *Transportation Research Record 1277*, 1991, pp. 80-89.

4. Bakeer, R.M., Hadj-Hamou, T., Duarte, F.M., and Satterlee, G.S., *Transportation Research Record 1277*, 1991, pp. 90-101.

5. Bathurst, R.J., "Instrumentation of Geogrid-Reinforced Soil Walls," *Transportation Research Record 1277*, 1990, pp. 102-111.

6. Jackura, K.A., "Performance of a 62-foot High Soil-Reinforced Wall in California's North Coast Range," *Transportation Research Record 1242*, 1989, pp. 39-45.

7. Duncan, J.M., Schaefer, V.R., Franks, L.W., and Collins, S.A., "Design and Performance of a Reinforced Embankment for Mohicanville Dike No. 2 In Ohio," *Transportation Research Record 1153*, 1987, pp. 15-25.

8. Hannon, J.B., and Forsyth, R.A., "Performance of an Earth Reinforcement System Constructed with Low Quality Backfill," *Transportation Research Record 965*, 1984, pp. 55-66.

9. Hannon, J.B., Forsyth, R.A., and Chang, J.C., "*Performance Comparison of Two Earthwork Reinforcement Systems,*" Transportation Research Record 872, 1983, pp. 24-32.

10. Chang, J.C., Forsyth, R.A., and Beaton, J.L, "Performance of a Reinforced Earth Fill," *Transportation Research Record 510*, 1974, pp. 56-68.

11. Bell, J.R., Barrett, R.K., and Ruckman, A.C., "Geotextile Earth-Reinforced Retaining Wall Tests: Glenwood Canyon, Colorado," *Transportation Research Record 916*, 1983, pp. 59-69.

12. Christopher, B.R., "Geogrid Reinforced Soil Retaining Wall to Widen an Earth Dam and Support High Live Loads," *Geosynthetics'87*, New Orleans, 1987, pp. 145-156.

13. Holtz, R.D., and Broms, B.B., "Wall Reinforced by Fabrics-Results of Model Tests," *International Conference on the Use of Fabrics in Geotechnics*, Paris, 1977, pp. 113-117.

14. Scott, J.D., Sego, D.C., Hofmann, B.A., Richards, E.A. and Burch, E.R., "Design of the Devon Geogrid Test Fill," *Geosynthetics'87*, New Orleans, 1987, pp. 157-168.

15. Sego, D.C., Scott, J.D., Richards, E.A., and Liu, Y., "Performance of a Geogrid in a Cohesive Soil Test Embankment," *4th International Conference on Geotextiles, Geomembranes and Related Products*, The Hague, Netherlands, 1990, pp. 67-72.

16. Su, C.K., and Chou, N.S., "A Test Embankment Reinforced by Four Types of Geosynthetics," *Geosynthetics'89*, San Diego, 1989, 291-303.

17. Fannin, R.J., and Hermann, S., "Creep Measurements on Polymeric Reinforcement," *Geosynthetics'91*, Atlanta, 1991, pp. 561-573.

18. Hayden, R., Schmertmann G.R., Qedan, B.Q., and McGuire, M.S., "High Clay Embankment over Cannon Creek Constructed with Geogrid Reinforcement," *Geosynthetics'91*, Atlanta, pp. 799-822.

19. Knight, M.A. and Valsangkar, A.J., "Instrumentation and Performance of a Tilt-Up Panel Wall," *Geosynthetics'93*, Vancouver, Canada, 1993, pp. 123-136.

20. Simac, M.R., Christopher, B.R., and Bonczkiewicz, C., "Instrumented Field Performance of a 6 m geogrid soil wall," *4th International Conference on Geotextiles, Geomembranes and Related Products*, The Hague, Netherlands, 1990, pp. 53-59.